APTA REPORT
ChemImage Biothreat, LCC
7301 Penn Avenue, Pittsburgh, PA 15208
Tel 412.241.7335 Fax 412.241.7311
www.chemimage.com

Report Title: Airborne Particulate Threat Assessment

Type of Report: Final Scientific

Reporting Period Start Date: October 1, 2005

Reporting Period End Date: December 31, 2008

Principal Author(s):

Treado, Patrick, J.; Klueva, Oksana; Beckstead, Jeffrey

Date Report was issued: March, 2009

DOE Award Number: DE-FC26-05NT42594

Name and Address of Submitting Organization:

ChemImage Biothreat LLC, 7301 Penn Ave, Pittsburgh, PA 15208

Dr. Patrick J. Treado, treado@chemimage.com

Contracting Officer's Representative:

Department of Energy, National Energy Technology Laboratory

ATTN: Pierina N. Fayish, DOE NETL (hard copy)
Don Martello, DOE NETL (e-copy)
Address: P.O. Box 10940 Mailstop B922/ R342C
Pittsburgh, PA 15236
Tel: (412) 386-5428
E-mail: Pierina.Fayish@NETL.DOE.GOV
Donald.Martello@NETL.DOE.GOV

Disclaimer:

Abstract:

Aerosol threat detection requires the ability to discern between threat agents and ambient background particulate matter (PM) encountered in the environment. To date, Raman imaging technology has been demonstrated as an effective strategy for the assessment of threat agents in the presence of specific, complex backgrounds. Expanding our understanding of the composition of ambient particulate matter background will improve the overall performance of Raman Chemical Imaging (RCI) detection strategies for the autonomous detection of airborne chemical and biological hazards. Improving RCI detection performance is strategic due to its potential to become a widely exploited detection approach by several U.S. government agencies.

To improve the understanding of the ambient PM background with subsequent improvement in Raman threat detection capability, ChemImage undertook the Airborne Particulate Threat Assessment (APTA) Project in 2005-2008 through a collaborative effort with the National Energy Technology Laboratory (NETL), under cooperative agreement number DE-FC26-05NT42594.

Table of Contents

1. Executive Summary

Aerosol threat detection requires the ability to discern between threat agents and ambient background particulate matter (PM) encountered in the environment. To date, Raman imaging technology has been demonstrated as an effective strategy for the assessment of threat agents in the presence of specific, complex backgrounds. Expanding our understanding of the composition of ambient particulate matter background will improve the overall performance of Raman Chemical Imaging (RCI) detection strategies for the autonomous detection of airborne chemical and biological hazards. Improving RCI detection performance is strategic due to its potential to become a widely exploited detection approach by several U.S. government agencies.

To improve the understanding of the ambient PM background with subsequent improvement in Raman threat detection capability, ChemImage undertook the Airborne Particulate Threat Assessment (APTA) Project in 2005-2008 through a collaborative effort with the National Energy Technology Laboratory (NETL), under cooperative agreement number DE-FC26-05NT42594.

During Phase 1 of the program, a novel PM classification based on molecular composition was developed based on a comprehensive review of the scientific literature. In addition, testing protocols were developed for ambient PM characterization. A signature database was developed based on a variety of microanalytical techniques, including scanning electron microscopy, FT-IR microspectroscopy, optical microscopy, fluorescence and Raman chemical imaging techniques. An automated particle integrated collector and detector (APICD) prototype was developed for automated collection, deposition and detection of biothreat agents in background PM.

During Phase 2 of the program, ChemImage continued to refine the understanding of ambient background composition. Additionally, ChemImage enhanced the APICD to provide improved autonomy, sensitivity and specificity. Deliverables included a Final Report detailing our findings and APICD Gen II subsystems for automated collection, deposition and detection of ambient particulate matter.

Key findings from the APTA Program include:

- Ambient biological PM taxonomy
- Demonstration of key subsystems needed for autonomous bioaerosol detection
- System design
- Efficient electrostatic collection
- Automated bioagent recognition
- Raman analysis performance validating Td<9 sec
- Efficient collection surface regeneration
- Development of a quantitative bioaerosol defection model

2. Project Objective

The objective of the APTA program was to advance the state of our knowledge of ambient background PM composition. Operation of an automated aerosol detection system was enhanced by a more accurate assessment of background variability, especially for sensitive and specific sensing strategies like Raman detection that are background-limited in performance. Based on this improved knowledge of background, the overall threat detection performance of Raman sensors was improved.

3. Project Statement of Work

The APTA Project conducted a qualitative and quantitative analysis of airborne PM including background interferants such as pollen, insecticides and industrial particulate matter. APTA program involved a development of ambient PM signature library. Review of the scientific literature identified major PM constituents. An audit of the CI/AFIP Bioagent library to determine its taxonomy and applicability to ambient PM detection revealed approximately 25% of the PM constituents were present in the CI/AFIP library. As part of Phase 2, we characterized another 25% of the PM classes. We carried out several

collections of ambient PM material at several indoor and outdoor locations. We characterized ambient backgrounds collected at NETL-supported ambient air collection facilities using techniques such as optical Raman and fluorescence chemical imaging, FTIR microspectroscopy and scanning electron microscopy.

ChemImage team undertook the following tasks:

Task 1: Refinement of the Knowledge Base

Task 2: APICD System Development

Task 3: Collection of Ambient Background Samples

Task 4: Detection

Task 5: Signature Database Compilation

Task 6: Final Report

In this Report, we describe our efforts in Phase 2 of the APTA program.

4. Task 1: Refinement of the Knowledge Base

Airborne particulate matter is one of the foremost and most complex air pollutants, diverse in chemical composition, size and origin. Suspended particulate matter (PM) influences climate changes and may be harmful to human health. The amount and composition of ambient particulate matter (PM) is highly variable with season, location and weather patterns. Such diversity leads to large uncertainties in physical and optical characteristics. While inorganic components of PM are fairly well characterized, the organic and biological contributors are generally measured “in bulk” as organic (OC) and elemental (EC) carbon without particular attention to composition. Classification of the organic components and their contribution to the PM mass strongly depends on the chosen techniques, particulate origin, formation mechanism, size, spatial and temporal location.

In the course of the APTA project, ChemImage has evaluated the current state of PM knowledge in respect to chemical composition by reviewing a body of scientific papers published in the last decade. In our examination of the literature, we have seen substantial gaps in the published quantitative studies on the PM chemical composition. These gaps are particularly obvious in regard to the biological fraction of PM. While pollen, fungal spores, animal allergens and bacteria types usually present in PM are well known from microscopy studies, no quantitative data exists on the mass contribution of biological components of PM due to different methods of detection and quantification for biological and non-biological particulates.

Based on our literature review, we proposed a classification of PM arising from chemical composition (**Figure 1**). We also used this methodology to classify our current Raman signature library (**Figure 2**). Additionally, we prepared a quantitative model for the chemical composition of the outdoor ambient PM based on the literature data. **Table 1** summarizes our findings for the chemical composition of outdoor ambient PM. PM data shows significant differentiation by size and location.

Table 1. Chemical Composition of Total Suspended Particulate (TSP) and its Fractions.

	Categories	Global TSP Data	North America TSP	North America $PM_{2.5}$
Inorganic	Mineral Dust	19.2%	10.5%	3.0%
	Sea Salt	6.5%	1.6%	0.5%
	Industrial	9.0%	4.7%	7.6%
	Sulfates	16.3%	23.7%	35.9%

	Ammonium salts	5.2%	8.3%	12.6%
	Nitrates	4.2%	4.0%	4.3%
Organic	Elemental carbon	4.0%	3.7%	4.7%
	WSOC	12.2%	7.9%	15.5%
	WINSOC	7.3%	4.7%	16.0%
	Pollen	6.6%	7.2%	0.0%
	Fungal Spores	3.1%	3.8%	0.0%
	Bacteria	7.0%	8.6%	0.0%
	Debris	10.4%	11.4%	0.0%

4.1. Outdoor PM Composition

4.1.1. Inorganic Particular Matter

The inorganic contribution includes mineral dust, sea salt, and secondary aerosols and can contribute from 6 to 95% to the mass of total suspended particulate (TSP). It is estimated that 50% of the atmospheric dust load can be attributed to anthropogenic factors.[1] Transportation, cement manufacturing, metallurgy, waste incineration and fossil fuel combustion are regarded as main anthropogenic sources and are heavily regulated. An Industrial PM category was added for inorganic particulate of anthropogenic origin related to industrial activity.

Crustal aerosol fraction, also called mineral dust, includes all-non-water soluble and non-carbonaceous components and makes up the majority of particulate matter less than 10 μm in size across the globe. Mineral dust contains minerals and other crustal earth material such as soil dust, fly ash and other windblown material from the deserts and dry lakebeds. Common mineral species in both PM_{10} and $PM_{2.5}$ fractions are calcite ($CaCO_3$), quartz (SiO_2), gypsum ($CaSO_4 \cdot 2H_2O$), dolomite ($CaMg(CO_3)_2$), feldspar ($XAl_{(1-2)}Si_{(3-2)}O_8$ where X = K, Na, Ca, Mg), hematite (α-Fe_2O_3), and anatase (TiO_2).[2] Iron, copper, zinc and lead contribute more than 90% of total mass of 11 measured metals, iron being the dominant metal in both PM_{10} and $PM_{2.5}$.[3] The finer fraction on average contains more water-soluble metallic species than the coarse function. Particulate may contain heavy and trace metals with heavy metal concentrations usually higher in urban and roadside locations as compared to rural sites.

Sea salt aerosol (0.05-10 μm), the second largest contributor to the global aerosol budget, consists principally of sodium chloride from seawater. Other components of seawater include magnesium chloride and organic compounds. Sea salt aerosols are formed during whitecap formation and depend strongly on wind speed. Other ions found in seawater include Na^+, Cl^-, Mg^{2+}, Ca^{2+}, K^+, SO_4^{2-}, HCO_3^-.

Suspended inorganic particulate includes secondary aerosols, produced by atmospheric oxidation of biogenic or anthropogenic compounds such as VOC, SO_2, NO_x, NH_3, sulfuric acid or nitric acid. Main species of secondary inorganic PM are sulfate, nitrate (NO_3^-) and ammonium (NH_4^+) ions. Sulfate aerosols consists of the sulfate anion (SO_4^{2-}) existing in various chemical states: sulfuric acid, ammonium bisulfate, ammonium sulfate, or as a dissociated anion in aqueous solution. Composition of secondary PM varies significantly with emission source and process conditions.

Airborne soil (60%) was the largest source of primary PM_{10} mass while soil contributed only 1% to $PM_{2.5}$ mass in a study conducted in Atlanta, GA[4]. The primary contributor to $PM_{2.5}$ mass was sulfate secondary

aerosol (56%) while elemental and organic carbon on average comprised approx. 8% and 40% of $PM_{2.5}$ respectively.[5] Invariably, NH_4^+ was associated with both the SO_4^{2-}-rich and NO_3-rich secondary aerosols.[4] Ultrafine PM_1 in the Atlanta study contained 74 % of organic and 1.5% of elemental carbon as percentage of particle mass.[6]

Iron, copper, zinc and lead contribute more than 90% of the total mass of 11 measured metals across all size fractions.[3] Particulate may contain heavy and trace metals with their concentration usually higher in urban and roadside locations as compared to rural sites. A study conducted in France[2] of PM_{10} detected large amounts of Al, Ca, Fe and K indicating mineral dust, Na+ and Cl^- related to sea salt as well as NH_4+, SO_4^{2-}, NO_3^-, Pb and Zn related to anthropogenic activity. Raman spectroscopy identified calcite ($CaCO_3$), quartz (SiO_2), gypsum ($CaSO_4 \cdot 2H_2O$), dolomite ($CaMg(CO_3)_2$), feldspar ($XAl_{(1-2)}Si_{(3-2)}O_8$ where X= K, Na, Ca, Mg), hematite (α-Fe_2O_3), anatase (TiO_2) in both PM_{10} and $PM_{2.5}$ fractions.

4.1.2. Organic Particular Matter

Non-mineral, carbon-containing compounds that constitute organic PM matter represent an important but poorly understood aerosol fraction. Globally about 20% of the total mass of atmospheric aerosols is carbonaceous material that may be separated into biogenic and non-biological fractions. The non-biological category contains combustion products and well as products of chemical processes in the soil and the atmosphere. The main sources for non-mineral, non-biological carbonaceous aerosol is the atmospheric oxidation of biogenic and anthropogenic VOCs, and burning of biomass and fossil fuel. Burning fossil fuels in factories, power plants, steel mills, smelters, diesel- and gasoline-powered motor vehicles and equipment generates most of the fine and ultrafine particles.

Secondary organic emissions are a complex mixture of the oxidation and condensation products originating from gaseous precursors and radical species such as O_3, OH, and NO_3. The low volatility products are usually condensed onto existing particles or nucleate and form new ones.[7] Composition and size of individual particles varies significantly with emission source and process conditions and can provide clues about their specific sources, i.e. combustion engines, explosives, forest fires, etc. and which helps elucidate potential health effects.

The total carbon content (TC) of particulate matter is traditionally expressed as the sum of all carbon present in the aerosol particles, except in the form of inorganic carbonates (0.5-3%) without attention to detailed chemistry. The TC is usually determined by catalytic oxidation of PM-laden filter to CO_2 to observe two fractions - organic carbon (OC – 70-90%) and elemental carbon (EC - 10–25%).[8] The fractions respective contribution to the PM mass strongly depends on the chosen technique, particulate origin, mechanism of formation, size, spatial and temporal location.

4.1.3. Biogenic Particular Matter

A significant part of organic fraction of particular matter is, or is produced by living things. Biogenic aerosols comprise 10-30% of total aerosol volume for both coarse and fine particulate fractions[9] and may include plant and insect debris, animal dander and saliva, microbial particles (bacteria, fungi, viruses, algae, pollen, spores, etc.) as well as semivolatile compounds emitted by plants directly or resulting from the chemical reactions in the atmosphere. The latter may form volatile organic compounds (VOC) or condense into humic-like substances that fall into the non-biological category in ChemImage's classification.

The sampling methods and analytical techniques associated with biogenic PM are varied and non-standardized. Collected microorganisms are grown and counted using optical or fluorescence microscopy. Other approaches include assays for specific microorganism constituents (i.e., ergosterol, muramic acid, glucans, allergens, mycotoxins, endotoxins) and molecular methods (i.e., polymerase chain reactions, gene probes, ELISA, LC-MS). Based on viable cultures, such approaches may underestimate microorganisms concentrations as fragments of pollen and fungi were found in PM fractions as low as 0.2 μm.[10] Nonviable fragments can remain toxic or allergenic, depending upon the specific organism.

Fungal spore size varies from 2-100 μm while many pollen species exceed 10 μm in size. The Bioaerosol Committee of the American Conference of Governmental Industrial Hygienists (ACGIH) stated[11] that outdoor airborne fungi concentration "routinely exceeds 1000 CFU/m^3 and may average near 10,000 CFU/m^3 in summer months." Airborne fungal spores contribute to the organic carbon of the atmospheric aerosol, mainly in the coarse PM range due to their spore size. Fungal contribution to the coarse size fraction can reach up to 9.9% of OC, while an average contribution may be only 0.9% of OC.[8] Other studies found the average spore mass percentage contribution to PM_{10} was 0.17% ± 0.13 for *Aspergillus/Penicillium*, and 0.95% ±1.63 for *Cladosporium* with assumed spore density of 1 g/cc.[12]The relationships between ambient airborne fungi and pollen with PM_{10}, $PM_{2.5}$, organic carbon, and other parameters were investigated in Cincinnati, OH.[12] Optical microscopy was used for identification and enumeration of a total of 28 fungal and 20 pollen genera. Mean concentrations of fungi and pollen were 102.7 spores/μg and 5.4 pollen/μg of total particulate matter with pronounced seasonal variations. The concentration levels of both PM_{10} and $PM_{2.5}$ were elevated during summer and fall months, similar to fungi and unlike pollen, which peaked in the spring. Predominant airborne fungi were: *Aspergillus/Penicillium* group (41.6%), *Cladosporium* (28.4%), *Ascospores* (10.6%), and *Basidiospores* (9.8%) relative to the total airborne fungal load. The dominant pollen types showed significant seasonal patterns, therefore, their contributions to the total airborne pollen load were determined at the time of pollen type seasonal occurrence. The following seasonal contributions were found: *Ambrosia* (Ragweed) - 88.0% (Fall); *Quercus* (Oak) - 51.3% (Spring); *Juniperus* (Juniper, Cedar) - 11.5% (Spring); *Ulmus* (Elm) - 8.8% (Spring), *Acer* (Maple) - 8.0%, *Pinaceae* (Pine, Fir, Spruce) - 4.8% (Spring), and *Poaceae* (Grass) - 3.3% (Summer) relative to the total pollen load.

Common airborne bacteria usually range from 0.5 to 2.0 μm but may be present as agglomerates. The bacterial load of PM is extremely low and difficult to quantify by methods other than colony counting after incubation and growth. Bauer *et al*. measured an average bacterial concentration of $1.2 \cdot 10^4$ cells/m^3, corresponding to 0.03% of OC[8] and carbon content of bacteria of 17 fg C/cell. [13] Measurements in Finland[14] found outdoor levels of bacteria to be lower by an order of magnitude in winter (12 CFU/m^3) than in summer (150 CFU/m^3) as expected due to snow coverage. Acceptable levels of airborne microorganisms have not been established.[15]

4.1.4. Quantitative Outdoor PM Composition Model

Our findings for the chemical composition of outdoor ambient PM, summarized in **Table 1,** shows significant differentiation by size and location. Particular emphasis has been placed on understanding molecular composition of ambient PM in North America, including detailed composition of $PM_{2.5}$. The differences between total suspended particulate detected globally and in North America differ mainly in the sea salt contribution, even though PM data over oceans was not included. The inorganic contribution includes mineral dust (whether natural or anthropogenic), sea salt, and secondary aerosols and can contribute from 6 to 95% to the mass of total suspended particulate (TSP), with an average value of 61.1%. The organic contribution describes carbon-based biogenic and anthropogenic particulate from plant debris to pollen and may vary 2.6 to 75.5% of TSP, with an average value of 33.5%. Airborne microorganisms contribute ~15% to ambient PM mass on average, with the mass fractions ranging from 0.2% to 32.5%.

Major differences in chemical composition were observed between crude and fine size outdoor PM fractions. While traces of biological species may be detected in fine $PM_{2.5}$ the amount is not easily quantified, while in PM_{10} the biological particulate fraction can dominate. The amount of mineral dust is greatly reduced in $PM_{2.5}$ while sulfates comprise more than a third of the fine particulate. The amount of industrial dust increased twofold for $PM_{2.5}$. Other categories remained approximately the same.

4.2. Indoor PM Composition

References describing indoor PM composition are limited to enumeration of biological genera since indoor bioaerosols are generally monitored as a part of industrial hygiene, for assessment of indoor air quality, epidemiological investigations, clean rooms or allergy research. Very little published data is

available comparing biological loads with the rest of indoor particulate. From ChemImage's experience, participating in government sponsored bioaerosal field studies, Table 2 describes some dominant indoor PM constituents.

Table 2. Possible Sources of False Alarms in Ambient Particulate Matter.

Pollen	Fungi	Allergens	Bacteria	Particulates
Kentucky Blue Grass (*Poa pratensis*)	*Neurospora crassa*	Cat dander/antigen (*Felis catus (domesticus)*)	*Staphylococcus epidermidis*	Upholstery Dust
Goldenrod Weed (*Solidago spp.*)	*Penicillium chrysogenum*	Dog Dander (*Canis familiaris*)	*Staphylococcus saprophyticus*	Arizona Road Dust
Mulberry Paper (*Broussonetia papyrifera*)	*Penicillium brevicompactum*	Guinea Pig Epithelia (*Cavia porcellus (cobaya)*)	*Micrococcus luteus*	Talc Powder (Hydrous magne-sium silicate)
Eastern Sycamore Tree (*Platanus occidentalis*)		Mouse Epithelia (*Mus musculus*)	*Bacillus thuringiensis*	Kaolin
Dandelion Flower (*Taraxacum officinale*)		Human Epithelia	*Bacillus mycoides*	Bentonite Powder
				House Dust
				Cellulose Flock

In general, a healthy indoor environment contains less bioaerosols and other PM than outdoor as the main source of indoor particulate is usually outdoor air. While outdoor PM levels influence indoor PM, their compositions have significant differences mostly in the organic and biological constituents. Excessive humidity and unsanitary conditions may result in large amounts of fungal spores and harmful bacteria. On the other hand, indoor environments have less mineral dust and different chemicals populating organic secondary PM (detergents, food, etc).

4.2.1. Qualitative Indoor Composition Model

The relationship between outdoor and indoor PM loads has not been sufficiently studied. A healthy indoor environment is assumed to contain less bioaerosols than outdoor although the opposite does not imply a healthy environment. Indoor microorganism concentrations as high 510 to 10,700 organisms/m^3, with 25-250 organisms/μg of PM_{10}, were measured in commercial buildings.[16]

The range of indoor air concentrations of airborne viable fungi is wide (10–10^4 cfu/m^3), and airborne concentrations of fungi greatly vary both temporally and spatially. Common indoor molds[17] in the US include:

1.) *Chaetomium globosum, Stachybotrys chartarum, Stachybotrys new species*;

2.) *Alternaria alternata, Aspergillus versicolor, Cladosporium sphaerospermum*;

3.) *Aureobasidium pullulans; Cladosporium cladosporioides, Penicillium brevicompactum,Penicillium chrysogenum, Ulocladium chartarum*;

4.) Acremonium strictum, Aspergillus niger;

5.) *Epicoccum nigrum, Eurotium amstelodami*;

6.) *Penicillium aurantiogriseum, Trichoderma harzianum*.

Measurements based on phosphlipids content (0.3% of spore dry weight) have suggested that about 12% to 22% of the OC or from 4% to 11% of the total $PM_{2.5}$ mass were of fungal origin.[18]

The bacteria found in indoor air generally is shed by building occupants or entered with outdoor supply air. Outdoor concentrations of airborne bacteria generally are higher than those indoors.[19] Concentrations of bacteria associated with normal human flora (e.g., Gram-positive cocci) were more

abundant in indoor air and in summer whereas those associated with soil and plant surfaces (e.g., Gram-positive and – negative rods) were more abundant in outdoor air, with little seasonal difference.

5. Task 2: Automated Particle Integrated Collector and Detector (APICD)

5.1. APICD Gen I Testing

The APICD Gen I System developed in Phase 1 employs electrostatic collection to deposit ambient PM on a stainless steel rod (**Figure 3**). Fluorescence triggering of Raman acquisition is being evaluated and based on the results may be included into the APICD system.

In Phase 2 of the project, the existing APICD Gen I system was further optimized for automated collection of PM and detection of biological samples within ambient background levels collected as part of indoor aerosol testing. Basic performance of the APICD Gen I system was characterized. (**Figures 4-6**) The results include:

Electrostatic Collection Tests:

- The electrostatic (ESTAT) Gen I device was exercised and collected PM for 13 continuous hours;
- Collection area on the steel rod was approximately 2 cm wide. Three distinct deposition zones were observed with color variation possibly due to compositional differences;

Imaging and Spectral Performance Tests:

- Dispersive and FAST Raman spectra were collected from known samples including acetaminophen, silicon wafer, NIST SRM 2422, Teflon, neon lamp, and aluminum slide;
- Dependence of power density on the sample as a function of laser voltage and zoom lens setting was obtained;
- Imaging cameras resolution was calculated from a USAF1951 resolution target;
- Modulation Transfer Function was measured.

FAST Imaging Characterization:

- Linear end of the multi-fiber bundle was correlated to the round end;
- Each fiber position on the spectral camera was determined and a FAST reconstruction map was built;
- FAST Reconstruction map is being tested using pinhole light source and polystyrene microspheres;
- Crosstalk between fiber channels was tested using polystyrene microspheres;
- Modulation Transfer Function has been measured.

The APICD Gen I system was used for semi-automated collection at the NETL site (see Task 3 for a full description).

5.2. Design of APICD Gen II Prototype

Figures 7-8 show the design concept for the Gen II prototype. The evolution of the design was based on a set of established requirements as seen in **Figure 9**.

5.2.1. Electrostatic Collector

ChemImage has teamed with Sceptor Industries to optimize Sceptor's electrostatic deposition technology for continuous aerosol collection and deposition. The basis for Gen II design is a drum concept that uses a rotating drum to enable continuous PM collection onto a continuously renewable surface for Raman detections.) The original concept used an axial air flow geometry. To increase the collection efficiency Sceptor has designed and built a closed drum prototype utilizing tangential flow of the sampled air stream. Sceptor presented a finalized engineering design incorporating access for targeting and Raman subsystems during a design review meeting (April 22, 2008). Gen I verses Gen II deposition patterns are seen in **Figure 10**. Two units of the Tangential Flow Drum Collector were assembled and tested (**Figures 11-13**). Under bulk collection conditions the deposition pattern is approx. 8 mm at its maximum which represents a significant improvement over the axial flow system (**Figures 14-15**).

As part of the development effort, new software was developed for the control of the tangential drum to enable autonomies control of the collection subsystem.

Sceptor engineers tested the performance of units 1 and 2 using fluorescent PSMS particles with 2 and 3 μm diameter. Fluorescent polystyrene particles were dispersed using a nebulizer and carried by airflow toward the electrostatic collector through ~3 meters of steel pipe (**Figure 16**). An airflow probe collected particles onto a reference filter to measure the reference particle concentration before deposition. Particles deposited on the drum are removed with a pre-weighed wipe; then the loaded wipe is placed into a centrifuge tube with a known volume of water. The reference filter was similarly placed into a known volume of water. Both centrifuge tubes are sonicated for 10 min to separate particles from the carrier. Concentrations of the fluorescent particles in the reference and drum suspensions are measured using a calibrated fluorometer and used to calculate % deposition efficiency.

Initial testing of TF unit 1 showed collection efficiency of 25% at the input airflow of 120 L/min. However, if the air flow rate was decreased to 40 L/min, the collection efficiency increased to 55%. Some scattering of the results was expected due to the incomplete recovery of particles from wipes, therefore, each measurement was repeated. Flow rates of 40-50 lpm gave the highest collection efficiency of 50-55% for 15 min collection on the stationary drum. Repeated measurements of collection efficiency as a function of time showed higher efficiencies as high as 80% around 20 minutes (**Figure 17**).

Similar experiments were carried out with rotating drum, in conditions closely approaching the intended operational conditions. The bead deposition pattern on the rotating drum was very faint with a well-defined top border. Nearly all the particles visible under the UV/Purple flashlight were inside a 3.75 mm stripe. Each measurement was repeated twice to confirm obtained efficiency values. The collection efficiency decreased with the flow rate with a maximum efficiency of 60% and minimum efficiency of ca. 40% at 100 lpm (**Figure 18**).

ChemImage recommended improvements for the 2nd unit based on the review of the 1st tangential flow drum Sceptor had made. Improvements to the 2nd unit design included brush disengagement, sealing around the drum and the mechanical interface.

5.2.2. Optical Targeting Subsystem

Ruda Associates were selected to aid in the design of the brightfield illumination optics. Optical system specifications were submitted to Ruda Associates for developing optimal coupling of the ultraviolet and white light LEDs to the Koehler illumination block. ChemImage performed the mechanical design to position these components (**Figures 19-20**). The magnification and sampling size of the imaging channel of the Brightfield Module are compared to design requirements in Table 3.

Table 3. Comparison of Specified and Measured parameters for Brightfield Optics in APICD Gen II.

	Brightfield Imaging Parameters	
	Design	**Actual**

Magnification	20x	20x
Field of View	1 mm	0.54 mm
Pixel Sampling Size	0.3-0.4 µm/pixel	0.29 µm/pixel
Image Resolution	600 lp/mm (1.6 µm)	645 lp/mm (1.5 µm)

5.2.3. Raman Subsystem

The Raman module was assembled and subsystem parameters were measured relating to laser and fiber coupling **Figure 21**. **Figure 22** shows the Raman subsystem and optical design as well as the first light measured using PEN, acetaminophen and polystyrene microspheres.

Laser Coupling

To aid in the development of an optical model of the Raman module, the lasers evaluated for this project were validated. Measurements included the beam profile as a function of distance from the laser head. These measurements were also taken when the *Laser Coupling Lens* was placed in the laser beam path, and finally after the objective at the objective's focal plane (the position of the drum surface). These measurements were compared to the results of the Raman laser delivery optical model developed by Ruda Associates. Possible improvements in the laser delivery optics were explored to reduce the beam size entering the objective's back aperture but will not be implemented at this time. **Figures 23-24**

Table 4. Raman System parameters for APICD Gen II

Test	Microscope Objective	Laser power, % max	Measured FWHM,* µm	FWHM Adjusted for System Magnification, µm
1	20x	25	1269.21	507.68
2	20x	80	1247.85	499.14
3	100x	25	965.41	386.16
4	100x	80	989.14	395.66

* - Average of horizontal and vertical values measured by precalibrated OPHIR CCD Beam Profiler.

** - Average values corrected by the system magnification of 2.5.

Fiber Coupling

The diameter of the Fiber Coupling Lens was found to be small for the efficient light collection and was increased. A mechanical mount for this lens and the Raman Fiber Bundle has been designed and fabricated. This mount allows the fiber to translate in three directions (one along the optical axis, two orthogonal. as well as rotate about the optical axis as well as the simple replacement of camera with the fiber mechanism for Raman alignment.

Using the Brightfield Imaging system, the performance of the new fiber lens has been evaluated using the new Fiber Coupling lens and the Brightfield camera.

5.2.4. Surface Regeneration

Automated regeneration of drum surface is a critical performance parameter of APICD Gen II. Gen II axial flow prototype drum was used for determining cleaning efficiency of the brush in the following way: (**Figure 25**).

1. A zoom lens with a video camera was setup to focus on the presumed Zero degrees position on the surface of the drum. Initial surface roughness was characterized over several fields of view.
2. 4 ml of 0.2% PSMS solution was dispersed for 90 sec Omcron nebulizer while electrostatic collector was active without rotation and the air blower was set to 10000 rpm.
3. The drum was rotated to bring deposited PSMS under the observation and 10 images were acquired.
4. The number of PSMS particles and their clusters in each field of view was determined and then particle density was calculated.
5. The surface cleaning brush was engaged and particle density was calculated over the same FOVs as a function of cleaning cycles.

On the axial drum prototype, 5 μm PSMS particles were deposited over 110 degrees of drum rotation, between 86 and 200 degrees. A small number of particles were detected at 205 degrees. Particle distribution was not even, with deposits near the beginning of the electrode pattern and larger clusters of 9-20 particles in the center of the deposition zone. These effects can be attributed to the particle-containing water droplets from the nebulizer condensing on the drum surface. Deposition of 5 μm polystyrene particles over 90 sec led to an average of ~10,000 particles/cm^2 within examined fields of view (**Figures 26-28**).

After the first cleaning cycle, the average density of PSMS particles and clusters was decreased to 624.39 particles/cm^2. Therefore, the single cleaning cycle achieved a 94% percent efficiency. A few of the ambient particles were still observed on the drum; and the deposition pattern at the beginning of the deposition zone was particularly difficult to remove even after 5 cleaning cycles. It is possible that forces other than electrostatic are holding larger clusters in place.

6. Task 3: Collection of Ambient Background Samples

Samples of outdoor and indoor particulate matter were collected using a dry electrostatic collection with APICD and several reference instruments at NETL. The operation of APICD was tested in field conditions. The purpose of concurrent collection was to validate APICD Collector by having conventional instrumentation collect particulate along with the APICD. In addition, the certified aerosol collection equipment at NETL was used to measure particle concentration and estimate particle density on the deposition surface.

PM collections were carried out in the Spring and Summer 2007 at two locations: ChemImage facilities (Pittsburgh, PA) and the Ambient Air Monitoring facility at NETL Bruceton Research center (Pittsburgh, PA). Sampling days were based on the absence of rain in the two days prior to the collection to ensure higher PM concentrations in the air.

Methodology Reference collections were carried out at Ambient Air Monitoring facility at NETL. The collection equipment schematic used at the NETL site is shown in **Figures 29-31.** The APICD, TEOM and ELPI™ instruments were turned on simultaneously for concurrent collection. DustTrak™ monitored particle loading continuously for several months, therefore, data relevant to the concurrent collection on August 1 and 3, 2007 was extracted from appropriate files. The NETL site lost power after Run 1, which required resetting of all instruments. The DustTrak™, TEOM and ELPI™ instruments were not impacted but APICD lost position settings, and positioning of the rod was continued with human operator intervention.

APICD APICD Gen I was used for an electrostatic PM collection at the NETL site. APICD Gen I developed by ChemImage includes a low-power, high-efficiency electrostatic collector. A fan forces PM-laden air inside the collector with at the rate of 100 L/min. An electrostatically charged stainless steel (SS) rod attracts the particulate for deposition.

ELPI The Electrical Low Pressure Impactor (ELPI™), manufactured by Dekati Ltd (Finland), is a particle size spectrometer designed to monitor aerosol particle size distribution in real time through electrical detection of aerosol particles. The ELPI™ uses 12 stages to measure particles ranging in size from 0.03 – 10 μm. The sampling flow rate is 30 L/min. In this study, aluminum impaction plates were used to minimize background signal in following chemical analysis. No grease was used to maximize particle retention on aluminum plates to avoid future interference with Raman detection. The inlet from the impactor was placed 10 feet from the ground. Data was collected in 1 min intervals using ELPIVI software v.13.1.

TEOM A Tapered Element Oscillating Microbalance (TEOM) Ambient Particulate Monitor equipped with an AccuSampler™ (Thermo Electron Co., former Rupprecht & Patashnick) continuously monitored the particulate mass concentration every 5 minutes. The TEOM was located near Ambient Air Monitoring lab with the inlet placed 6 feet from the ground.

DustTrak™ A DustTrak™ Aerosol Monitor (TSI Inc) is a portable, battery-operated laser photometer measuring real-time particle mass concentration. A pump draws the sample aerosol corresponding to the $PM_{2.5}$ fraction. The sensing mechanism consists of a laser diode directed at the aerosol stream. Scattered light is collected with optics and a photodetector at 90° to the light beam. The intensity of the scattered light is proportional to the particle mass concentration.

The DustTrak™ Aerosol Monitor was mounted at the NETL site, on a platform near the Ambient Air Monitoring lab. The inlet was placed 10 feet from the ground. Particle mass concentration was detected every 5 min.

6.1. Collections

In the Spring and Summer of 2007, 16 collections were carried out as seen in **Table 5**.

Preliminary outdoor and indoor collections were carried out at the ChemImage facility to estimate the fluorescent fraction of ambient PM for use in the APICD Particle Accounting model. A 10-day collection (April 3-12, 2007) of indoor witness sample was carried in ChemImage's Manufacturing area. A 24-hr witness sample collection of outdoor dust was performed at the on April 3-4, 2007 (**Figures 32-35)**.

Table 5. Collection Schedule.

#	Description	Collection Date			Collection method	Location
		Start	End	Duration		
1	Spring Outdoor Collection	3-Apr-07	4-Apr-07	24 hrs	gravity	Point Breeze, PA
2	Spring Indoor Collection	3-Apr-07	12-Apr-07	10 days	gravity	Indoor, Point Breeze, PA
3a	Summer Outdoor Collection, Run 1	1-Aug-07 12:50 EST	1-Aug-07 13:50 EST	1 hr	ELPI	NETL
3b	Summer Outdoor Collection, Rod 1	1-Aug-07 12:50 EST	1-Aug-07 13:50 EST	1 hr	APICD	NETL
3c	Summer Outdoor Collection, Run 1	1-Aug-07 12:50 EST	1-Aug-07 13:50 EST	1 hr	TEOM	NETL
3d	Summer Outdoor Collection, Slide 1	1-Aug-07	2-Aug-07	1 day	gravity	NETL

3e	Summer Outdoor Collection, Run 1	1-Aug-07 12:50 EST	1-Aug-07 13:50 EST	1 hr	DustTrak	NETL
4a	Summer Outdoor Collection, Run 2	1-Aug-07 14:08 EST	1-Aug-07 15:58 EST	1.5 hr	ELPI	NETL
4b	Summer Outdoor Collection, Rod 2, PSMS spiked	1-Aug-07 14:08 EST	1-Aug-07 15:58 EST	1.5 hr	APICD	NETL
4c	Summer Outdoor Collection, Run 2	1-Aug-07 14:08 EST	1-Aug-07 15:58 EST	1.5 hr	TEOM	NETL
4d	Summer Outdoor Collection, Run 2	1-Aug-07 14:08 EST	1-Aug-07 15:58 EST	1.5 hr	DustTrak	NETL
4e	Summer Outdoor Collection, Slide 2, PSMS spiked	2-Aug-07 14:35 EST	2-Aug-07 15:37 EST	1.5 hr	gravity	NETL
5a	Summer Outdoor Collection, Run 3	2-Aug-07 14:35 EST	2-Aug-07 15:37 EST	1 hr	ELPI	NETL
5b	Summer Outdoor Collection, Rod 3, PSMS spiked	2-Aug-07 14:35 EST	2-Aug-07 15:37 EST	1 hr	APICD	NETL
5c	Summer Outdoor Collection, Run 3	2-Aug-07 14:35 EST	2-Aug-07 15:37 EST	1 hr	TEOM	NETL
5d	Summer Outdoor Collection, Run 2	2-Aug-07 14:35 EST	2-Aug-07 15:37 EST	1 hr	DustTrak	NETL

Three outdoor collections were carried out at DOE-NETL location in Pittsburgh, PA using APICD Gen I, ELPI™, TEOM and DustTrak concurrently at similar conditions **(Figure 36).** Two witness samples were collected by gravity deposition of suspended PM on Al-slide. Successful deposition of PM was confirmed by optical microscopy. Sampling times varied from 60 to 90 min as our previous research have shown that longer collection times may overload the rod surface with PM.

Table 6. Weather conditions at NETL site during the collection. Weather Conditions Are Equivalent For Three Collections.

	DATE	TIME	AVERAGE WIND SPEED (MPH)	AVERAGE WIND DIRECTION (DEGREES)	AVERAGE AIR TEMPERATURE 2M (DEGREES F)	AVERAGE RELATIVE HUMIDITY 2M (PERCENT)	AVERAGE SOLAR RADIATION (WATTS/M^2)	AVERAGE PRESSURE (MILLIBARS)
	8/1/2007	12:45	2.89	64.96	84.7	91.6	326.0	980
	8/1/2007	13:00	3.10	49.15	85.5	91.6	843.0	980
	8/1/2007	13:15	3.59	14.6	86.1	91.7	840.0	980
	8/1/2007	13:30	2.40	180.7	86	91.7	673.6	980
	8/1/2007	13:45	3.72	1.519	86	92.1	588.6	980
RUN 1		**MEAN**	**3.14**	**62.19**	**85.66**	**91.74**	**654.2**	**980.00**
	8/1/2007	14:15	4.17	305.1	87.5	91.9	532.6	979
	8/1/2007	14:30	2.51	319.3	87.8	91.8	841.0	980
	8/1/2007	14:45	3.20	334.4	88	91.9	541.1	979
	8/1/2007	15:00	2.14	233.2	87.9	91.9	530.3	979
	8/1/2007	15:15	2.40	285.2	88.6	91.9	711.0	979
	8/1/2007	15:30	2.39	283.7	88.7	91.8	845.0	979
	8/1/2007	15:45	3.47	331.9	89.3	91.9	592.7	979
RUN 2		**MEAN**	**2.90**	**298.97**	**88.26**	**91.87**	**656.2**	**979.14**
	8/3/2007	14:30	5.92	258.7	90.2	91.7	816.0	978
	8/3/2007	14:45	4.26	269.9	89.8	91.8	744.0	978
	8/3/2007	15:00	5.46	250.4	89.1	91.9	370.5	978
	8/3/2007	15:15	5.35	243.1	88.7	92.2	501.4	978
	8/3/2007	15:30	5.03	252.1	89.7	91.8	738.0	978
	8/3/2007	15:45	5.90	248.6	88.5	91.8	295.8	978
RUN 3		**MEAN**	**5.32**	**253.80**	**89.33**	**91.87**	**577.6**	**978.00**

ELPI™ stages 1 to 8 collected particulate with aerodynamic diameter of ≤2.5 µm corresponding to $PM_{2.5}$ measured by other instruments and therefore, were used for comparison of mass concentration of fine particulate in the air. As ELPI™ data had the highest time resolution of 1 minute, 5 minutes averages were compared with DustTrak™ and TEOM readouts.

Mass concentration of $PM_{2.5}$ ranged from 15 to 130 µm/m^3 during the Summer 2007 collection (**Figure 37**). The obtained data was on the same order of magnitude for three particle monitors. DustTrak™ produces the highest readings. Discrepancy in the mass concentration reading is a result of the fundamentally different approaches to measuring mass, as well as high humidity (91%) during the sampling periods. The DustTrak™ particle monitor uses light scattering for mass measurement, which depends on particle size, refractive index, shape and orientation of the particle. Therefore, highly variable composition of PM with unknown optical properties, may lead to inaccuracy in measuring particle mass concentration.

The TEOM uses a direct relationship between oscillator mass and oscillating frequency, so it should provide more accurate data in real time. However, heating of the sampler leads to loss of water and substantial evaporation of volatile and semi-volatile organic components (organics, ammonium nitrate) on particles entering the TEOM, while ELPI measures particle number concentration at an ambient humidity. Additionally, ELPI™ operated close to the limit of detection for this stage (6.3 µg/m^3) during the first two runs. Run 3 was carried out during an air quality day with a high concentration of particulate in the ambient air, and there was a better agreement between DustTrak and ELPI data **(Figure 38)**.

Particle size distribution is shown in **Figure 39**. Ultrafine particulate constitutes the majority of the collection. ELPI™ stages 8 to 12 collected particulate with aerodynamic diameter of 1 –10 µm that corresponds to the size most likely to be detected by APICD. Particle number concentration for these stages were added and averaged to yield 1000 to 8000 particles/L. As expected, the last run had the highest particle concentration of 6985± 712 particles/L.

Deposition of fluorescent particles from Run 2 was investigated and 17 fluorescent particles were detected. Calculated fluorescent particle density was 257 particles/mm^2 (2.6E4 particles/cm^2). Overall

deposition surface of the rod (4.7 cm^2) was extrapolated to contain 1.2E5 fluorescent particles. As fluorescent particles comprise 38% of particulate in 1-10 μm size range, the total rod loading was estimated to be 3.2E5 particles.

The data above was used to approximate APICD collection efficiency. During Run 2 average 1 L of air contains 2364 of APICD-detectable particles; a 90-min collection with a flow rate of air 100 L/min exposes the collector to 2.1E7 such particles. The collector's efficiency overall was estimated for collection of particles in the 1-10 μm size range to be 1.5%. Overall collection efficiency is higher as particles in this range are a small fraction of overall particulate.

7. Task 4: Detection

In this task, collected particulate matter underwent rigorous analysis to validate identities obtained by APICD Gen I device and other methods in Task 3 and by APICD Gen II device in Task 2.4. APICD results were confirmed by laboratory analysis conducted by trained ChemImage scientists.

We analyzed a part of the summer collection at NETL. Witness sample of Run 1 on an aluminum-covered slide was analyzed to determine fluorescence particle fraction (**Figure 40**). This sample is an aluminum-covered slide that was exposed to the ambient PM during Run 1 of summer collection. This witness sample is being analyzed to correlate gravity-deposited PM with the ambient concentration of PM collected by the Dekati collector at NETL. The initial step is the estimation of particle size distribution and the relative fraction of fluorescent particles

Ambient PM collected by the Dekati collector at NETL was analyzed to determine fluorescence fraction to correlate both sets of data. A 5x5 BFR and FLI montage was collected for stages 6, 8, 10, and 12 of the APTA Dekati Outdoor Collection Sample. For stages 6 and 8, the 100x objective was used to collect the BFR and FLI montages, and a 20x microscope objective was used for the remaining stages. Manual counting was performed for both BFR and FLI montages. The average fluorescence fraction of summer 2007 collection collected by the Dekati apparatus was 12%.

8. Task 5: Signature Database

8.1. Continue development of the Ambient PM signature library

Characterization and database coverage of both biothreat and interferent materials is critical to robust operation of detectors in real environments. ChemImage has a substantial experience with the efficient collection of biothreat signatures which are arranged into a Raman Chemical Imaging biothreat database. This biothreat database and underlying analysis software have been shown to be effective in the detection of biothreats in complex mixtures.

The APTA Project conducted a qualitative and quantitative analysis of airborne PM including background interferents such as pollen, insecticides and industrial particulate matter. Interferents causing possible false positives for Raman-based detection were identified and studied. ChemImage uses ChemDB, a database developed to manage signature libraries developed in support of biomedical and biodetection projects. ChemDB database includes 1059 entries, consisting of threat agents, near neighbors and common interferents (**Figure 2**). 413 entries were liquids or other materials that were unlikely to be found in particulate matter so they were omitted and the database was reclassified. A review of the database classification indicated insufficient population of the pollen and fungi categories that comprise a large part of coarse suspended matter and are ubiquitous in the environment. Audit of the CI Bioagent library to determine its taxonomy and applicability to ambient PM detection revealed 20 out of 82 major PM constituents were present in CI/AFIP library. During the APTA Project, an additional 22 materials were characterized using the following methods:

Primary Methods:

- Brightfield reflectance

- Polarized Light Microscopy
- Differential Contrast Microscopy
- Fluorescence Light Microscopy
- Dispersive Raman microspectroscopy

Secondary Methods:

- Fluorescent Chemical imaging
- Fourier Transform Infrared microspectroscopy
- Raman Chemical Imaging
- Near Infrared Chemical Imaging
- Scanning electron microscopy (SEM) with X-ray fluorescence energy dispersive spectroscopy (EDS)

As Raman spectroscopy is the basis for a searchable library of signatures, particular attention was paid to collection of reference quality Raman spectra. Due to the complex nature and variability of components comprising particulate matter, each reference sample was characterized by 10 Raman spectra taken at different areas of the bulk sample.

As part of Task 5, ChemImage has initiated a harmonization of the Raman Spectral Library with developing guidelines being formulated for the evaluation and testing of bioagent detectors. We have cross-referenced the Raman Signature Database against the developing guidelines. The terms *inclusivity* or *sensitivity* describe the ability of a detection method to detect the target analyte from a wide range of strains. *Exclusivity* or *specificity* is the lack of interference in a detection method from a relevant range of nontarget strains, which are potentially cross-reactive. **Table 7** represents an analysis of inclusive and exclusive biological agents currently in the library. **Table 8** represents an analysis of various environmental interferents currently in the library.

Table 7. Inclusive and Exclusive Biological Agents.

Inclusivity	***In Library?***		***Exclusivity***	***In Library?***
Bacillus anthracis Canadian bison	X		*B. cereus* G9241	X
Bacillus anthracis V770-NP-1R	X		*B. thuringiensis* subsp. *Israelensis*	X
Bacillus anthracis PAK-1	X		*B. thuringiensis* subsp. *kurstaki*	X
Bacillus anthracis BA1015	X		*B. mycoides*	X
Bacillus anthracis Ames	X		*B. megaterium*	X
Bacillus anthracis SK-102 (Pakistan)	X			
Bacillus anthracis Vollum 1B	X			
Bacillus anthracis BA1035	X			
Bacillus anthracis RA3	X			
Bacillus anthracis Pasteur	X			
Bacillus anthracis Sterne	X			
Bacillus anthracis Turkey #32	X			

Table 8. Environmental Interferants.

Environmental Interferant	In library?
Additional Biothreats	
Bacillus anthracis Ames	X
Yersinia pestis Colorado-92	X
Francisella tularensis subsp. tularensis Schu-S4	X
Burholderia pseudomallei	X
Brucella melitensis	X
Ricinus communis	X
Clostridium botulinum Type A Hall Strain	X (not sure of strain)
Cultivatable Bacteria	
Acinetobacter lwoffii	X
Bacillus megaterium	X
Burkholderia cepacia	X
Deinococcus radiodurans	X
Escherichia coli K12	X
Neisseria lactamica	X
Pseudomonas aeruginosa	X
Staphylococcus aureus	X
Stenotophomonas maltophilia	X
Streptococcus pneumoniae	X
Vibrio cholerae	X
Listeria monocytogenes	X
Microbial Eukaryotes (Fungi)	
Alternaria alternata	X
Aspergillus penicilloides change to fumigatis	(terreus)
Aureobasidium pullulans	X
Cladosporium cladosporioides	X
Cladosporium sphaerospermum	X
Epicoccum nigrum	X
Penicillum chrysogenum	X
Higher Eukaryotes (Plants)	
Pollen from Pinus spp. (pine)	X
Cotton	X
Homo sapiens(HeLa) human	X
Biological Insecticides	
B. thuringiensis subsp. israelensis	X
B. thuringiensis subsp. kurstaki	X
Powders and Chemicals	
Bacillus thuringiensis powders (e.g., Dipel)	X
Powdered milk	X
Powdered coffee creamer	X
Powdered sugar	X
Talcum powder	X
Flour	X
Baking soda	X
Chalk dust	X
Dry wall dust	X
Cornstarch	X
Baking powder	X

GABA (Gama aminobutyric acid)	X
L-Glutamic acid	X
Kaolin	X
Chitin (n-acetylglucosamine)	X
Chitosan	X
$MgSO_4$	X
Boric Acid	X
Popcorn salt	X

8.2. Improve algorithms for autonomous operation and decision-making

ChemImage is improving algorithms for autonomous data acquisition and developing decision-making methods for better fitting between target spectra and signature libraries.

Figure 41 describes the detection sequence for PM collection, analysis and identification. Aqueous solution of 5 μm polystyrene microspheres (PSMS) was placed in a metered dose pump spray bottle. The dispenser was primed 5 times and dispersed 25 sprays of PSMS solution in the vicinity of the collector. Ambient PM was collected for 60 min on a previously regenerated post. The post was placed into the detection position and was screened for the presence of PSMS among PM. Brightfield reflectance (BFR) and total fluorescence (FLI) linear montages were collected at 20x with automated focusing between the frames to compensate for surface roughness of the collection post. An automated targeting algorithm analyzed size, shape and brightness of fluorescence montages and selected two sub-frames containing maximum amount of targets. A list containing positions of the identified targets is generated for subsequent analysis at 100x. After manual switch to a 100x microscope objective and centering the object in the FOV, the automated acquisition software brings the object into focus, takes a BFR and FLI images, and switches to the Raman mode. In Raman mode, the software function monitors photobleaching using a pre-set 5% change threshold, and upon reaching the target threshold snaps a spectral image using a pre-set time. The spectral image is automatically converted into 19 Raman spectra corresponding to each fiber and each spectrum is classified. The final results of identification are displayed as a table of the top three matches.

Currently ChemImage software and application group efforts were directed toward further improvement of system control and decision-making software algorithms such as:

1) *Autofocus*

Ability of APICD Gen I to focus was demonstrated previously for 20x and 100x microscope objectives. Automated focusing in BFR mode precedes all APICD measurements in fluorescence mode. The current focusing algorithm uses a Step-Scan method based on monitoring sharpness of the video image while changing the z-position of the sample. The maximum sharpness position is considered the focal plane position. Step size and number of steps are flexible and can accommodate different magnifications.

ChemImage has developed a faster auto-focusing method which uses a Rapid Scan technique for coarse focusing and Successive Approximation method for fine focusing. Rapid Scan allows stage movement while acquiring a stack of images and processes them in the background. This approach works well for finding the analysis surface at low magnification. The Successive Approximation Method is used for fine focusing to find the frame with the maximum sharpness. It is similar to the Step-Scan approach but changes direction and reduced step size based on the sharpness differential.

2) *Automated Targeting*

The APICD Targeting User Function analyzes size, shape and brightness of particle in total fluorescence montage collected at 20x. A ranked list containing positions of the identified targets is generated for subsequent analysis at 100x.

Several changes were made to the *Targeting* algorithm. In the new version, each frame in the montage is flat-fielded after conversion to a gray-scale image. An intensity threshold is applied to the background corrected image to generate a binary image. In the binary images, particles are analyzed by size (Maximum Chord) and shape to eliminate specific sizes and shapes. The remaining targets are ranked according to their similarity to an "ideal threat". A ranked list of targets is generated and loaded into the *AutoID* function for further analysis at 100x. This list can be saved and loaded separately **(Figure 42).**

A statistical model was developed to describe the targeting performance of APICD Gen I. A witness sample on Al slide for 1-hr indoor collection (March 07, 2007) spiked with polystyrene microspheres (PSMS) was used to test algorithm performance. Single 5 μm polystyrene spheres served as the analyte of interest. Manual counting and identification were used as gold standard method to correctly identify events. Three runs were carried out and the targeting results are shown in **Figures 43-44.** Targeting sensitivity and specificity for PSMS are above 90% with low false positives and false negatives rates as seen in **Figure 45**.

An additional option for targeting in brightfield reflectance mode was also developed and tested.

3) *Automated Acquisition and Identification Functions*

Automated Acquisition software allows user-free collection of focal plane images of Raman signals from multiple targets, comparison of resulting Raman spectra to the library, and displaying target identity in the form of a confusion matrix.

After a manual switch to a 100x microscope objective, *Automated Acquisition* brings the target into focus, centers the object in the FOV (new function), and takes BFR and FLI images. After switching to Raman mode, the software photobleaches the sample and snaps a spectral image using a pre-set time. The spectral image is automatically converted into 19 Raman spectra corresponding to each sampling fiber, which are run against the library using Mahalanobis distance. The final results of identification are displayed as a Mahalanobis Statistics matrix of top three matches. Images and spectra generated during the targeting and identification are automatically saved under standardized names reflecting target rank.

Initially, photobleaching time (PBT) varied based on the percent change in the fluorescence and a flexible acquisition time based on preset SNR. This approach was found inefficient, particularly with highly fluorescent samples. The current algorithm has added the ability to pre-set photobleaching and exposure times. PBT of 10-15 sec and exposure of 10 sec at 3 kW/cm^2 power density at the sample usually results in a reasonably good Raman signal from the test samples. A statistical model was developed to describe the identification performance of APICD Gen I. Targets obtained from a witness sample from a 1-hr indoor collection (March 07, 2007) spiked with 5 μm PSMS was used to test algorithm performance.

Raman identification was carried out in the automated mode using Mahalanobis Distance identifier with 5 Principal components in 800-1800 and 2800-3200 cm^{-1} spectral ranges. The model was based on the library containing 4 classes (aluminum, polystyrene, Bt and Bg). APICD Identification had perfect specificity (100%) rejecting non-polystyrene particles with no False Positives. Three runs were carried out and the results for each run and the summary of runs are shown in **Figure 46.** The system sensitivity was ~30%. Insufficient SNR and baseline correction along with focusing failure at 100x contributed to the false negative rate.

4) Data Logger

ChemImage is developing a data logger to display APICD Gen II results. In APICD Gen II the collector drum would rotate, presenting a narrow strip of deposited particulate to the detector. The data logger would keep track of: particles in the respirable range; fluorescence particles in the respirable range, and threat probability as a function of time. As the cumulative threat probability reaches a set threshold, The APICD software would trigger an alarm.

ChemImage exploited APICD Gen I data to develop a data-logging concept to assist the software team. Bt on Al slide deposited by inkjet aerosol generator in 5 μm clusters was used to represent threat PM. Three random areas of the sample were arbitrarily chosen undergo analysis. A data logger was

constructed in Excel to display respirable particles, for fluorescence respirable particles, and threat probability (**Figure 47**).

5) Time Logger

Time Logger was developed to monitor the timing of APICD Gen I subsystems and how long each *Auto Acquisition* process takes. The output is stored as a text file for each particle. Each run has a summary of the total experimental time of the run, time spent on the Raman portion of the run and average Raman experimental time, including photobleaching and exposure times, per target.

6) Spectral Calibration

Correct identification of biothreat agents is highly dependent on good spectral calibration of the spectrometer. The APICD Gen I device uses Fiber Array Spectral Translation (FAST) technology to obtain spatially resolved 19 Raman Spectra. The routine for spectral image calibration uses an average spectrum of acetaminophen standard. While such an approach may result in adequate calibration of the 19-fiber system, APICD Gen II will use 80+ fibers for better spatial resolution. Misalignment of 80+ fibers with detector pixels can results in a systematic shift of peaks in the resulting spectra. Anticipating Gen II development, ChemImage software team developed an algorithm for individual calibration of each FAST fiber.

8.3. Enhance System Performance Model

ChemImage prepared a Particle Accounting Model (PAM) model for electrostatic collector to test feasibility of PM detection. PAM is a useful exercise based on the efficiency estimate for every stage of the collection and detection process for electrostatic collection coupled with Raman detection which allows us to evaluate the feasibility of system use in field conditions.

APICD Gen II Particle Accounting model was updated based on the experimental collection and cleaning efficiencies obtained by Sceptor and ChemImage. We also utilized experimentally measured average fluorescence fraction of 12% for summer 2007 collection (Task 4.1). Independent investigation allowed for a better estimate of the time necessary for FCI targeting based on the reduced number of frames and faster frame rate. The updated model based on these experimental parameters **(Figures 48-51)** was used to calculate time to alarm of 14 minutes for 10% BT concentration (**Figures 52-54**).

9. Conclusions

The ChemImage team collected and reviewed a body of scientific papers in order to develop the APTA Project knowledge base. Based on the literature review, we proposed a novel particulate material (PM) taxonomy based on the underlying chemical structure of PM constituents. In addition, we developed a quantitative model for outdoor PM composition. PM components are broadly grouped into inorganic and organic fraction. The inorganic contribution includes mineral dust, sea salt, and secondary aerosols and can contribute from 6 to 95% to the mass of total suspended particulate (TSP). The organic contribution describes carbon-based particulate of various origins and may vary 2.6 to 75.5% of TSP, with an average value of 33.5%. Airborne microorganisms contribute ~15% to ambient PM mass on average, with PM bioloading ranging from 0.2% to 32.5%.

As part of the APTA project, in the Spring and Summer of 2007, 16 aerosol collections were carried out. The Summer 2007 collections were carried out at NETL in order to make use of the NETL PM monitoring instruments for validation of the APICD collector. The APICD Collector successfully operated in both automatic and semiautomatic modes. Multiple samples were collected to enable evaluation of particle density, composition and APICD collection efficiency for particles in the 1-10 µm size range.

In Phase 2, efforts to develop a database of reference materials specific to airborne Particulate Matter involved harmonization with developing bioagent test guidelines.

Finally, emphasis was placed during Phase 2 on the development and validation of subsystems appropriate for future automated Raman bioaerosol monitors. These development efforts have been

successful, and validate the APICD design as a credible, future potential technology area for continuous, reagentless PM monitoring and identification in complex aerosols.

10. List of Figures

49. Task 5 Particle Accounting Model-1
50. Task 5 Particle accounting Model-2
51. Task 5 APICD Gen II Performance Compared for 3 Scenarios
52. Task 5 Time to Alarm Model for 9% Biothreat in PM
53. Task 5 Time to Alarm Model for 50% Biothreat in PM
54. Task 5 BT "Threat" Detection Simulation

11. References

[1] Tegen I, Fung I. Contribution To The Atmospheric Mineral Aerosol Load From Land Surface Modification, *Journal of Geophysical Research*, **1995**, *100 (18),* 707-18,726.

[2] Batonneau Y, Sobanska S, Laureyns J, Bremard C. Confocal Microprobe Raman Imaging of Urban Tropospheric Aerosol Particles, Submitted to *Environmental Science & Technology,* **2005**.

[3] Air Quality Expert Group. *Particulate Matter in the United Kingdom*. 2nd Report. **2005.** This document is at: http://www.defra.gov.uk/environment/airquality/aqeg/particulate-matter/index.htm

[4] Kim E, Hopke PK, Edgerton ES. Source identification of Atlanta aerosol by positive matrix identification, *The Journal of the Air & Waste Management Association,* **2003**, *53*, 731-739.

[5] Lim HJ, Turpin BJ. Origins of primary and secondary organic aerosol in Atlanta. *Environmental Science & Technology,* **2002***, 36*, 4489-4496.

[6] Solomon P, et al. Overview of the 1999 Atlanta Supersite project. *Journal of Geophysical Research*, **2003**, *108 (D7),* 8413.

[7] Seinfeld JH, Pandis SN. Atmospheric Chemistry and physics: From air pollution to climate change, **1998**, John Wiley, New York, 724-727.

[8] Bauer H, Kasper-Giebl A, Loflund M, Giebl H, Hitzenberger R, Zibuschka F, Puxbaum H. The contribution of bacteria and fungal spores to the organic carbon content of cloud water, precipitation and aerosols. *Atmospheric Research*, **2002**, *64*, 109-119.

[9] Matthias-Maser S, Jaenicke R. The Size Distribution Of Primary Biological Aerosol Particles With Radii >0.2 μM In An Urban-Rural Influenced Region. *Atmospheric Research,* **1995**, *39*, 279-286.

[10] Menetrez MY, Foarde KK, Ensor DS. An Analytical Method for the Measurement of Non-Viable Bioaerosols. *J. Air & Waste Manage. Assoc.*, **2001**, *51*, 1436-1442.

[11] ACGIH. Step two: On-site investigation, pp. 1-8; Fungi, pp. 1-10; Bacteria, pp. 1-7. Committee on Bioaerosols, eds. In *Guidelines for the Assessment of Bioaerosols in the Indoor Environment*. American Conference of Governmental Industrial Hygienists, Cincinnati, OH, **1989**.

[12] Adhikari A, et al. Correlation of ambient inhalable bioaerosols with particulate matter and ozone: A two-year study. *Environmental Pollution*, **2006**, *140*, 16-28.

[13] Bauer H, Kasper-Giebl A, Zibuschka F, Hitzenberger R, Kraus G, Puxbaum H. Determination of the carbon content of airborne fungal spores. *Analytical Chemistry*, **2002**, *74*(1), 91-5.

[14] Reponen T, Nevalainen A, Jantunen M, PelikkaM, Kalliokoski P. Normal Range Criteria for Indoor Air Bacteria and Fungal Spores in a Subarctic Climate. *Indoor Air*, **1992**, *2*, 26-31.

[15] Rao, CY, Burge H, Chang JS. Review of quantitative standards and guidelines for fungi in indoor air. *J. Air Waste Man. Assoc*., **1996**, *46*, 899-908.

[16] Reynolds SJ, et al. Indoor Environmental Quality in Six Commercial Office Buildings in the Midwest United States. *Applied Occupational and Environmental Hygiene*, **2001**, *16*(11), 1065–1077.

[17] McGinnis M. Relationship Between Moulds and Health. **2002** This presentation is at: http://www.doctorfungus.org/lecture/environ.htm

[18] Womiloju TO, Miller JD, Mayer PM, Brook JR. Methods to determine the biological composition of particulate matter collected from outdoor air. *Atmospheric Environment*, **2003,** *37*, 4335-4344.

[19] Tsai FC, JM Macher JM, Y-Y Hung Y-Y. CONCENTRATIONS OF AIRBORNE BACTERIA IN 100 U.S. OFFICE BUILDINGS. *Indoor Air*, **2002**, 353-358.

Task 1 Classification of Ambient Particulate Matter

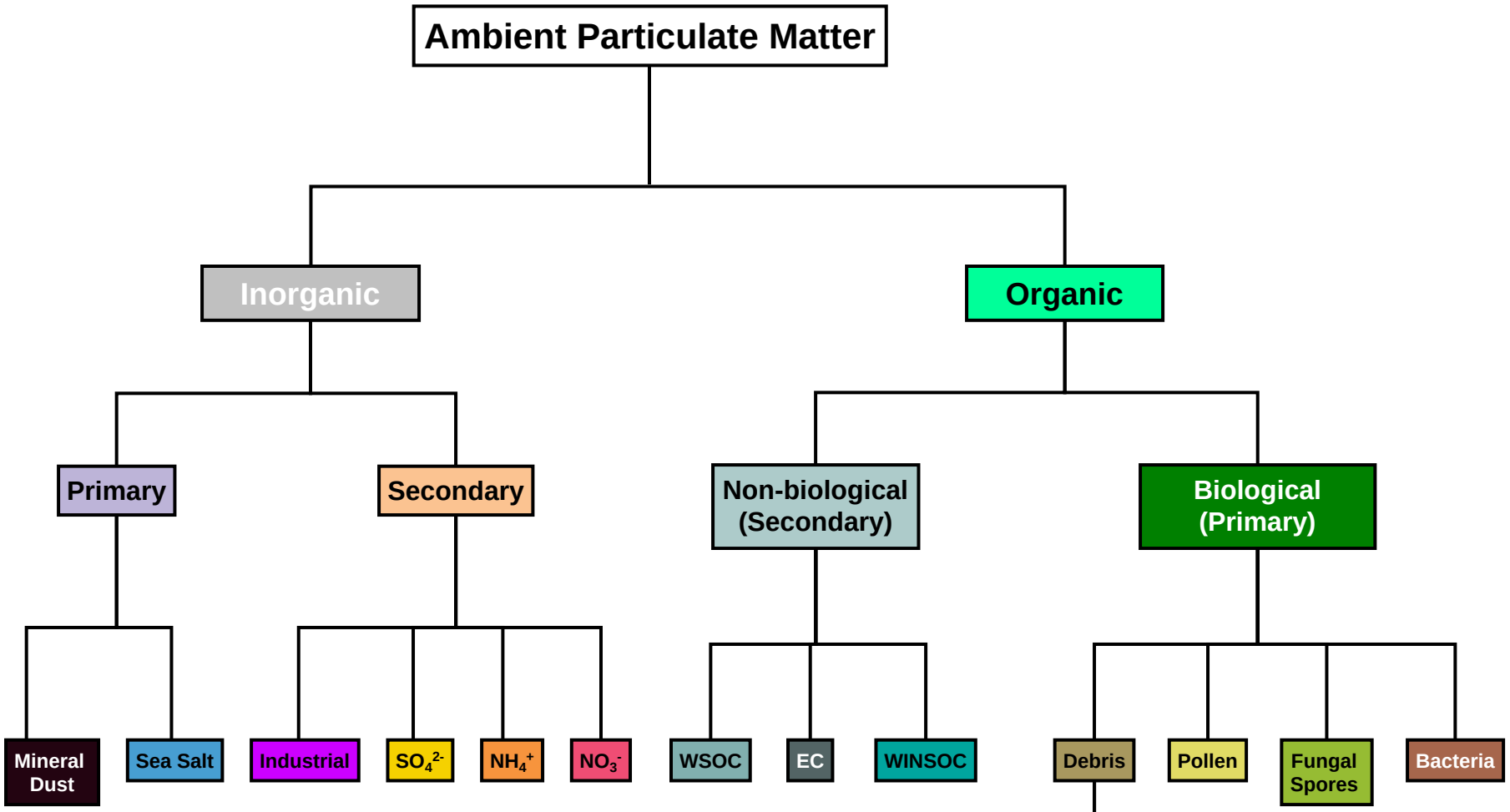

EC– Elemental Carbon
WSOC – Water-soluble Organic Carbon
WINSOC – Water-insoluble Organic Carbon
Debris - Plant and insect parts, Skin flakes, Dander

ChemImage™

Task 1 Raman Signature Library Taxonomy

1059 entries (Pathogens, CWA, Explosives, TICs, TIMs, simulants and interferents)

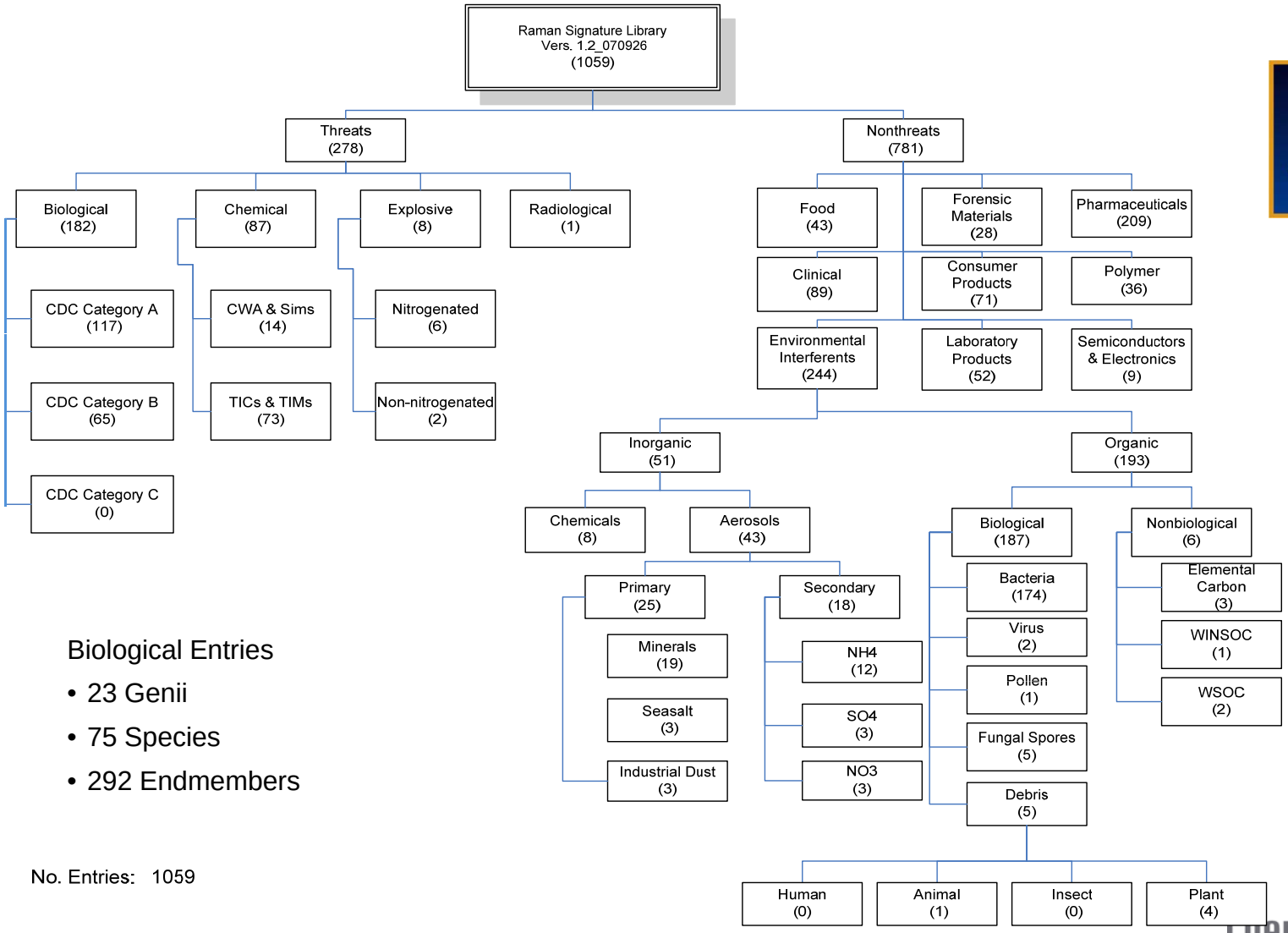

Biological Entries

- 23 Genii
- 75 Species
- 292 Endmembers

No. Entries: 1059

Task 2 APICD Gen I Assembly

Micron/pixel Resolution	APICD Gen I
Video Camera at 20x	0.48
Video Camera at 100x	0.10
FCI Camera at 20x	0.24
FCI Camera at 100x	0.05

Status:

- Fabrication of APICD Gen I system is complete
- Initial performance evaluations are complete
- Gen I enables evaluation of :
  - ESTAT collector performance
  - Detector autonomy (autofocus; autotarget, autoID)
  - Performance models
  - Need for bio-enrichment
  - Manual surface cleaning procedure (as a precursor to the automated procedure)
- Performance evaluation drives APICD Gen II design

Task 2 APICD System Using Headwall Spectrometer

FAST Spectra of 10 μm PSMS at 20x on Headwall

BFR

FLI

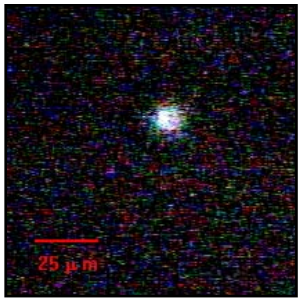

FAST at 1000 cm^{-1}

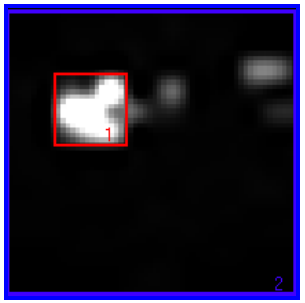

Bias, NIST, Bsln, Normalized, Expanded

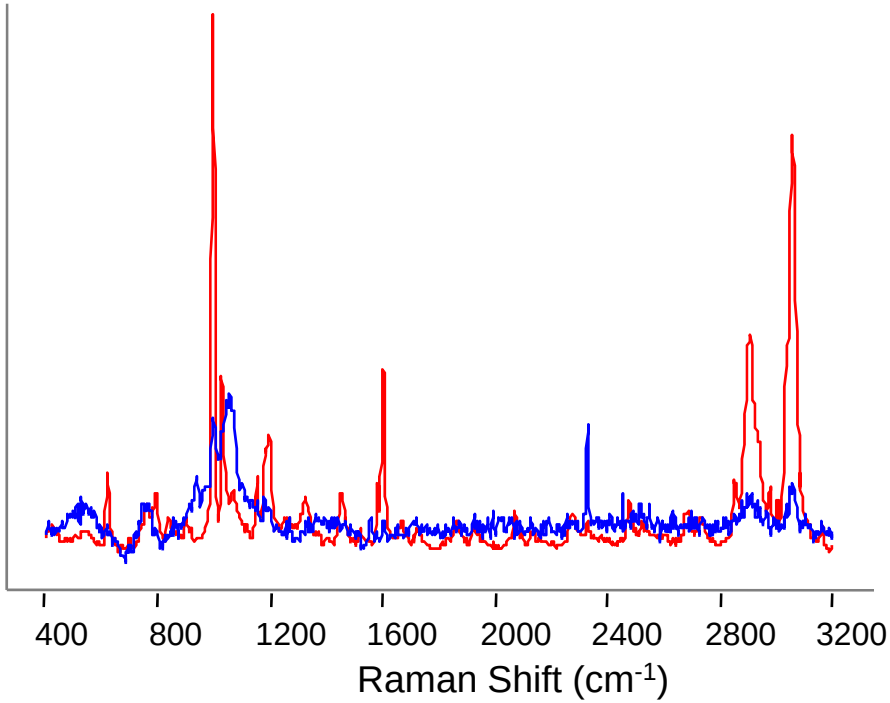

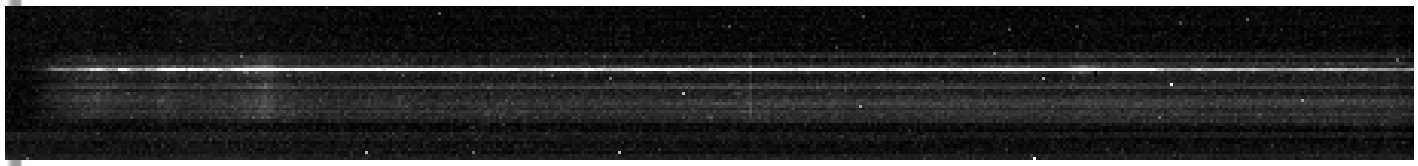

ChemImage™

Task 2 Characterization of APICD Imaging Performance at 20x

BFR montage

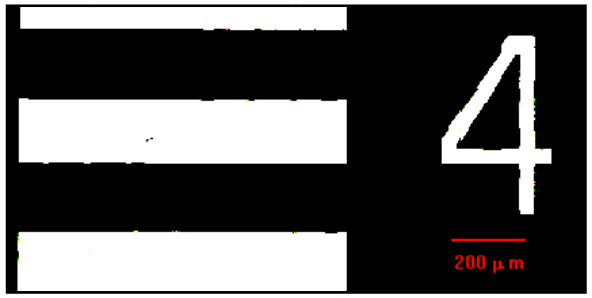

FAST montage at 3500 cm^{-1}

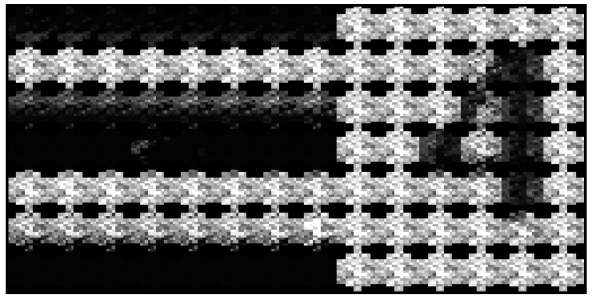

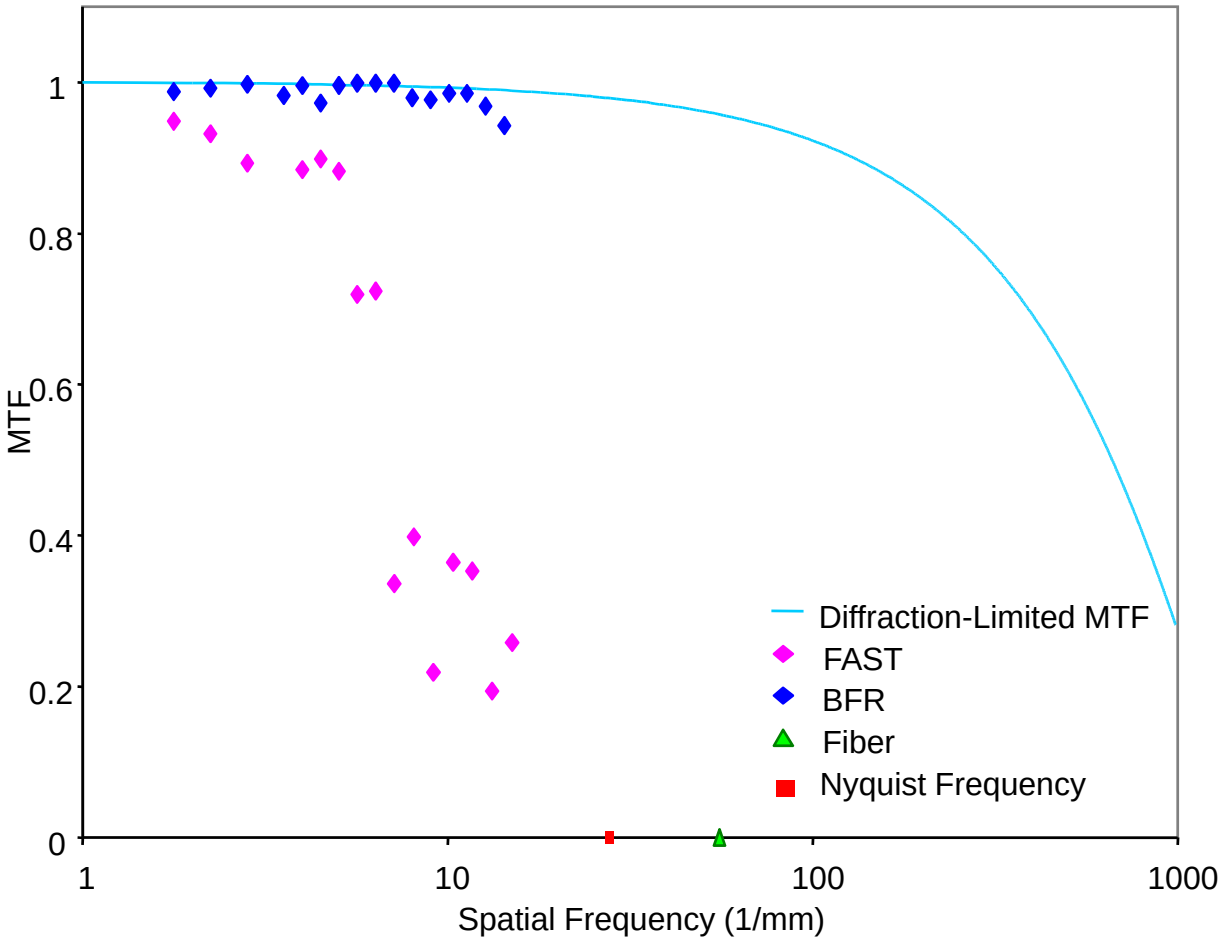

ChemImage™

Task 2 APICD Gen I Discrimination Performance at 100x

3 classes, 800-1800 cm^{-1}, 5 PC

Clean post

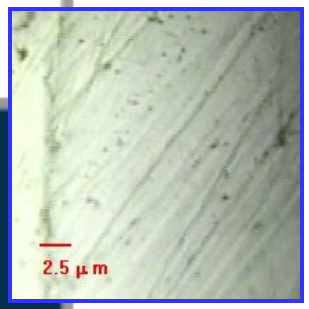

5 µm PSMS

Background PM

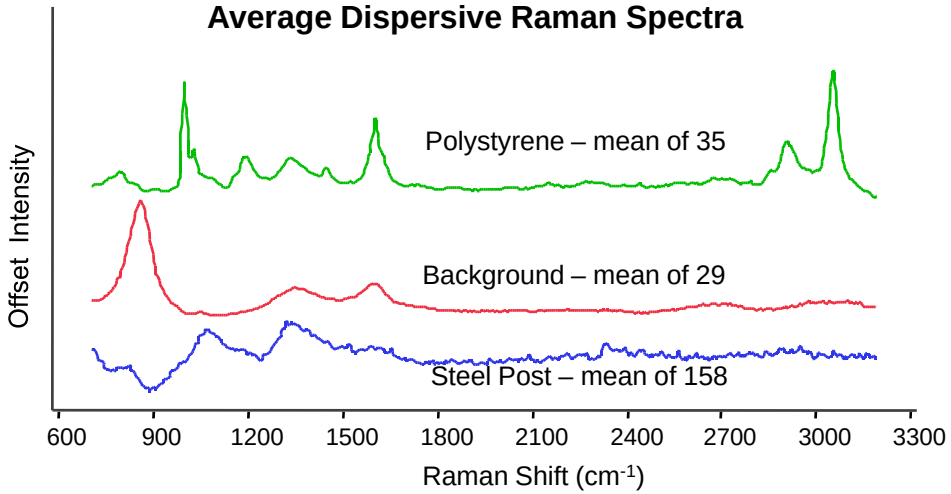

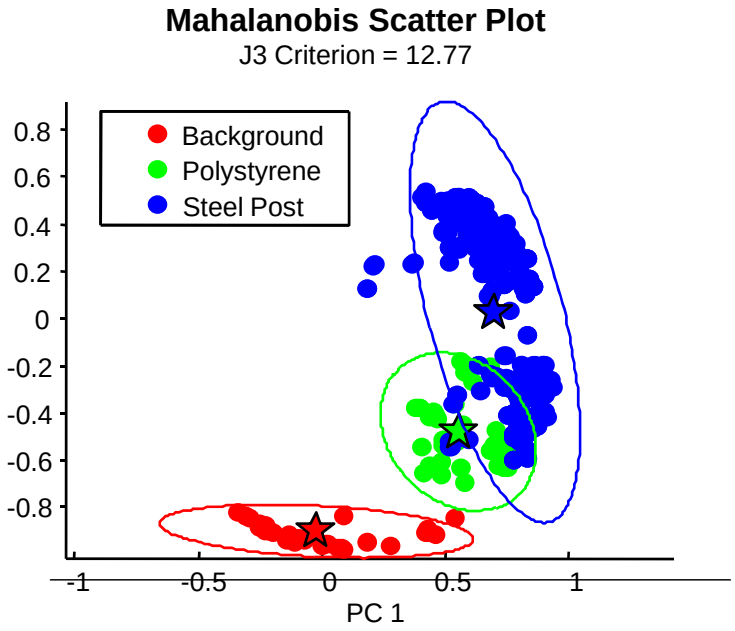

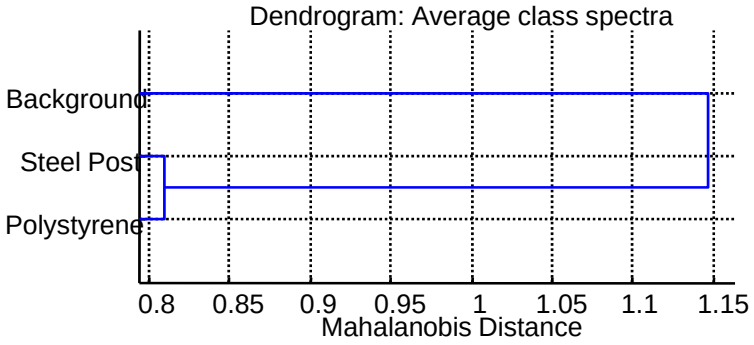

	Background	Polystyrene	Steel Post
Background	100.00	0	0
Polystyrene	0	100.00	0
Steel Post	0	0	100.00

Misclassification Rate: 0.00 %

ChemImage™

Task 2 Design Concept For APICD Gen II.

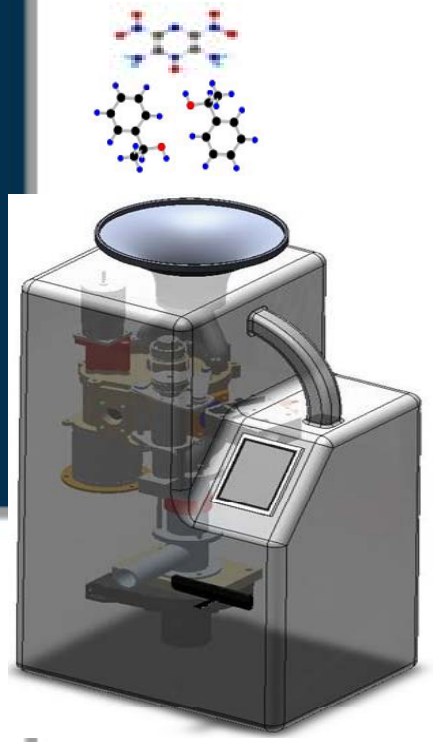

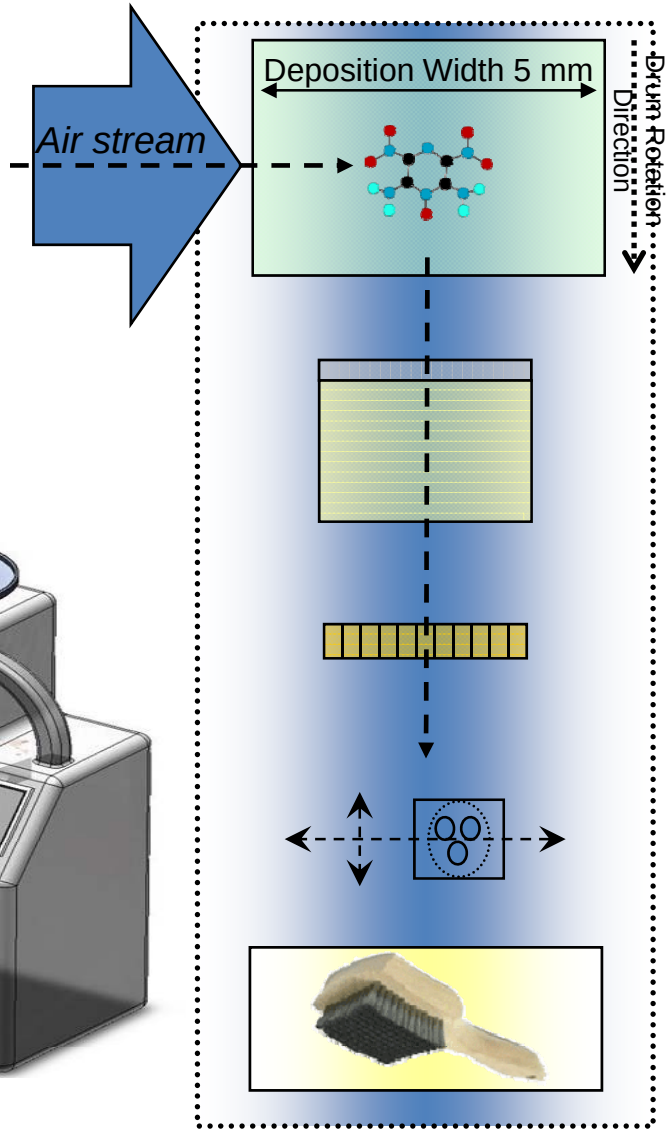

1 *Deposition Zone*

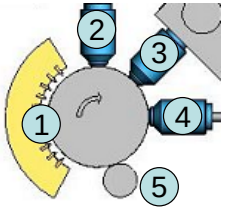

2 3 *Targeting*

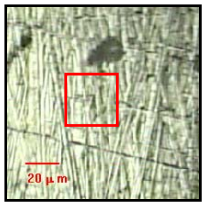

Fluorescence Spectral Cube

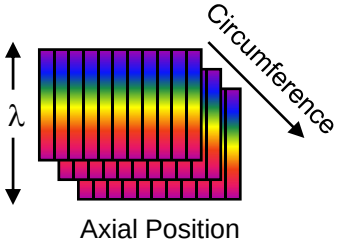

4 *FAST Raman Spectra*

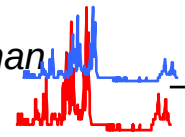

Library Search → Identified Threat

5 *Surface Regeneration*

ChemImage™

Task 2 APICD Gen II Concept Layout

Targeting – 2D Imaging
- •White Light (Bright field)
- •Total Fluorescence

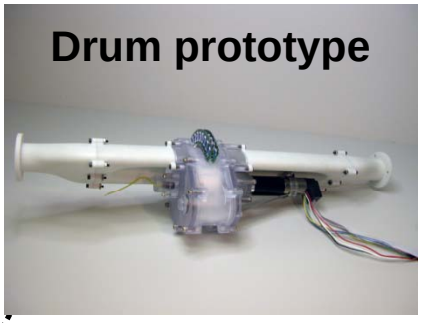

Drum Diameter = 3 in
Rotation Speed = 1- 500 RPM
Stepper motor driven

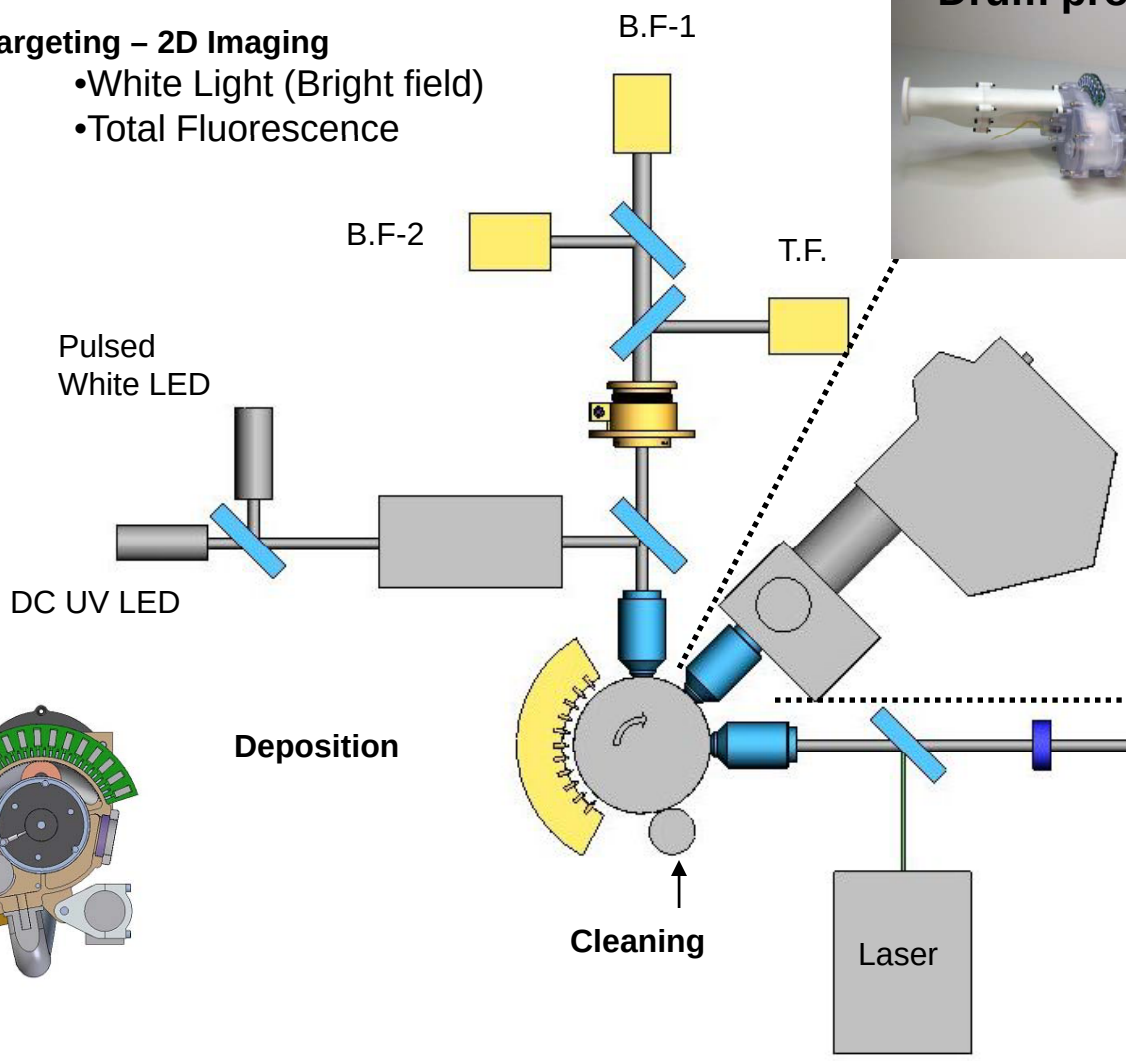

Targeting - Fluorescence Spectral Imaging

Raman Detection
(RBI/Polly-like with higher NA objective)

ChemImage™

Task 2 APICD Evolution

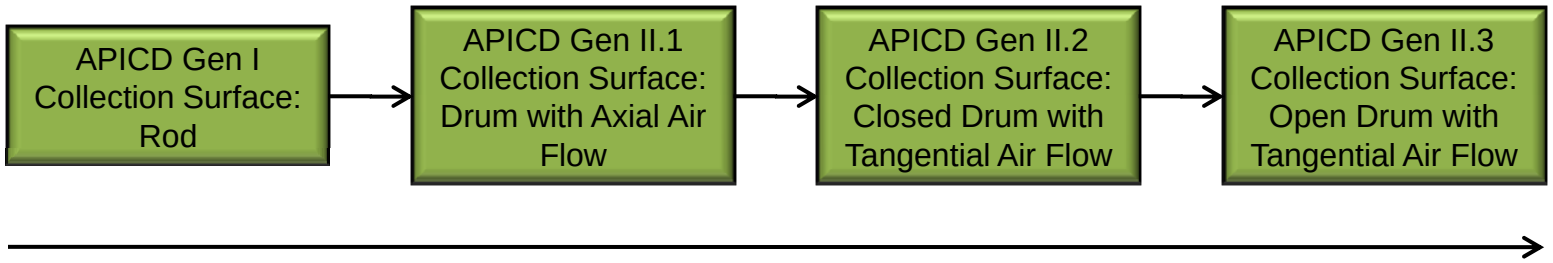

Phase 1	Phase II O4	Phase II O6	Phase II O7
In house	In house	In house	CDR 4/22/08
			Under construction

Requirements:

- Optimized collection efficiency and deposition pattern
- >145° free access to drum
- Positional Accuracy and Feedback
  - Thor Labs motor and GPI Encoder
- Replaceable drum surface
- "GOOD" surface regeneration and dis-engagable brush
- Particulate Load Monitoring
- All-Weather Operation (100% non-condensing humidity)

ChemImage™

Task 2 Deposition Pattern of PM

Obtained on APICD Gen I and APICD Gen II drum prototype

Weekend Collection September 28 – October 1, 2007

APICD Gen I Deposition

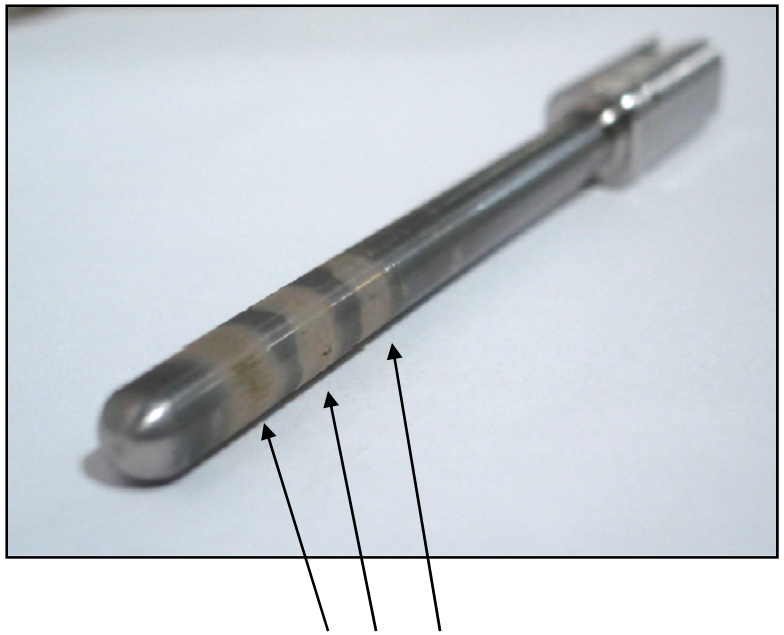

APICD Gen II Deposition

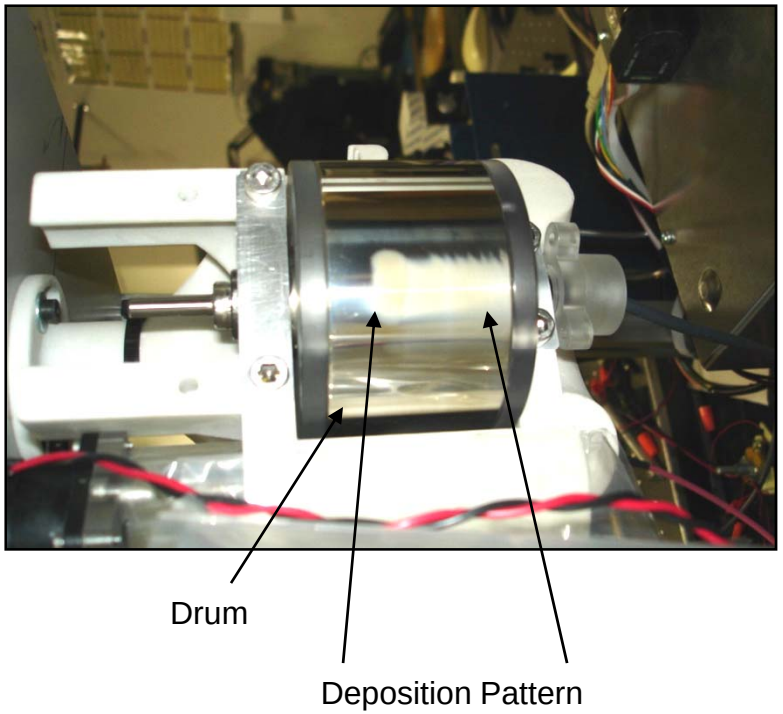

ChemImage™

Task 2 Model and a Prototype of a Tangential Flow Collector

- Requirements:
- Optimized collection efficiency and deposition pattern
- >145° free access to drum
- Positional Accuracy and Feedback
  - Thor Labs motor and GPI Encoder
- Replaceable drum surface
- "GOOD" surface regeneration and disengagable brush
- Particulate Load Monitoring
- All-Weather Operation (100% non-condensing humidity)

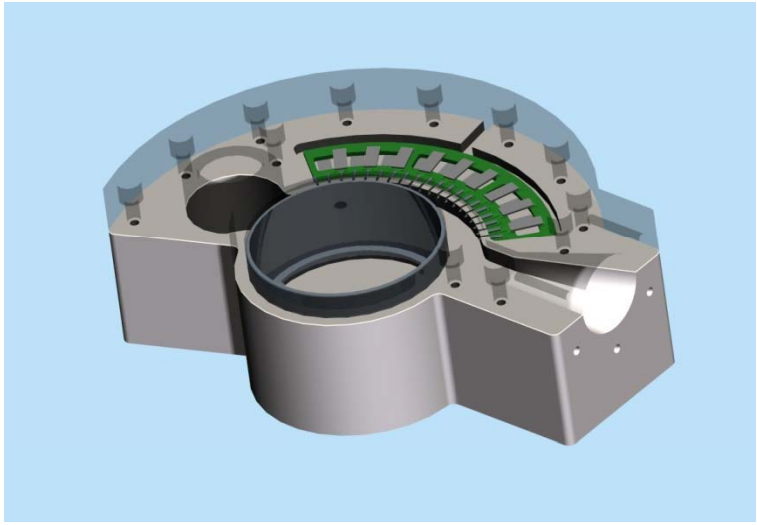

CAD model with transparent cover plate showing electrode region and collection zone.

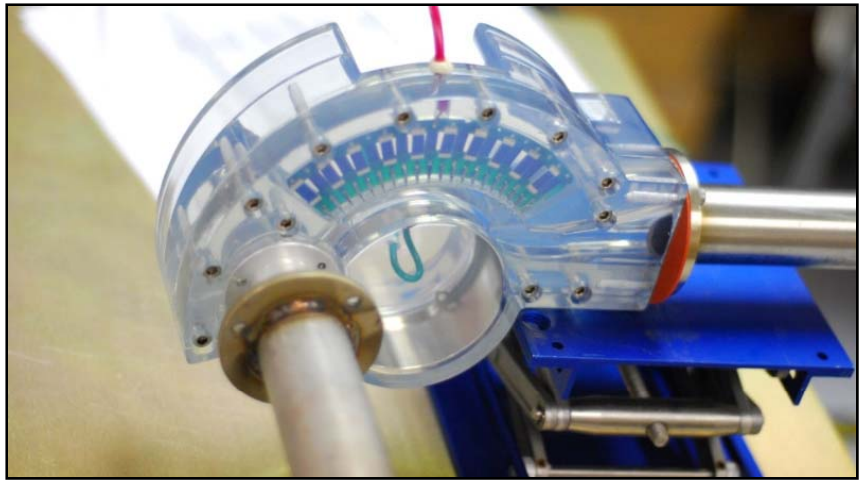

ChemImage™

Task 2 Finalized Engineering Design for APICD Gen II with Tangential Flow

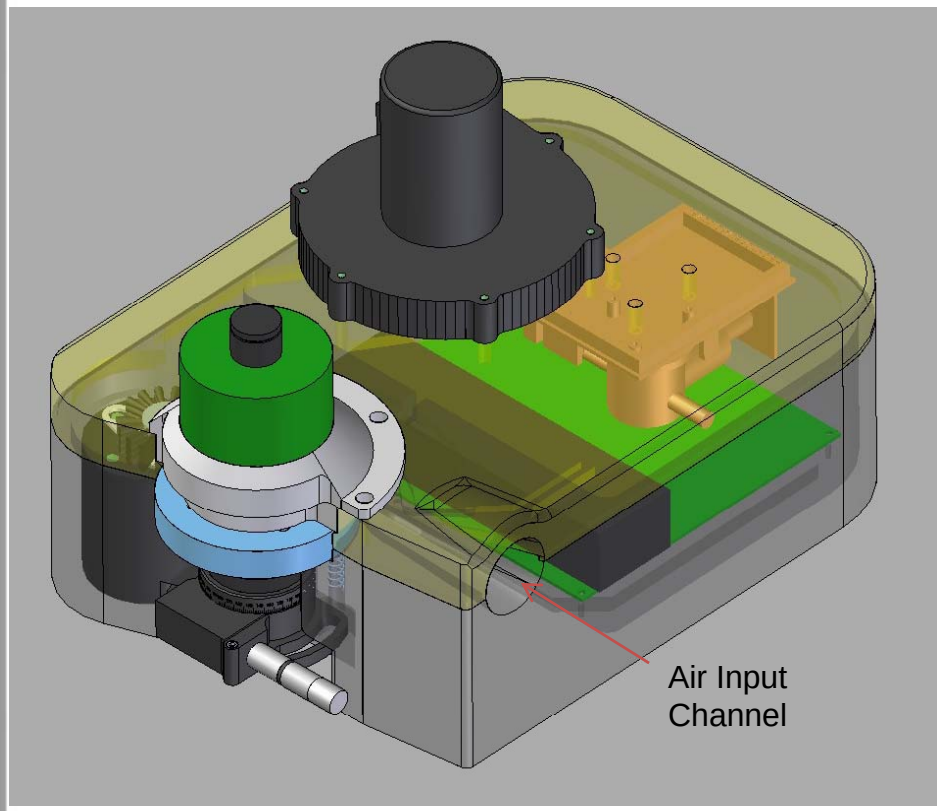

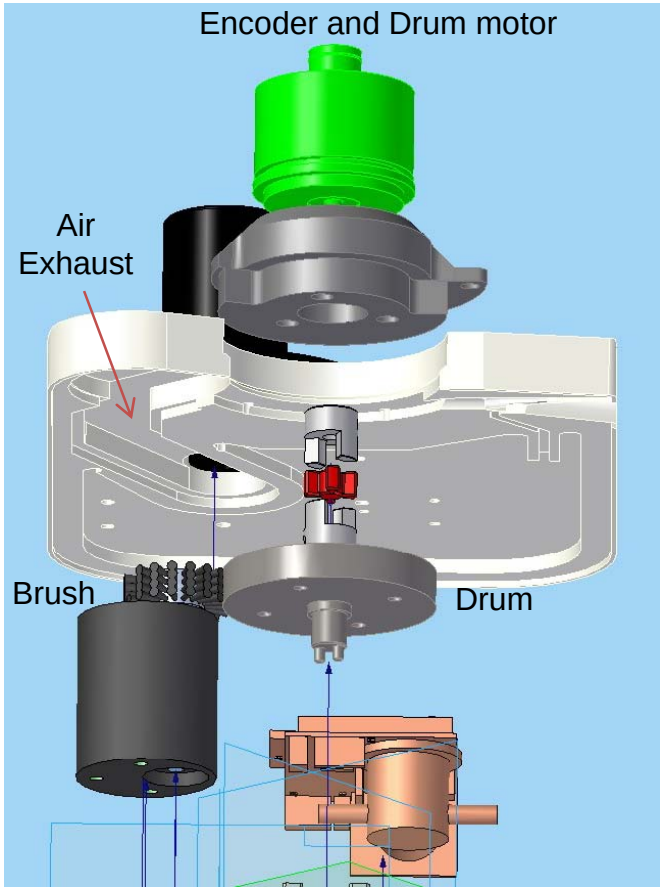

ChemImage™

Task 2 Finished Tangential Flow Unit 1

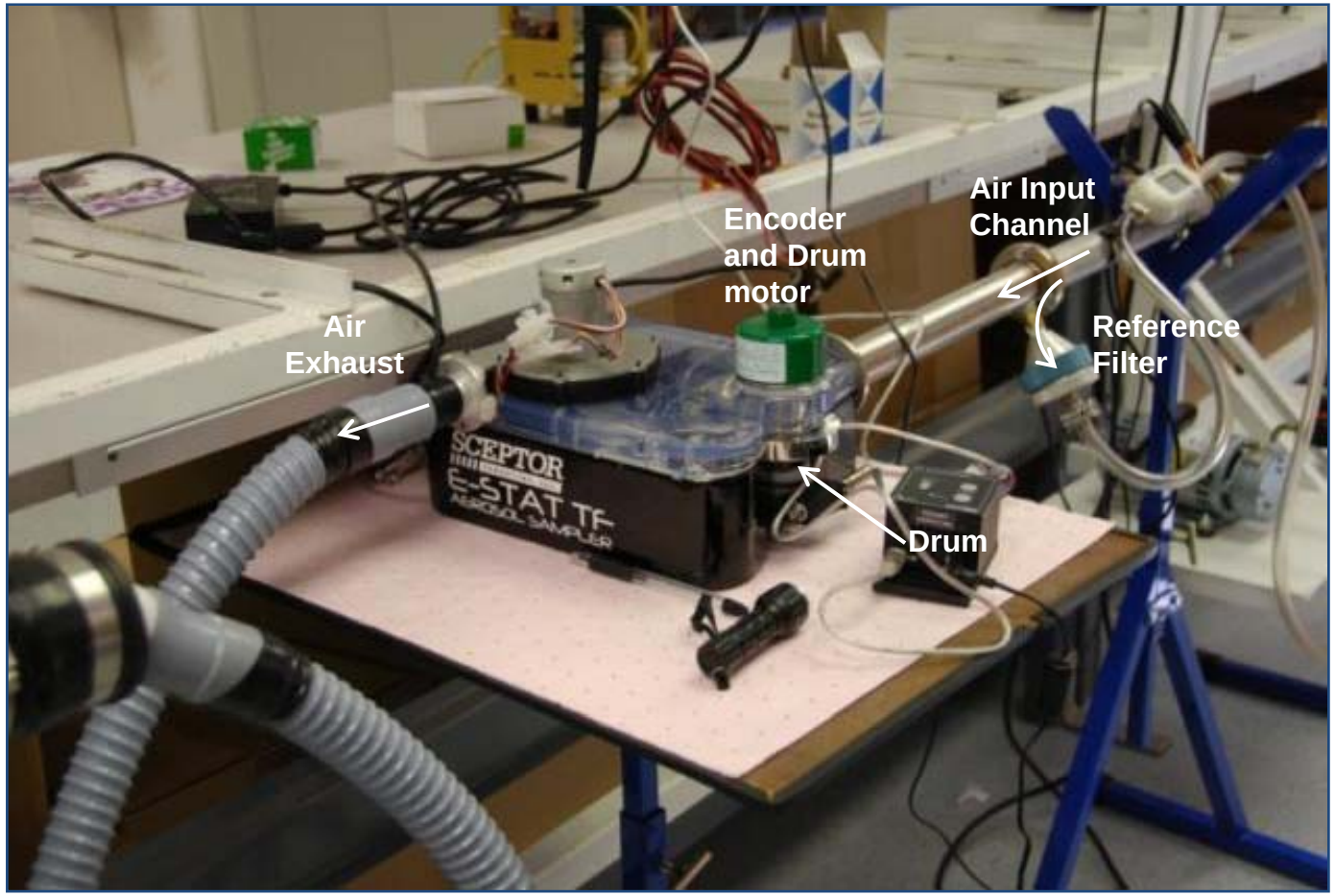

Task 2 Test Deposition Pattern on the Modified Drum

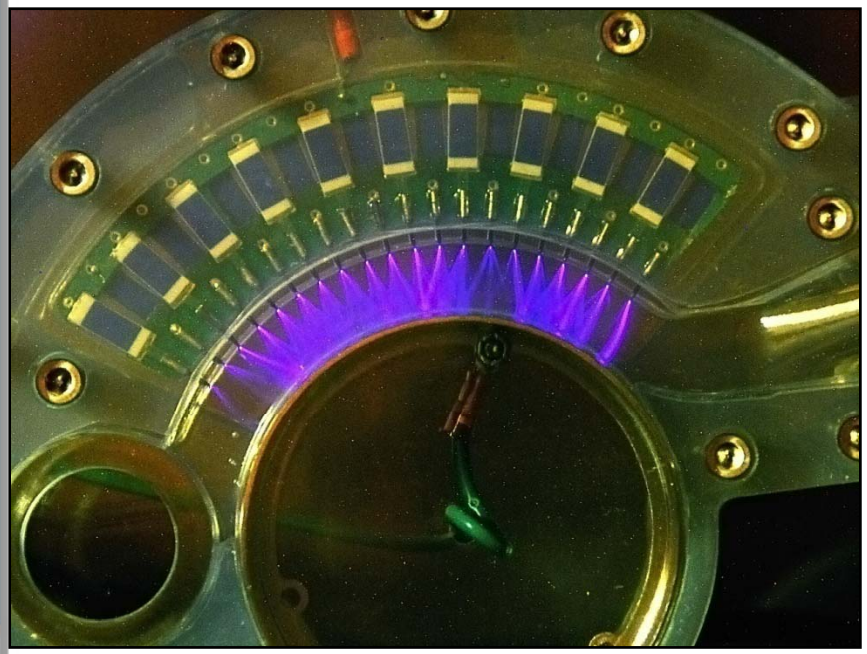

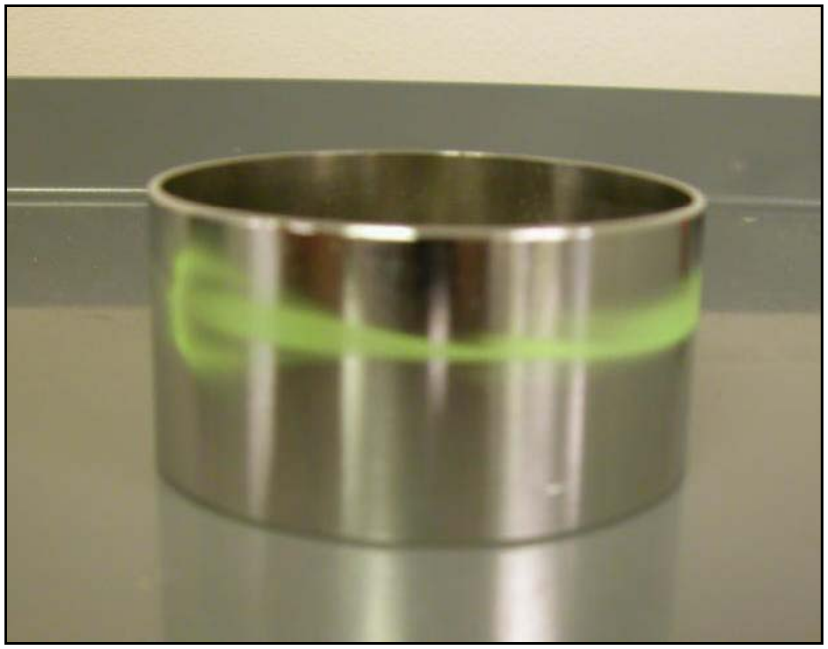

Image of corona ring of closed tangential flow prototype

ChemImage™

Task 2 Deposition Pattern for the Tangential Flow Unit

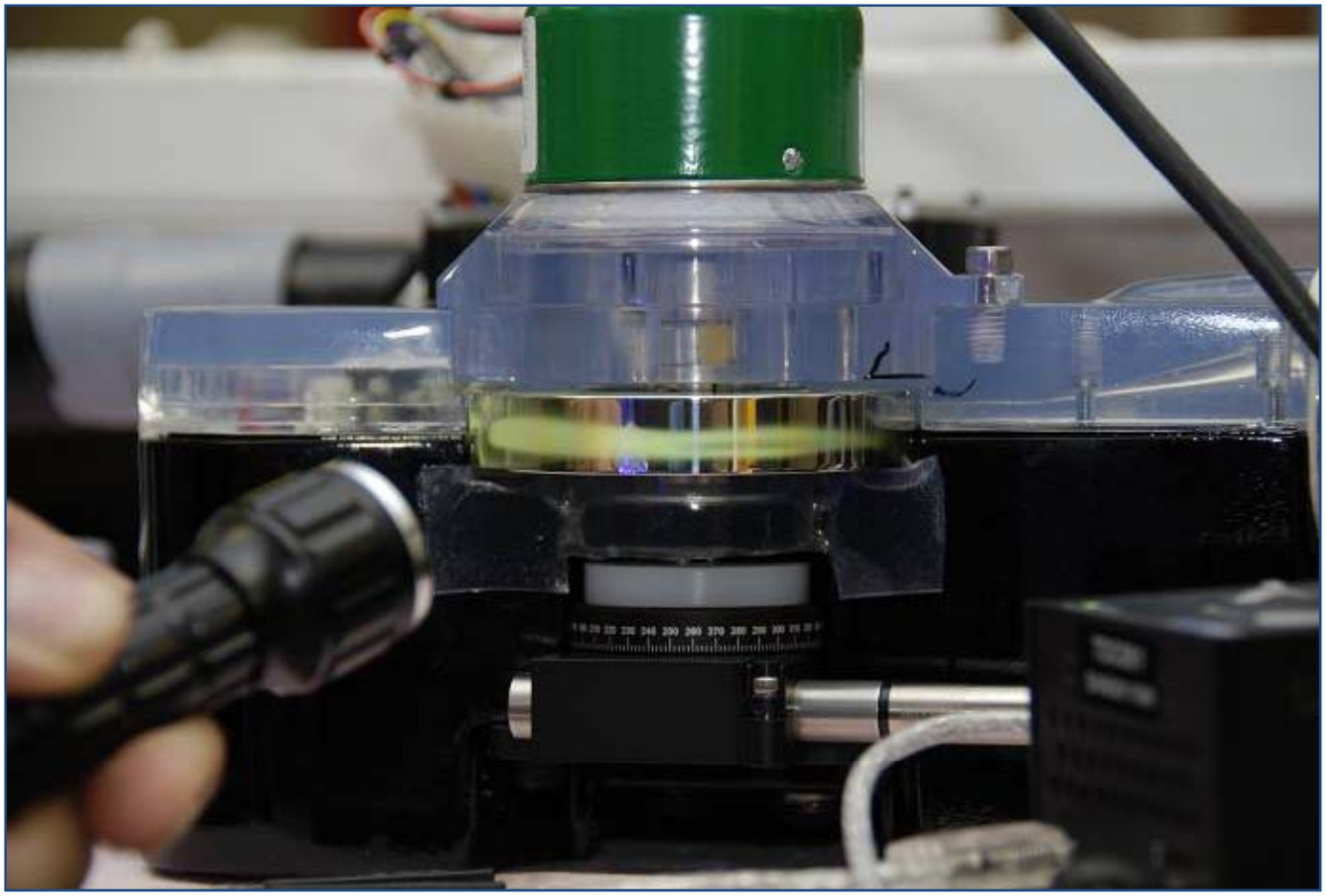

Task 2 Test fixture for Studying deposition Pattern and Collection Efficiency

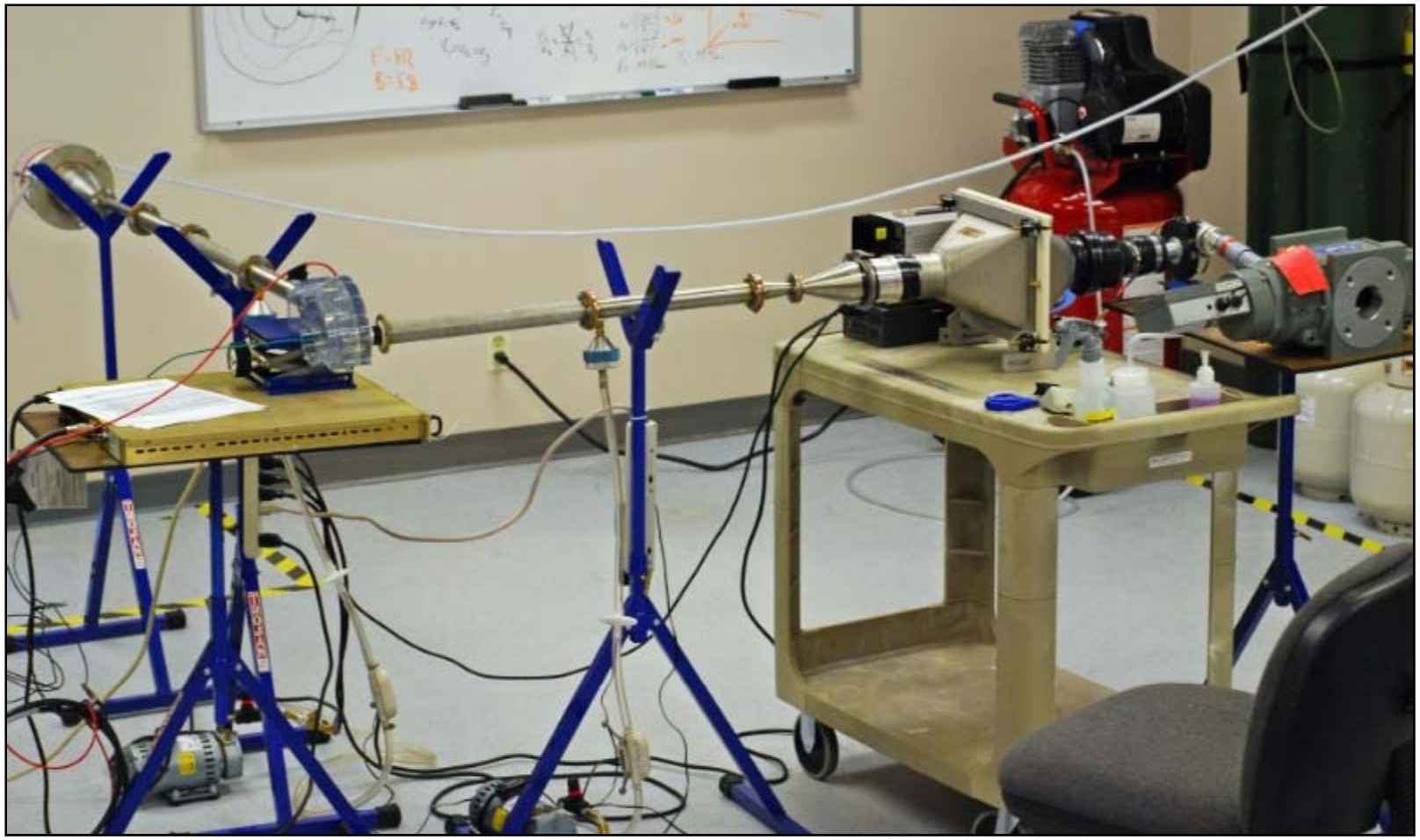

ChemImage™

Task 2 Collection Efficiency for Stationary Drum, Unit 1

Dependence on Flow Rate

15 min Collection time, 3 micron polystyrene microspheres

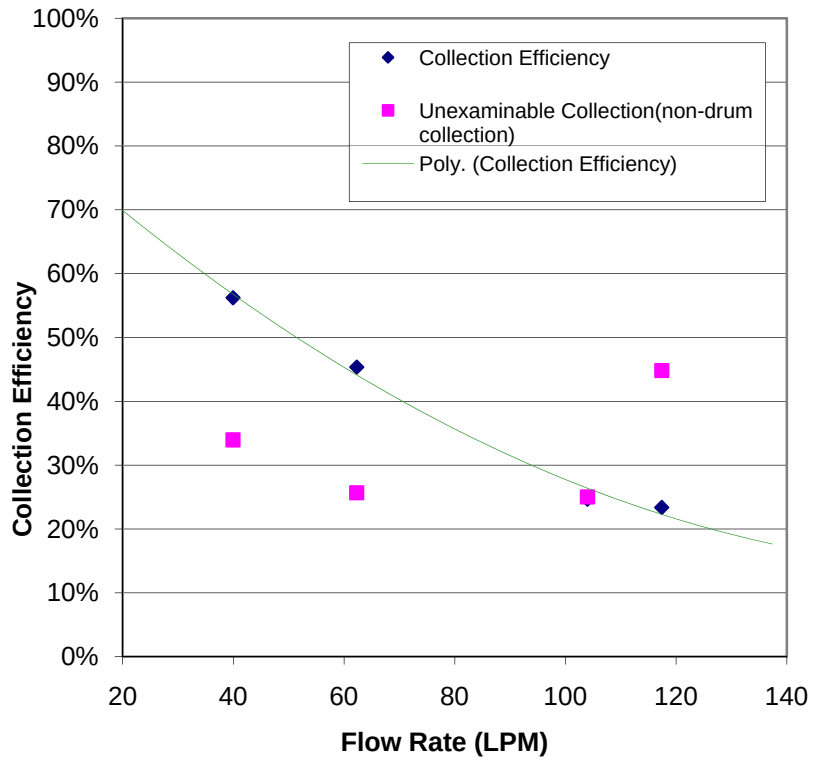

Dependence on Collection Time

Flow Rate 50 LPM, 2 micron polystyrene microspheres

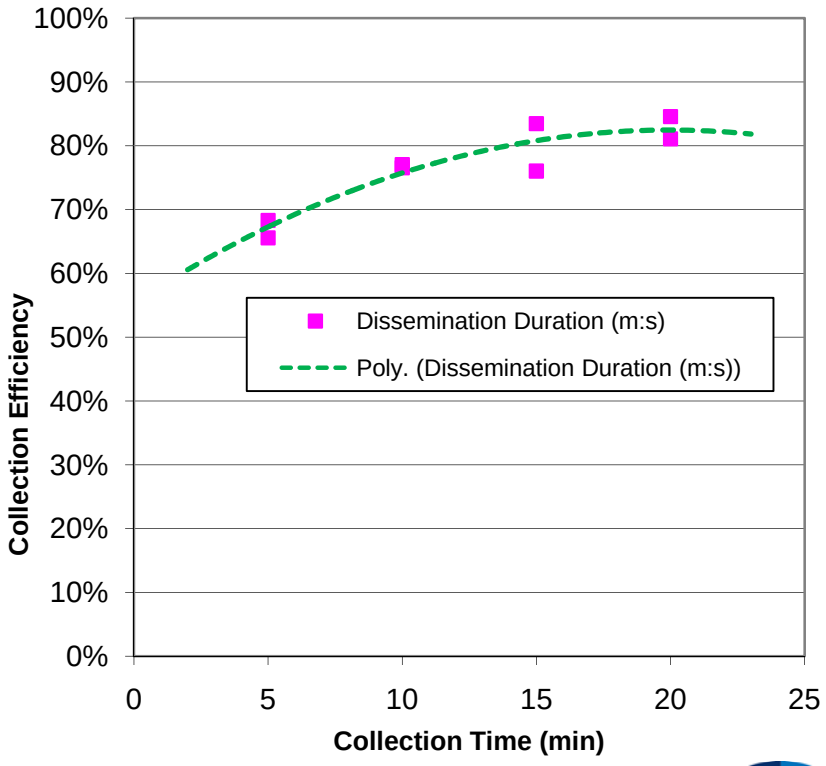

SCEPTOR Industries, Inc.

ChemImage™

Task 2 Collection Efficiency for Rotating Drum, Unit 1

10 min Collection time, 2 micron polystyrene microspheres

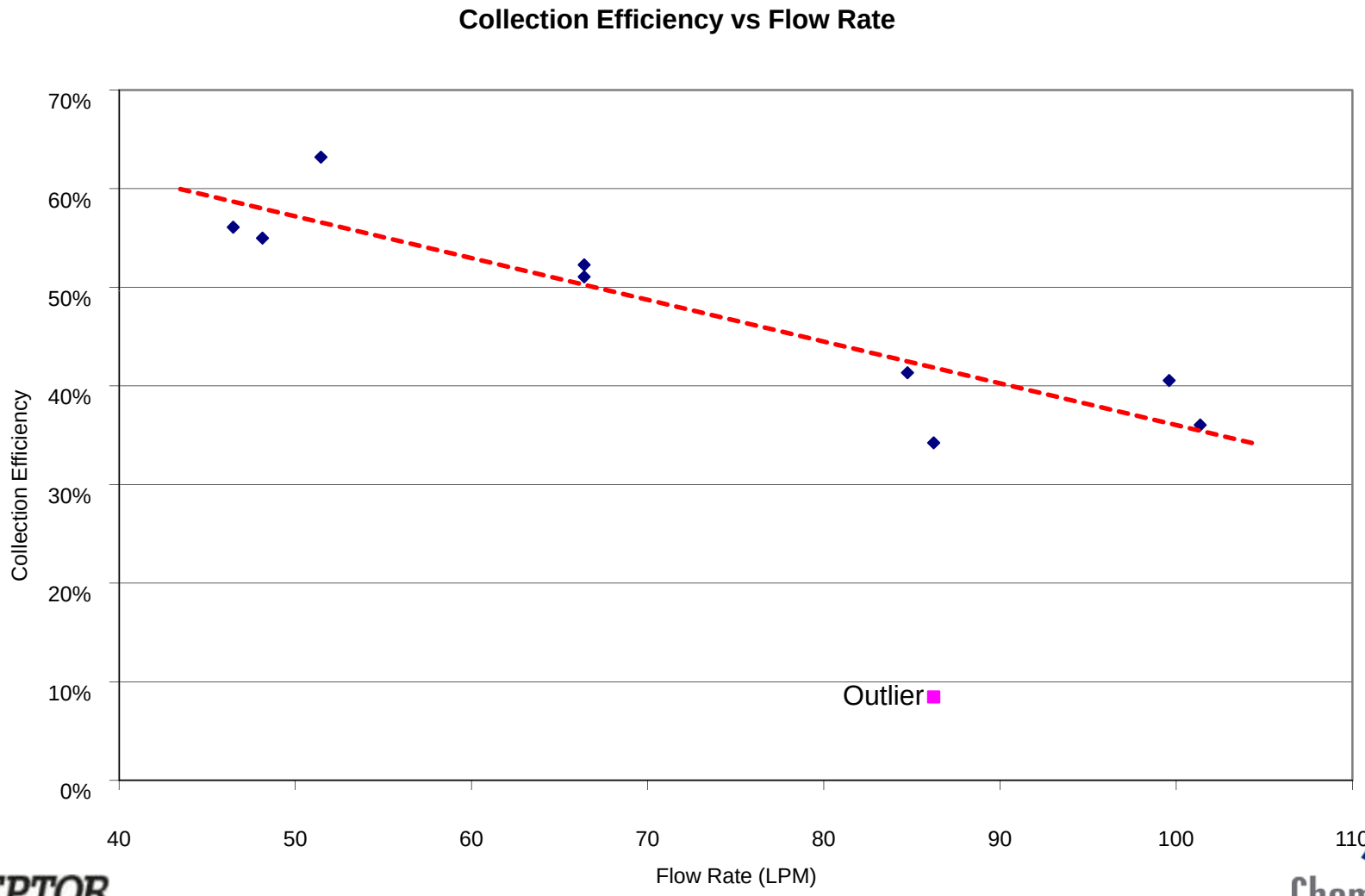

SCEPTOR Industries, Inc.

ChemImage™

Task 2 New Design for Koehler Brightfield Illuminator

White light ray trace

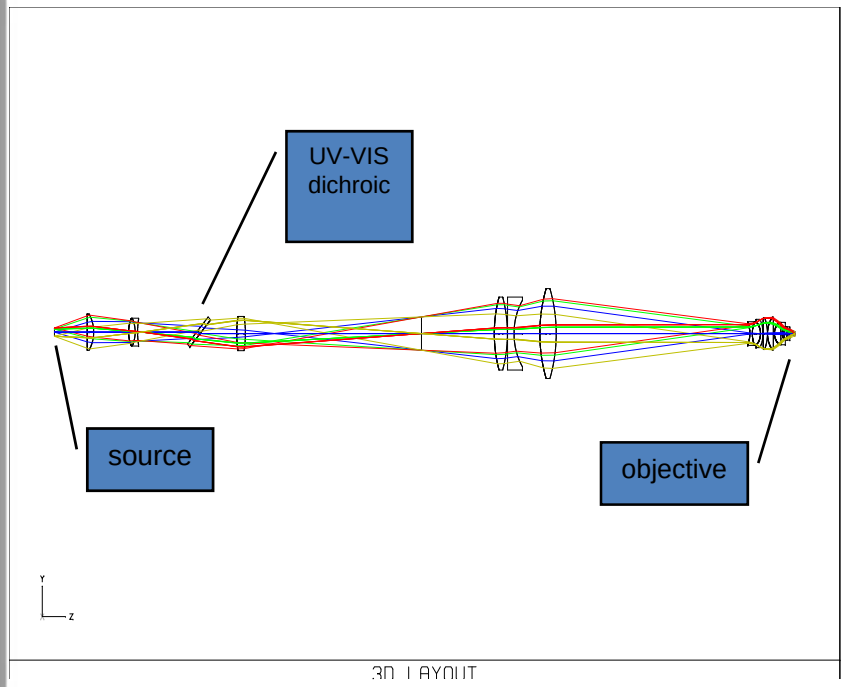

UV light ray trace

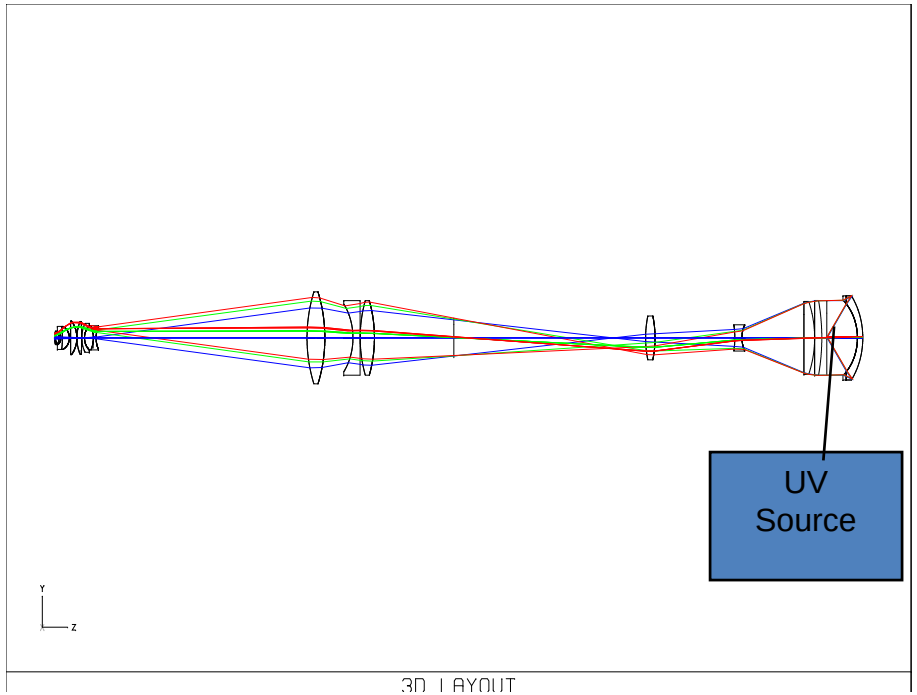

RUDA & Associates

ChemImage™

Task 2 Irradiance on Focal Plane in APICD Gen II Illuminator

- White light irradiance pattern

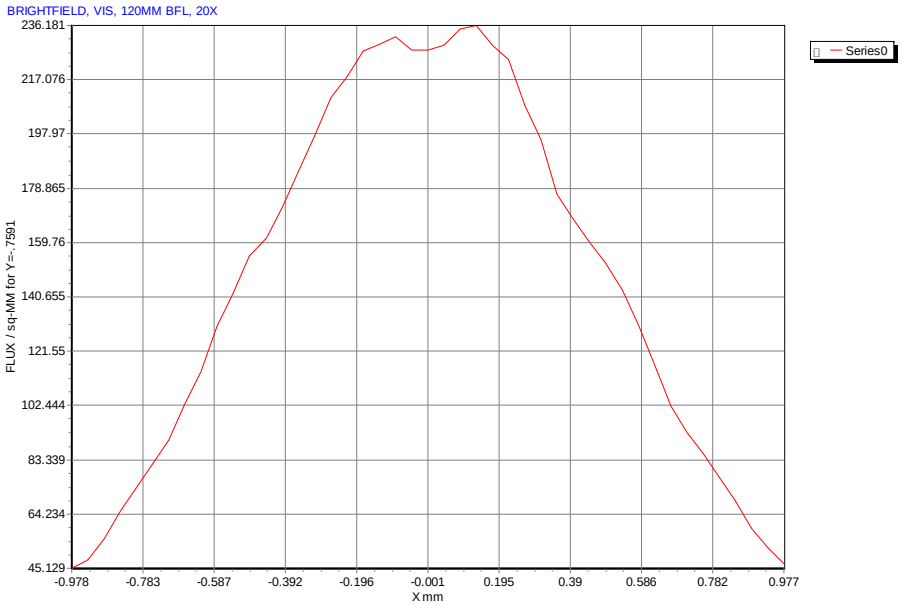

- UV light irradiance pattern

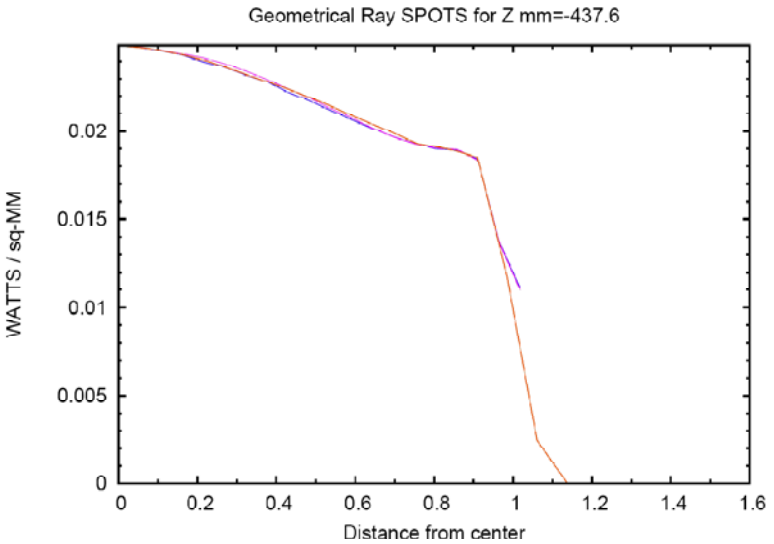

- The modeled microscope objective may not be an accurate representation of the actual Olympus objective

RUDA & Associates

ChemImage™

Task 2 Raman Targeting Subsystem in APICD Gen II

Optical layout and prototype

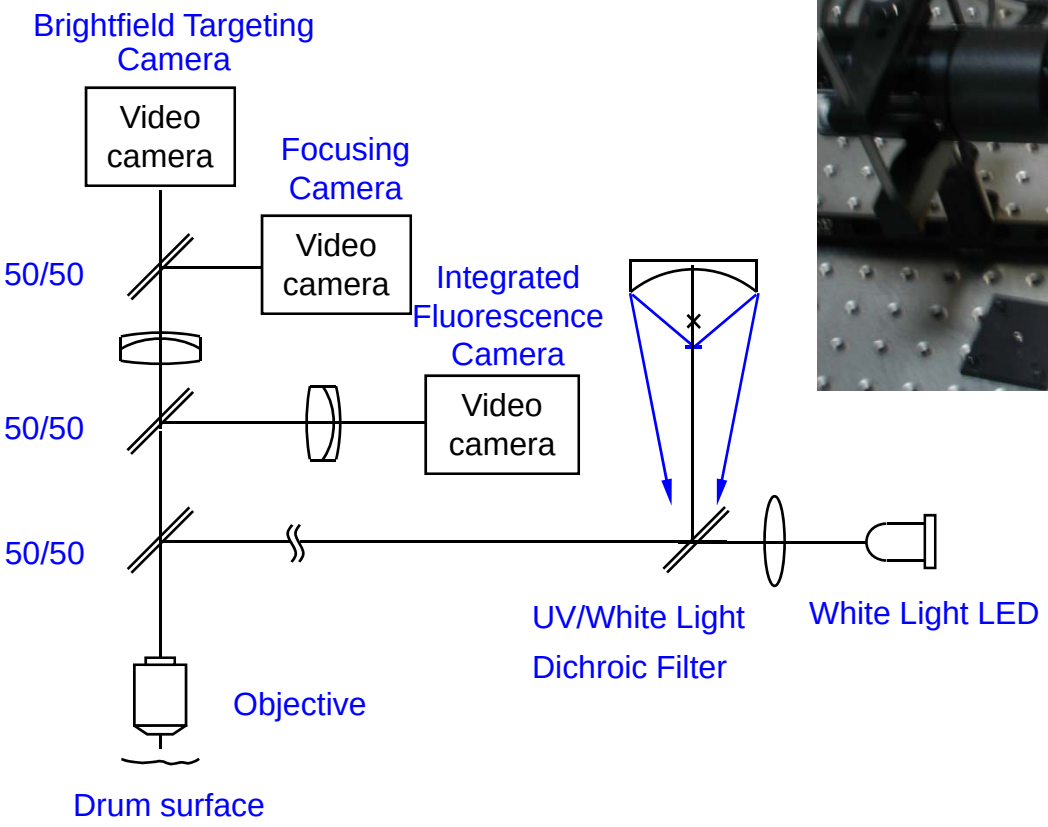

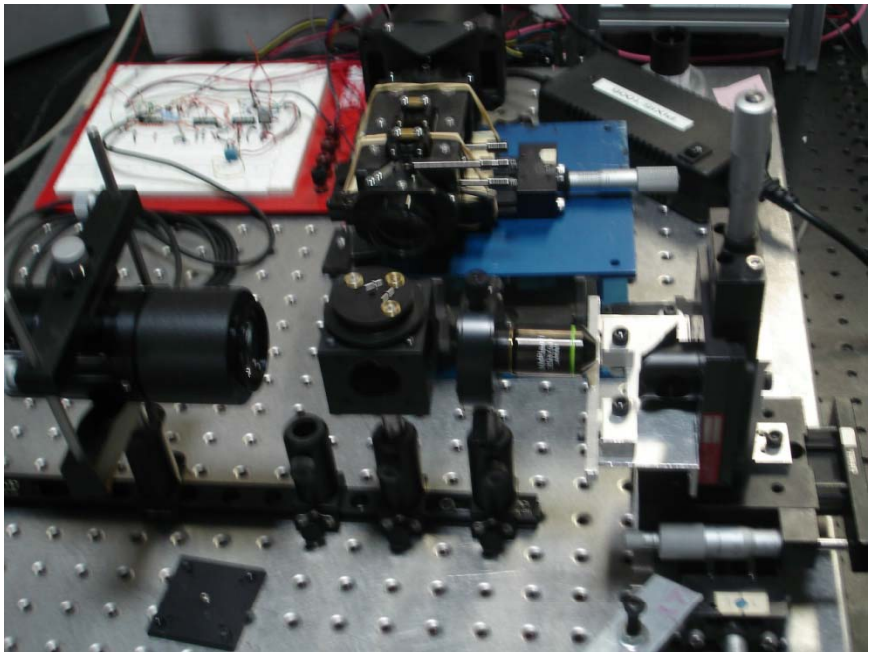

Task 2 Raman Threat Identification Subsystem
APICD Gen II

First Light testing of the Raman module

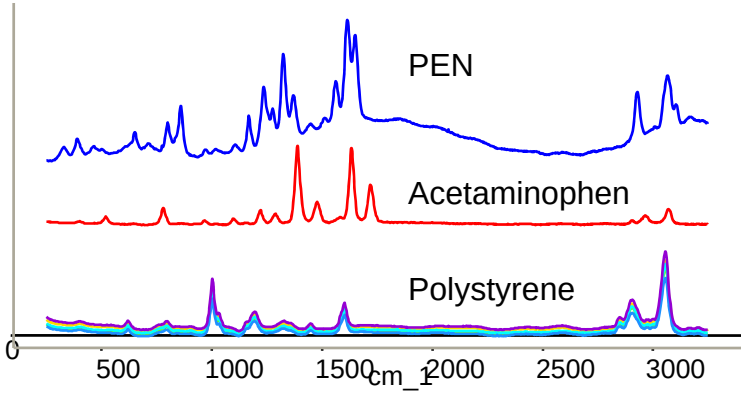

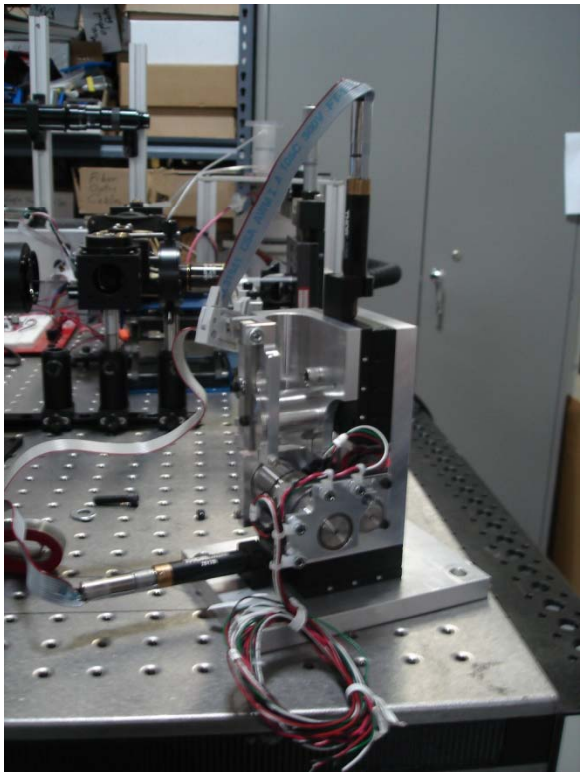

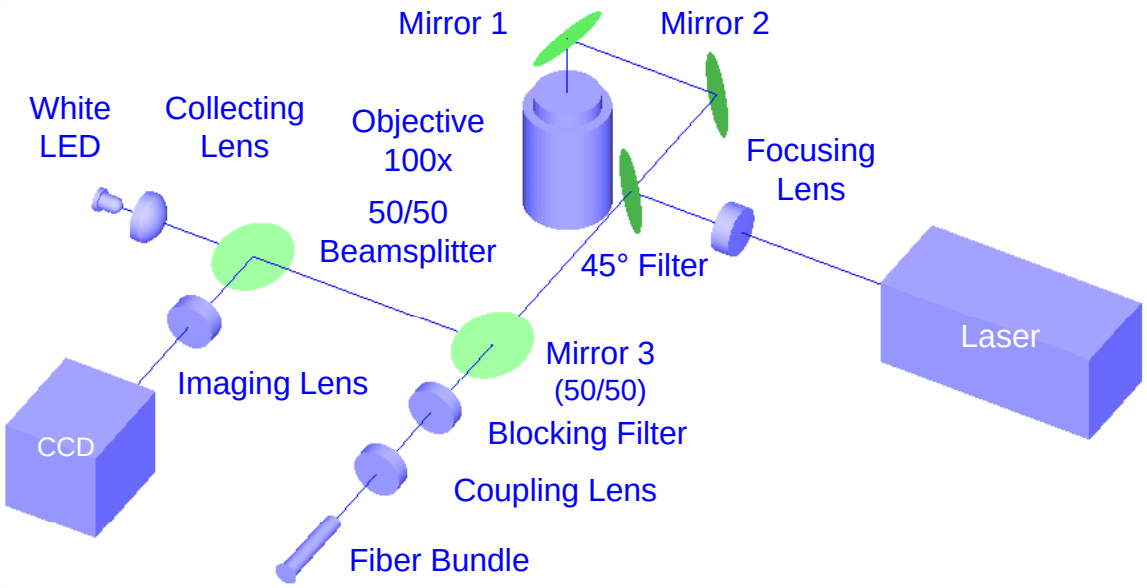

ChemImage™

Task 2 Measured Beam Size for 100x Microscope Objective

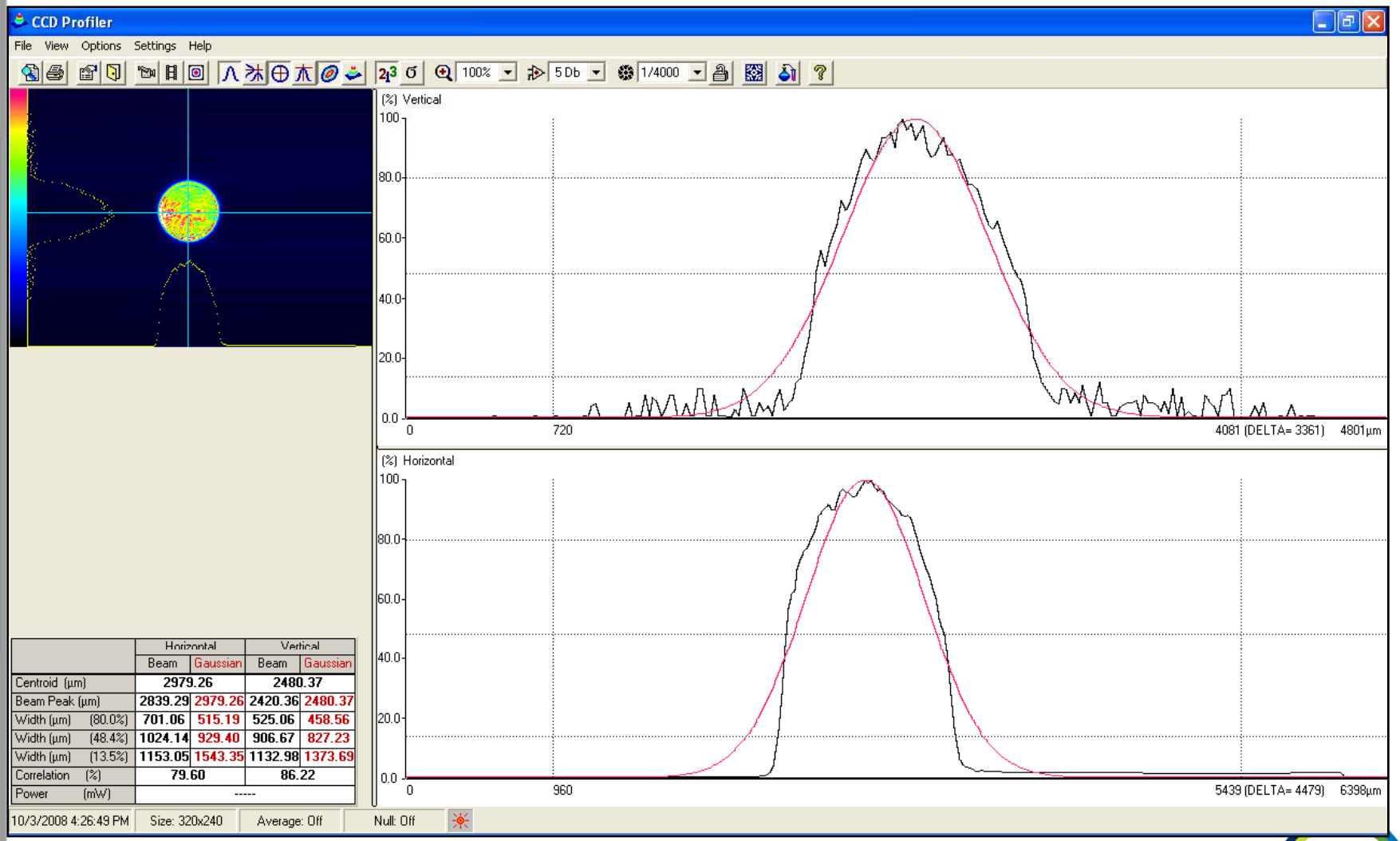

	Horizontal		Vertical	
	Beam	Gaussian	Beam	Gaussian
Centroid (µm)	2979.26		2480.37	
Beam Peak (µm)	2839.29	2979.26	2420.36	2480.37
Width (µm) (80.0%)	701.06	515.19	525.06	458.56
Width (µm) (48.4%)	1024.14	929.40	906.67	827.23
Width (µm) (13.5%)	1153.05	1543.35	1132.98	1373.69
Correlation (%)	79.60		86.22	
Power (mW)	-----			

ChemImage™

Task 2 Laser Illumination in Focal Plane of 100x Microscope Objective

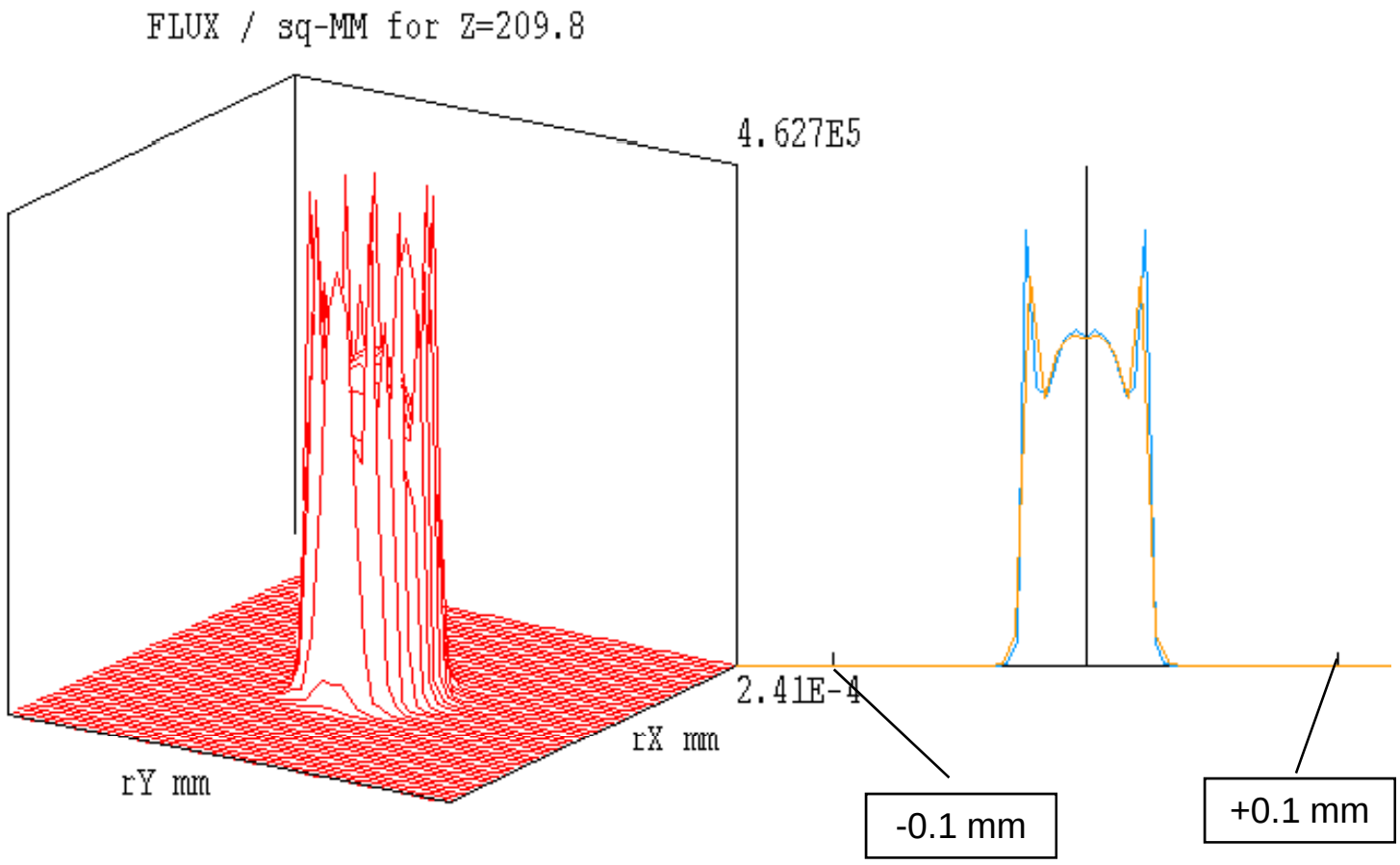

RUDA & Associates

ChemImage™

Task 2 Experimental Setup for APICD Cleaning Performance

- APICD Gen II axial flow prototype drum was cleaned.
- Zoom lens was focused on the presumed Zero degrees position on the surface of the drum.
- 1 ml of 1% aq. sln of 5.3 micron PSMS solution was diluted by 4 ml of deionized water. Obtained 0.2% PSMS solution was placed into Omcron nebulizer and dispersed for 90 sec while electrostatic collector was active without rotation.
- Air blower was set to 10000 rpm
- Drum was rotated for 86 degrees to bring PSMS deposition under the observation. PSMS particles were deposited between 86 and 200 degrees of rotation of the drum. Insignificant number of particles was detected at 205 degrees.

86 degrees

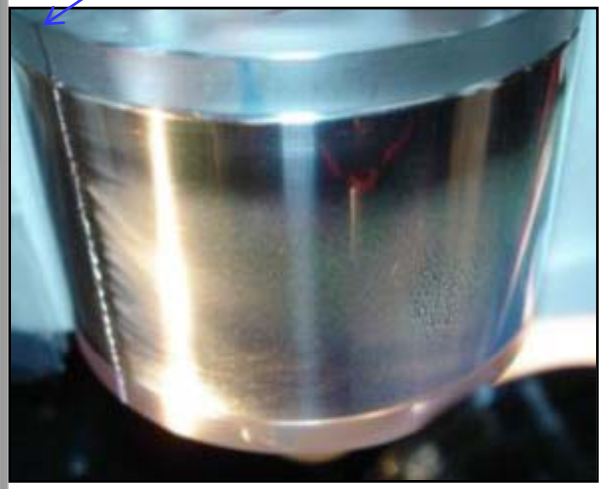

View from Above

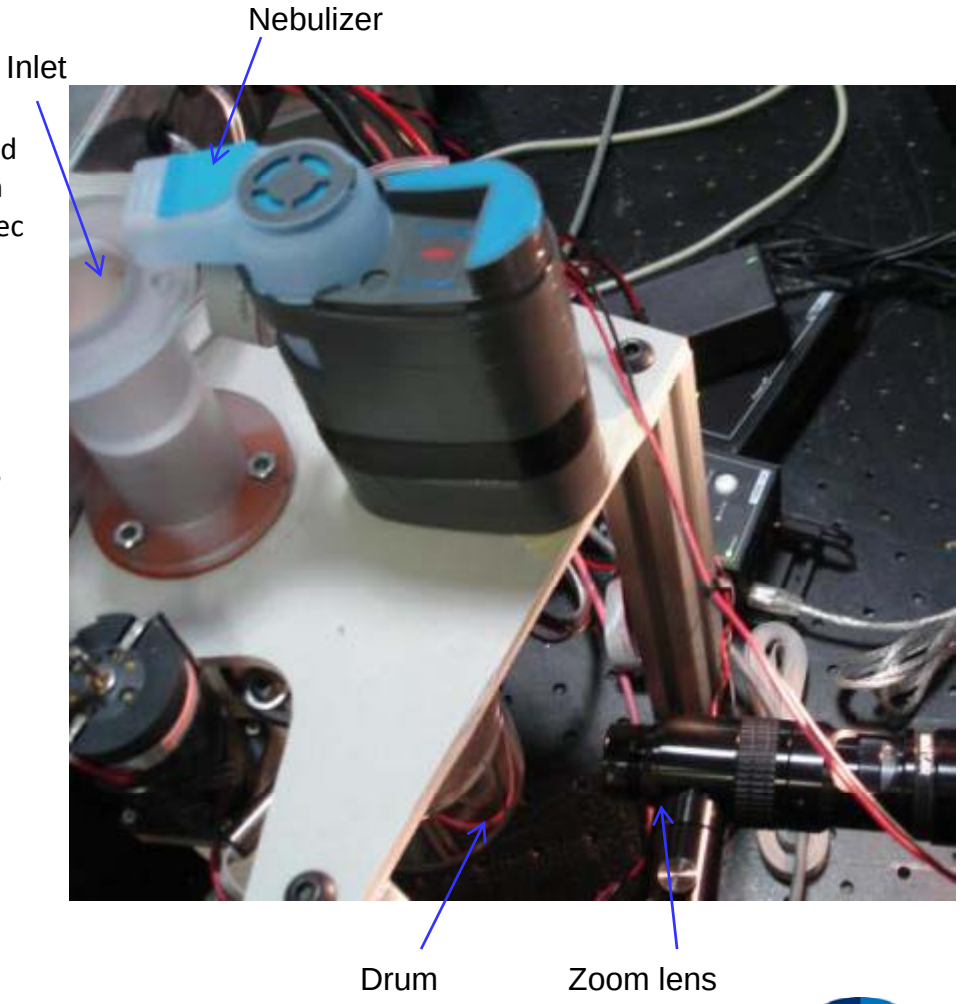

ChemImage™

Task 2 Particle Counts and Density after 90 sec Dispersal

85 degrees

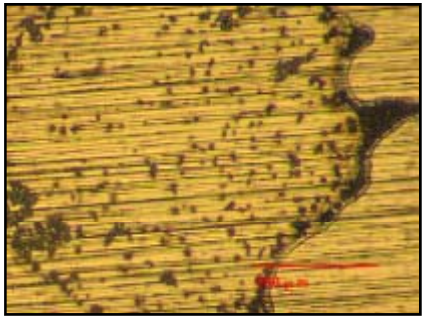

105 degrees

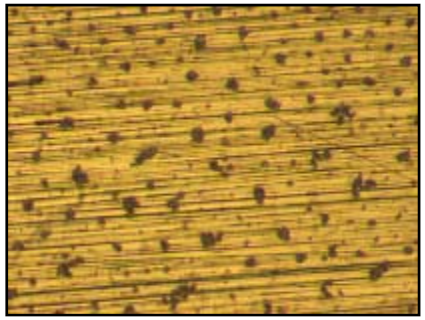

125 degrees

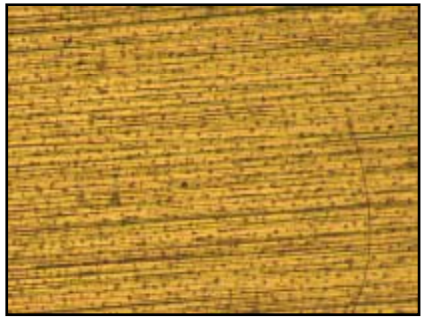

	FOV at rotation	Particle Count	Particle /cm^2
1	95 degrees	180	5483.88
2	100 degrees	220	6702.52
3	105 degrees	357	10876.35
4	110 degrees	412	12551.98
5	115 degrees	464	14136.21
6	125 degrees	310	9444.45
7	140degrees	250	7616.49
8	150 degrees	292	8896.07
9	180 degrees	285	8682.80
10	200 degrees	486	14806.46
11	205 degrees	5	152.33
	Average*:	**325.6**	**9919**

* Only first 10 FOV were included in average calculation
Clusters of PSMS were counted as one particle.
Each FOV is 657.84 x 498.96 micron = 328,235.85 um^2 = 0.0328235 cm^2

ChemImage™

Task 2 After 1st Cleaning Cycle – 94% Cleaning Efficiency

105 degrees

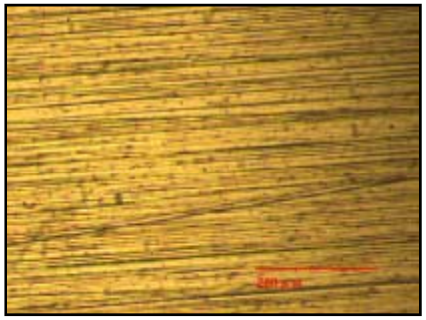

120 degrees

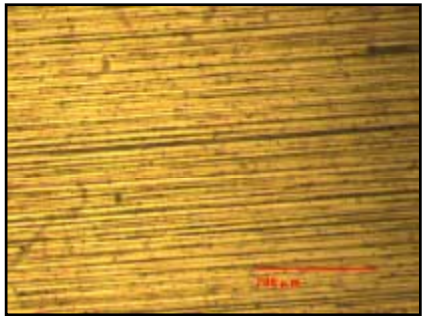

140 degrees

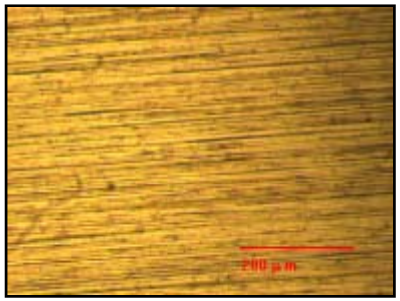

FOV at rotation	Particle Count	Particle density per cm^2
105 degrees	45	1370.97
100 degrees	17	517.92
130 degrees	10	304.66
140 degrees	18	548.39
150 degrees	16	486.46
180 degrees	17	517.92
Average	**20.5**	**624.39**

Only PSMS particles were counted, therefore, 94% refers to PSMS cleaning efficiency. Visual inspection shows that some small particles remained on the drum.

ChemImage™

Task 2 Representative BFR images of 5 μm PSMS on Al slide dispersed using a Omcron Nebulizer

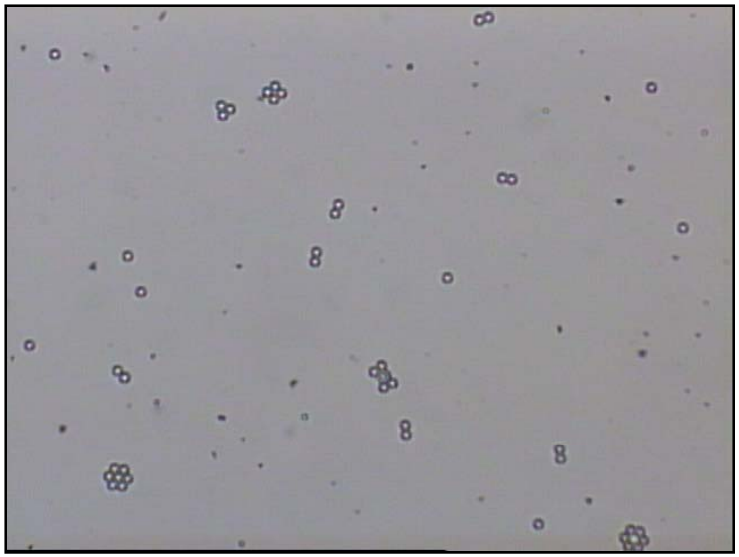

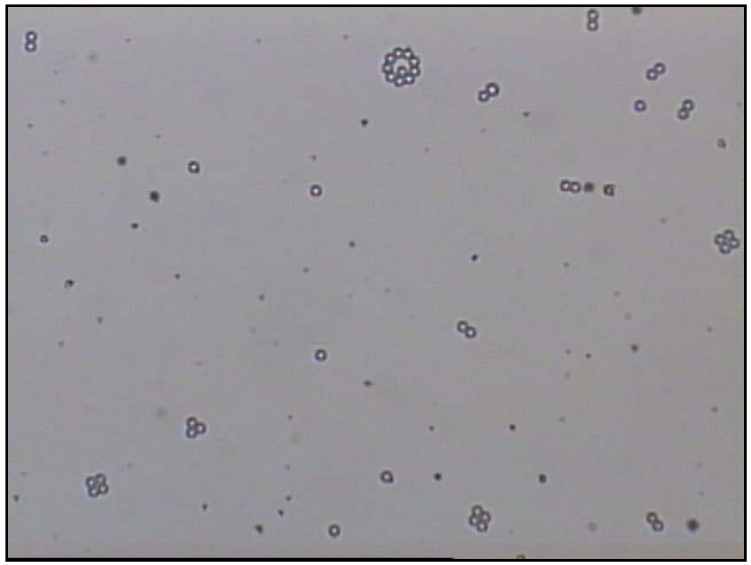

ChemImage™

Task 3 Setup for Characterization of Deposition Efficiency

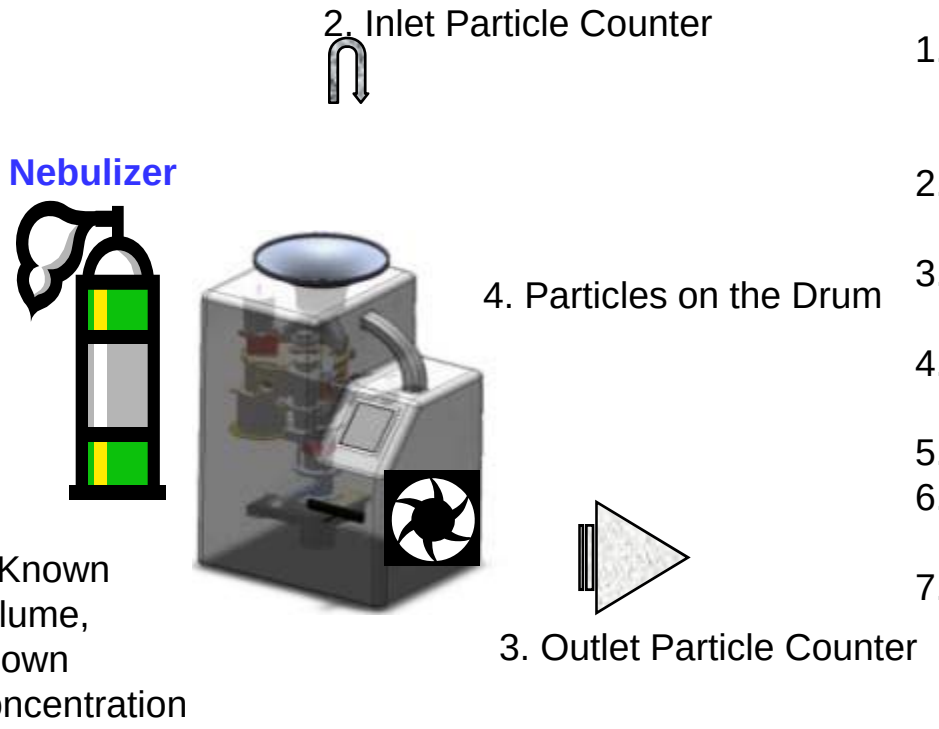

1. Disperse known amount of PSMS using Omcron Nebulizer while running electrostatic collector
2. Measure particle count entering the APICD drum inlet. NB May contain water droplets.
3. While collecting, measure amount of particles on the outlet of the APICD drum
4. Count number of particles deposited on the drum in at least 10 FOVs
5. Estimate particle deposition efficiency
6. Turn off electrostatic collector and turn on cleaning brush
7. Count number of particles remaining on the drum in the same FOVs after 1, 2, 3 cleaning cycles

ChemImage™

Task 3 Particulate Matter Test Chamber

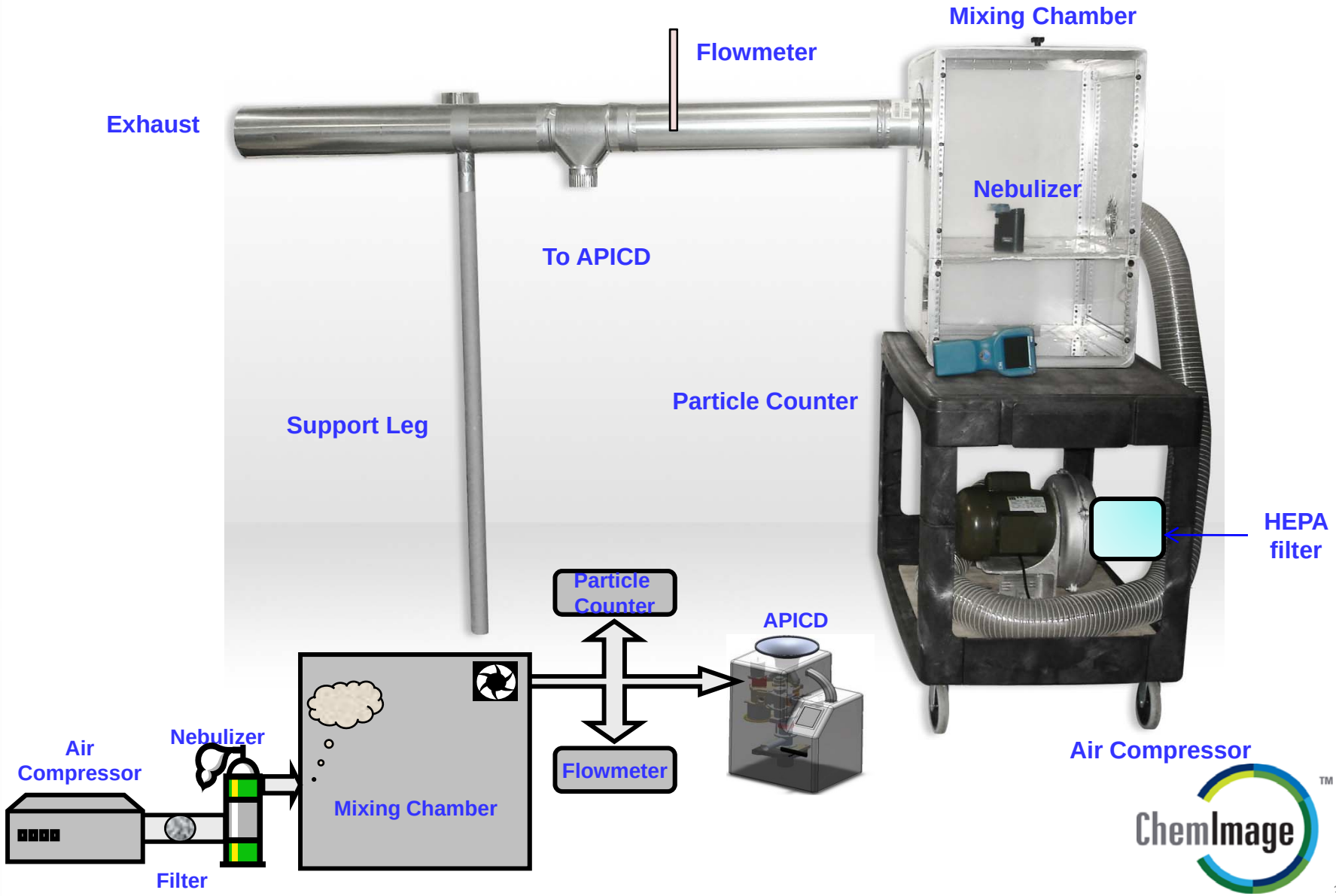

Task 3 Collection Equipment Schematic

Setup for Concurrent Collection at NETL

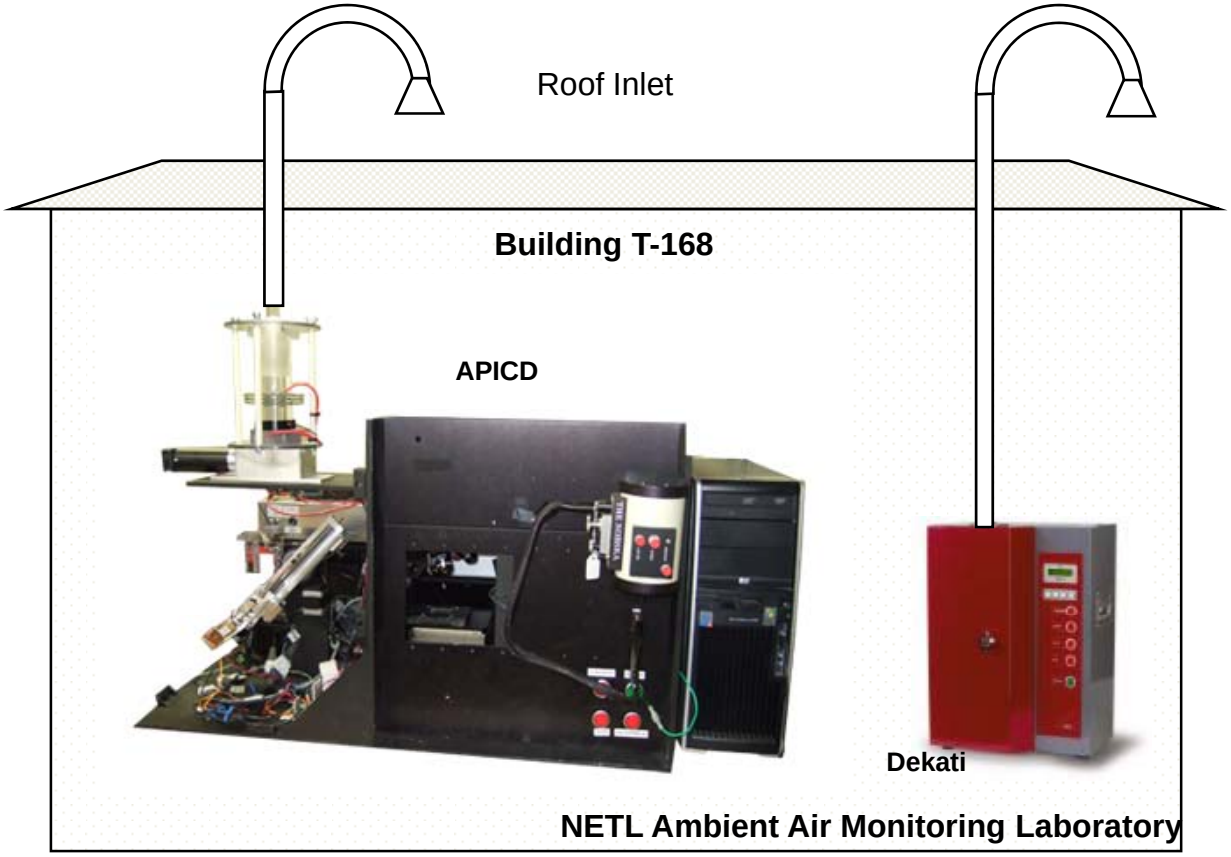

DustTrak

Task 3 Particle Size Distribution: 10 min Average

Manufacturing Area Reference Measurement on March 12, 2008

Particle Fraction	Particle Count		
	10 min Average (Counts/m³)	St Dev	1 Hrs Average (PPL)
0.3-0.5 µm	32,620,197	3.36%	195,721
0.5-1.0 µm	4,019,623	10.94%	24,118
1-3 µm	458,457	20.37%	2,751
3-5 µm	91,663	28.77%	550
5-10 µm	29,450	37.71%	177
>10 µm	4,277	34.10%	26
TOTAL:	**37,223,666**		**223,342**

Ambient Particle Size Distribution

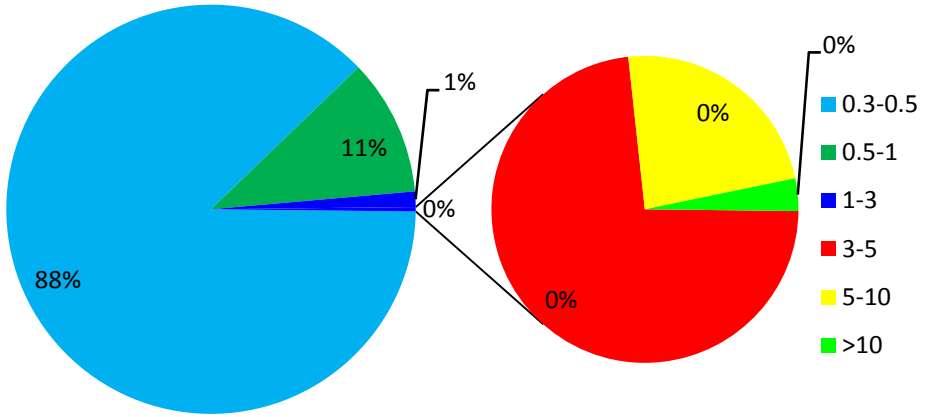

Task 3 Fluorescent Fraction of Spring Outdoor Witness Sample

Characterization of the Outdoor Witness Sample (s4161)

Digital Photograph of Outdoor Witness Sample

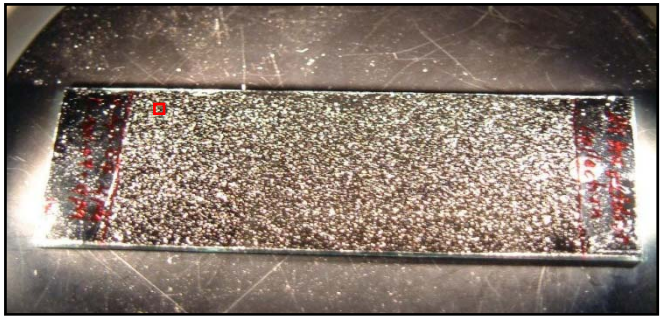

0.5 % Area of the slide investigated

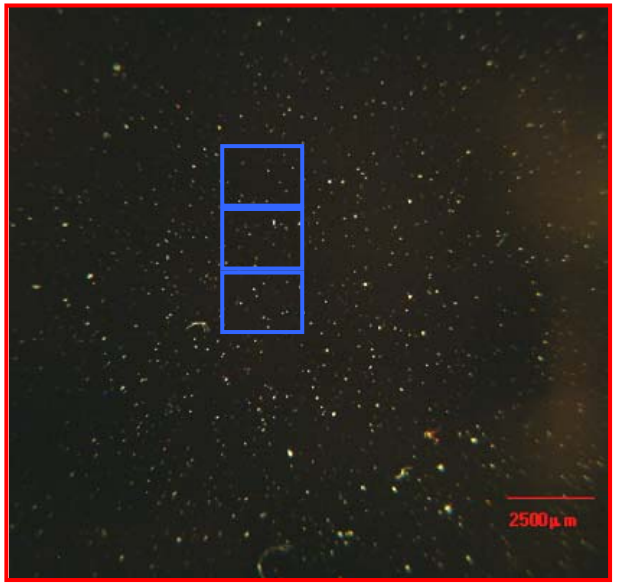

BFR Montages at 20x overlaid with FLI data

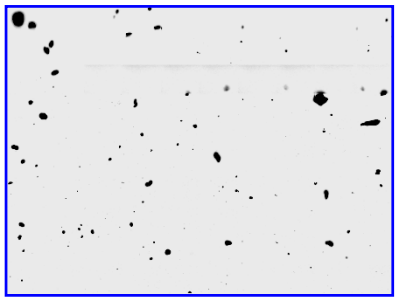

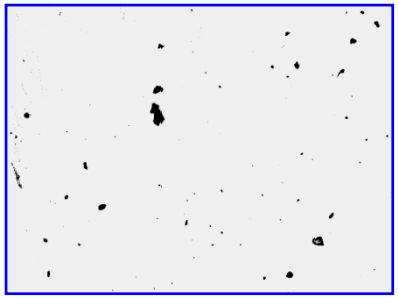

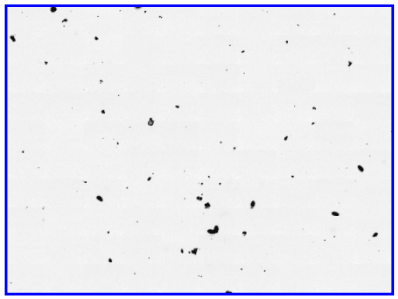

	Particles	
	Manual Counting	CI Xpert
BFR total	937	1502
BFR 1-10 µm	-	651
FLI total	369	541
FLI 1-10 µm	-	245
Fluorescent Fraction (all sizes)		36%
Fluorescent Fraction (1 – 10 µm)		38%

ChemImage™

Task 3 Particle Size Distribution for 69 hrs

Empty Particle Chamber Measurement

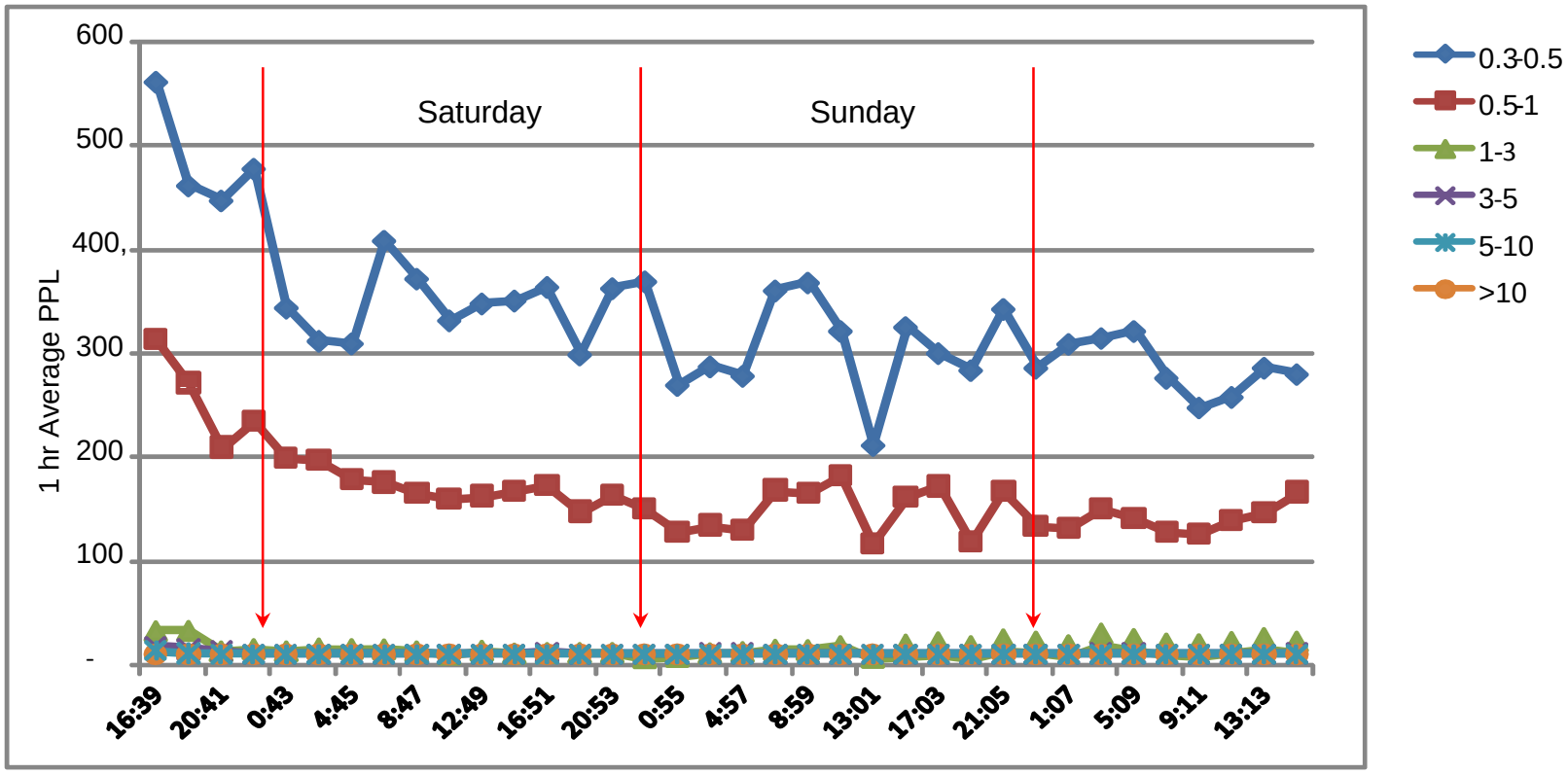

Particle Count	Particle Fraction						Total
	0.3-0.5 µm	0.5-1.0 µm	1-3 µm	3-5 µm	5-10 µm	>10 µm	
2 hr Average (Counts/m³)	670,944	333,392	27,208	1,305	255	10	1,033,109
% St Dev	21%	24%	43%	218%	427%	600%	
1 Hrs Average (PPL)	335	167	13	0.6	0	0	516

ChemImage™

Task 3 Particle Size Distribution for 23 hrs

Empty Particle Chamber Measurement

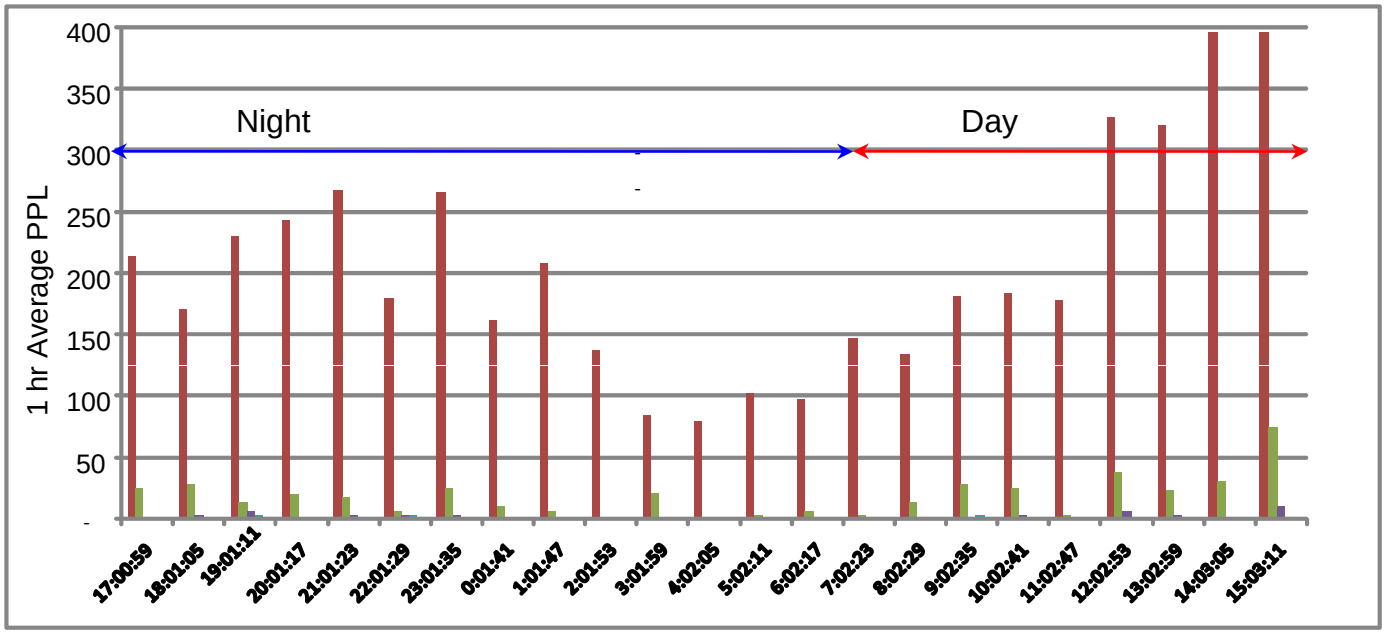

Particle Count	Particle Fraction						Total
	0.3-0.5 µm	0.5-1.0 µm	1-3 µm	3-5 µm	5-10 µm	>10 µm	
1 hr Average (Counts/m³)	2,641,752	210,070	18,804	2,002	465	-	2,873,093
% St Dev	52%	49%	88%	149%	264%	-	
1 Hrs Average (PPL)	2,641	210	18	2	0.5	-	

ChemImage™

Task 3 $PM_{2.5}$ Maps of US for Outdoor Collections at NETL

Daily 24-Hour AQI for $PM_{2.5}$ (midnight to midnight)

Runs 1 and 2

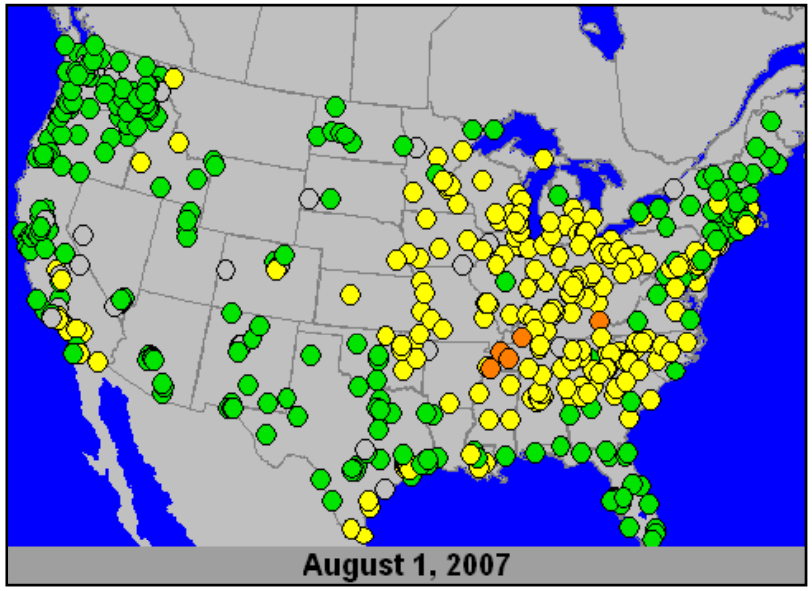

Run 3

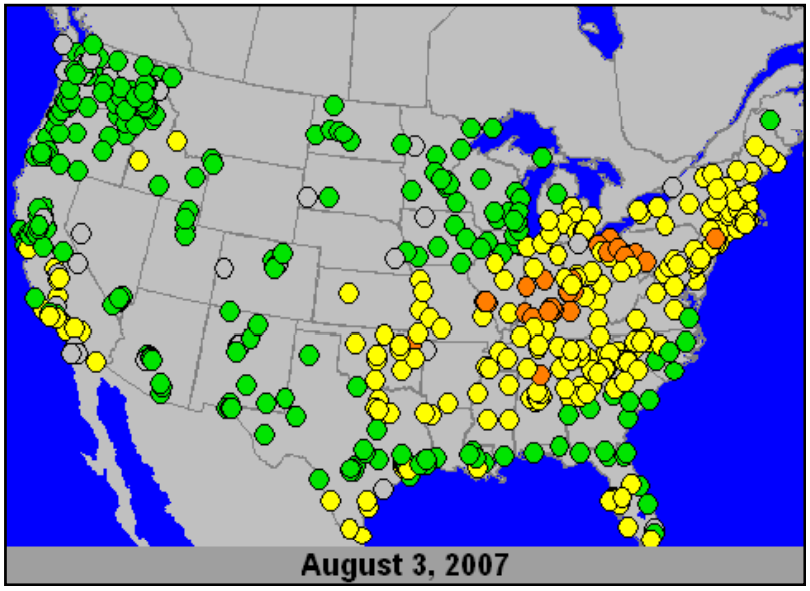

http://www.airnow.gov

	DATE	START	END	COLLECTION DURATION (MIN)
RUN 1	8/1/2007	12:50	13:50	60
RUN 2	8/1/2007	14:08	15:38	90
RUN 3	8/3/2007	14:25	15:37	60

Air Quality Day

ChemImage™

Task 3 $PM_{2.5}$ Mass Concentration For Three Runs

Measured by TEOM, ELPI and DustTrack particulate monitors

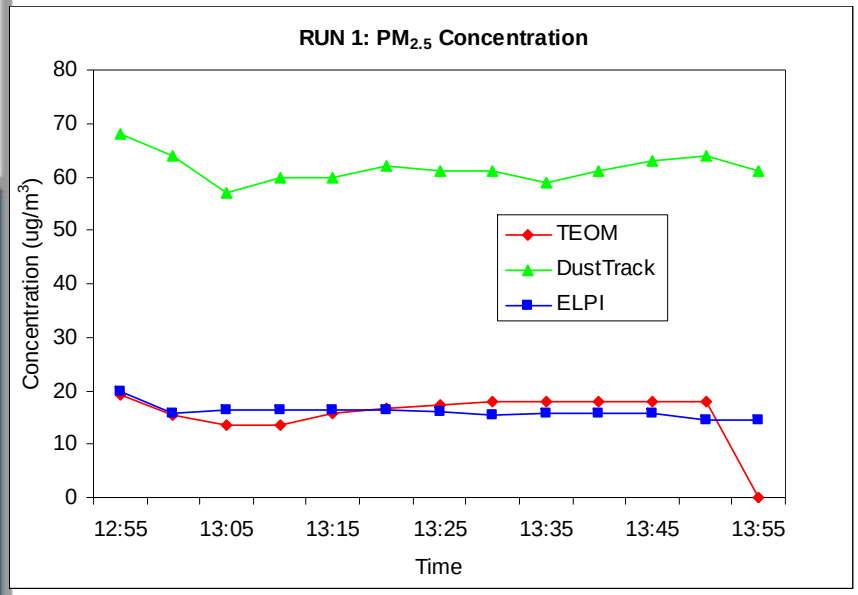

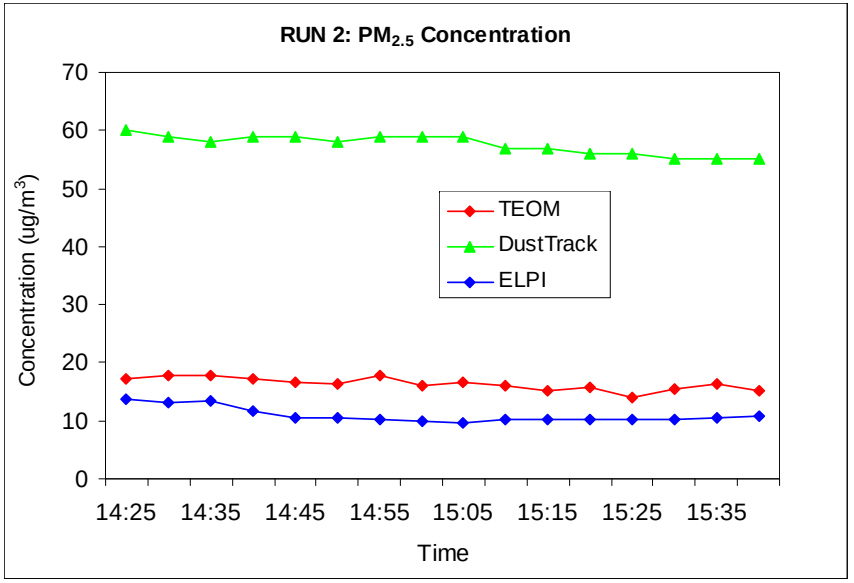

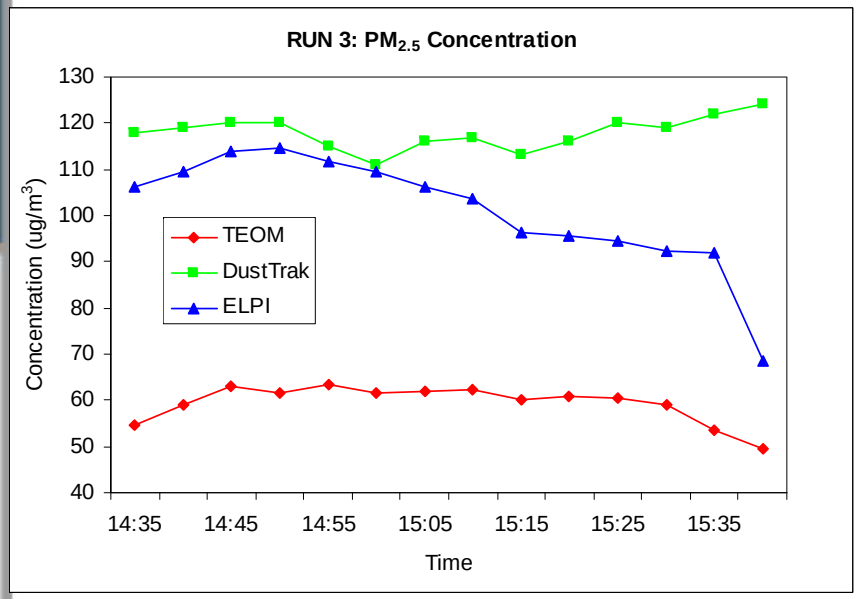

ChemImage™

Task 3 Concentration of 1-2.5 μm Particles in Three Runs

Measured by ELPI instrument

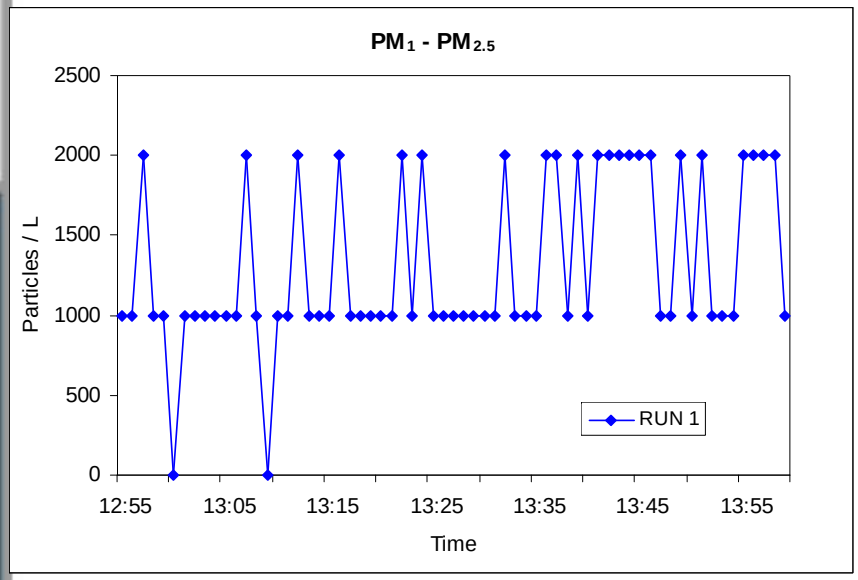

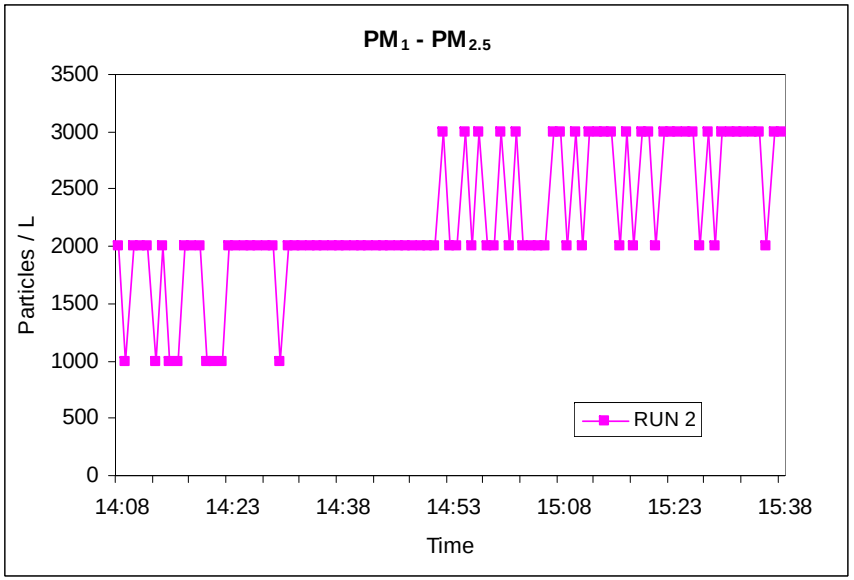

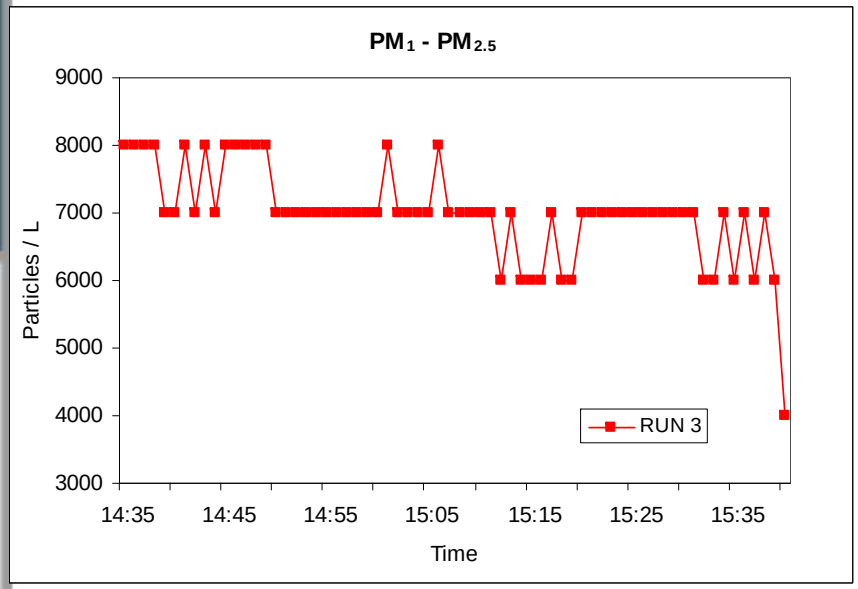

	DATE	MEAN PM_1-$PM_{2.5}$ CONCENTRATION (# / L)	STD (%)
RUN 1	8/1/2007	1308	40%
RUN 2	8/1/2007	2364	27%
RUN 3	8/3/2007	6985	10%

ChemImage™

Task 3 Particle Size Distribution For Three Runs

Measured by ELPI

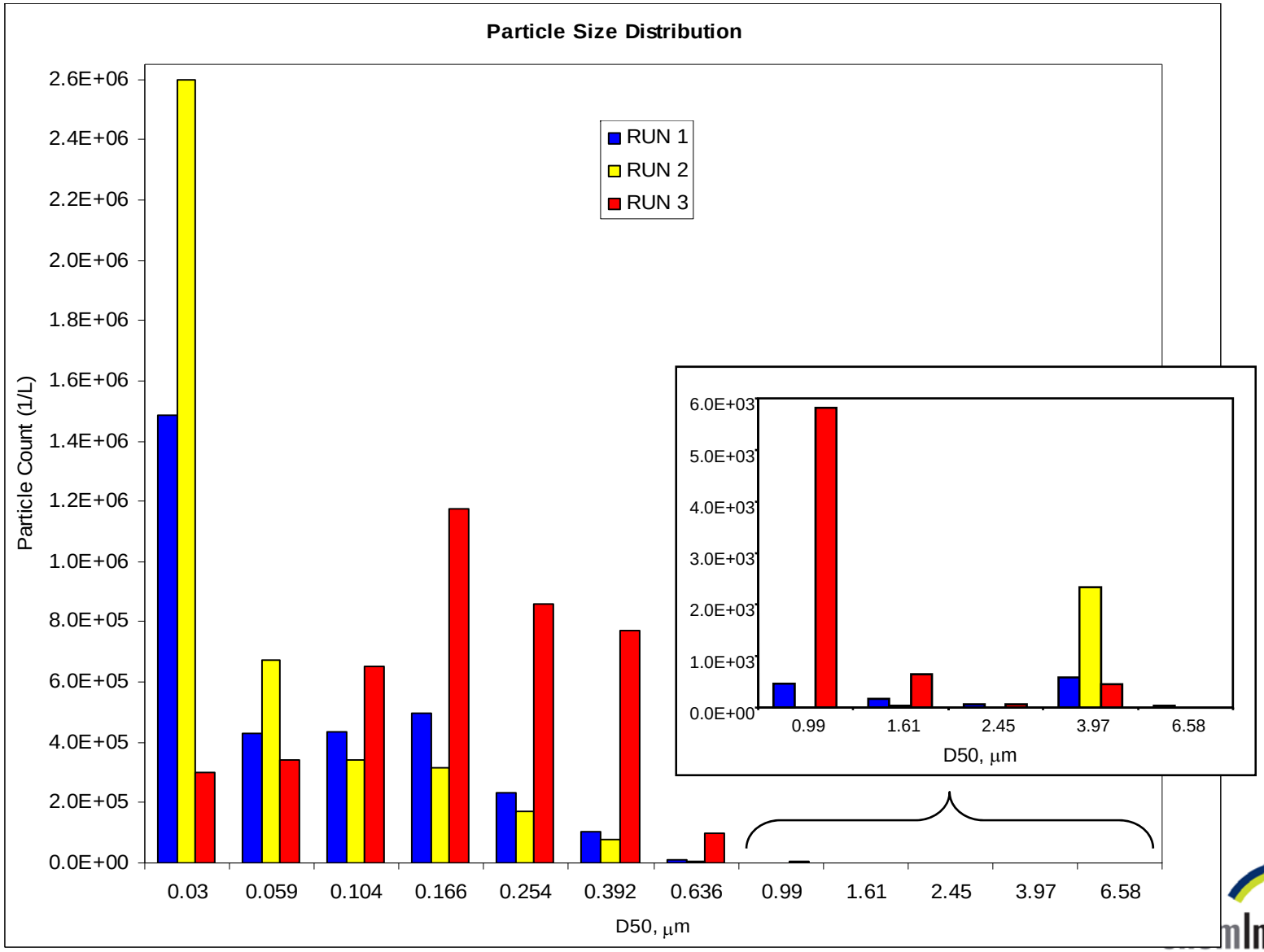

Task 4 Analysis of Outdoor Summer Collection: Witness Sample

Particle Count (Manual)	Brighfield Reflectance	Fluorescence	Fluorescent Fraction
Less than 1 μm	120	10	8.3%
All Particles	252	34	13.5%

BFR montage at 20 x

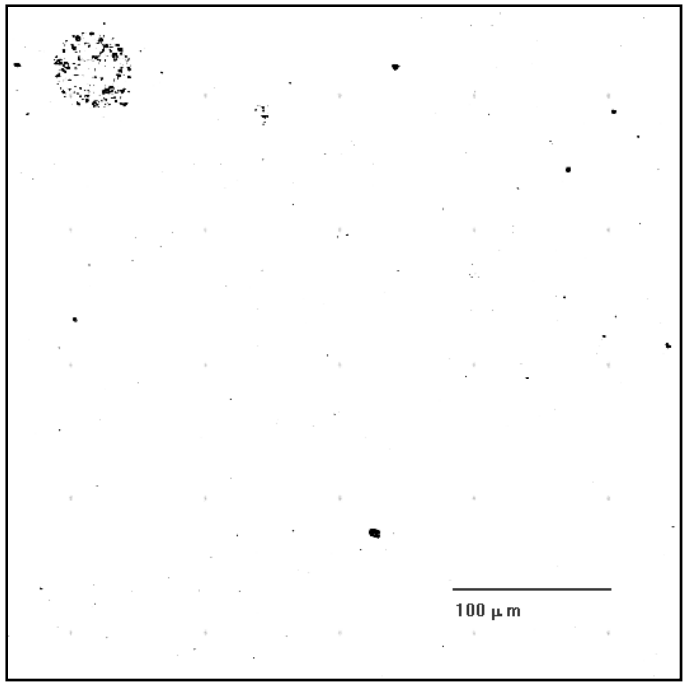

FLI montage at 20 x

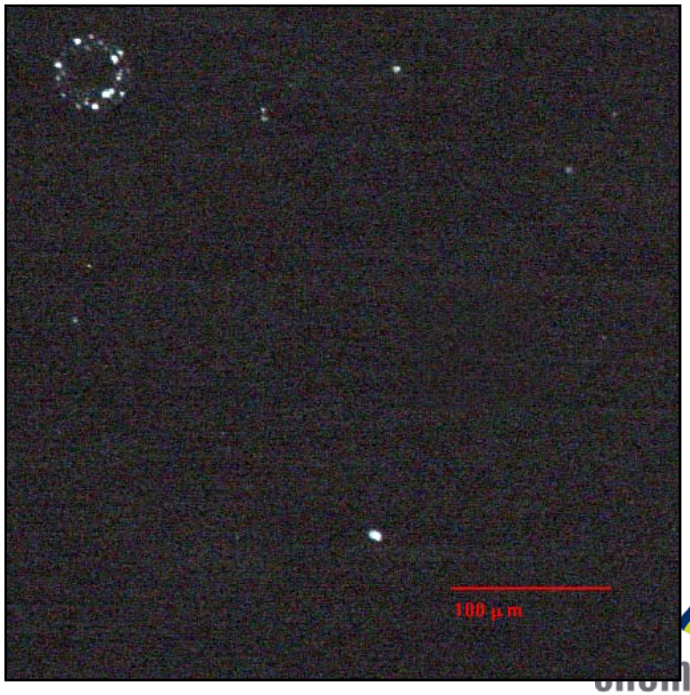

Task 5 Detection Sequence for PM Collection, Analysis and Identification

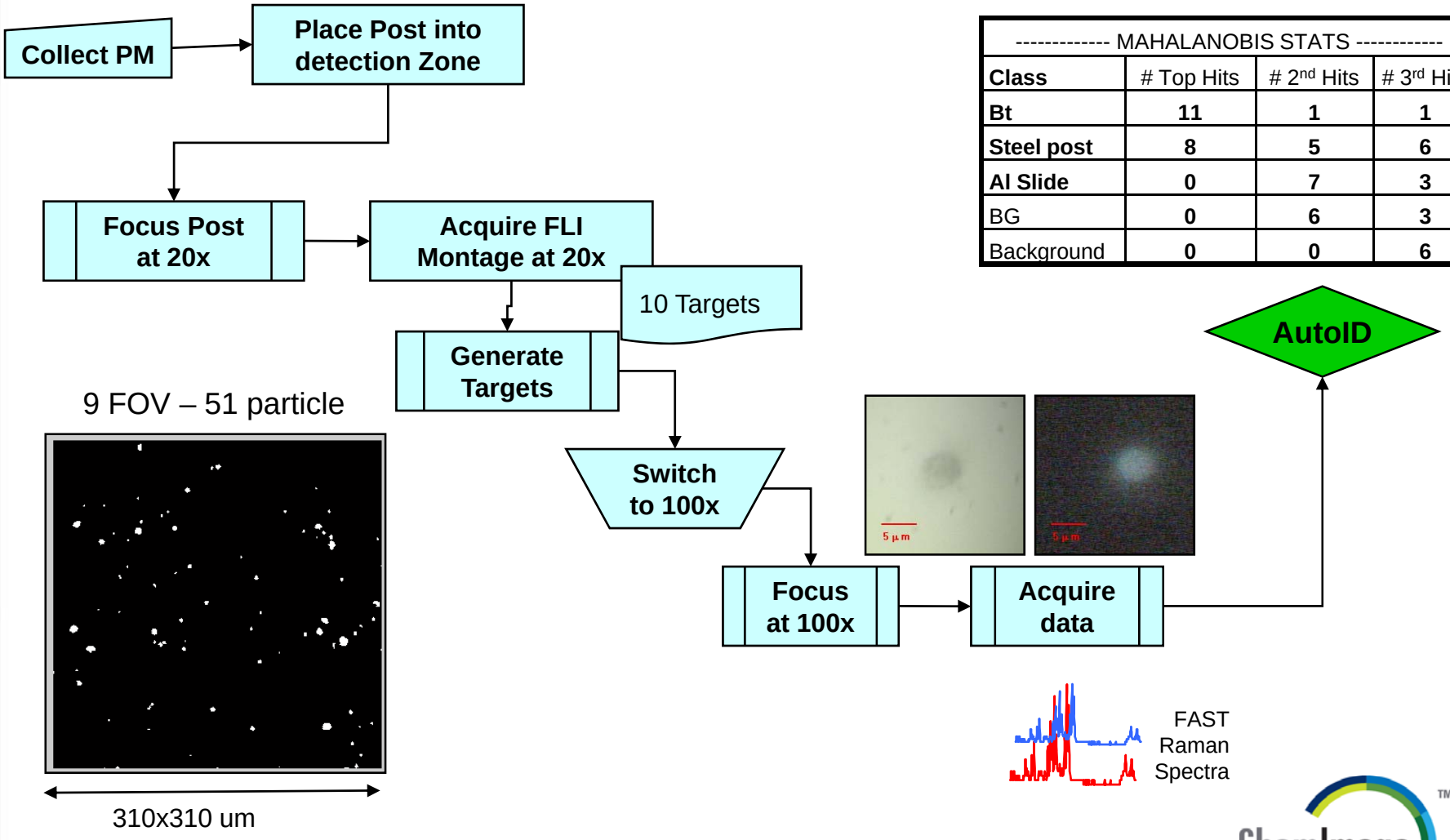

---------- MAHALANOBIS STATS ----------			
Class	# Top Hits	# 2nd Hits	# 3rd Hits
Bt	**11**	**1**	**1**
Steel post	**8**	**5**	**6**
Al Slide	**0**	**7**	**3**
BG	**0**	**6**	**3**
Background	**0**	**0**	**6**

ChemImage™

Task 5 Automated Targeting Algorithm

Preprocessing

Integrated Fluorescence Image

- Noise smoothing
- Background correction

Median, Wiener filtering
Background division

Binarization

Thresholding

Image scaled between 0-1
Threshold = 0.7

Particle Ranking

Calculate particle parameters

(Area, Centroid, Major Length, Eccentricity)

Remove non-targets
based on expected parameter values

(Min and Max Diameter, Eccentricity < 0.8)

Rank targets
based on similarity to "ideal" particle

Ideal Expected Target:
High Fluorescence Intensity
Ø 7.5 μm, Perfect Circularity

Report and Display Results

Particle Location List

Image Overlay

FLI Montage at 20x

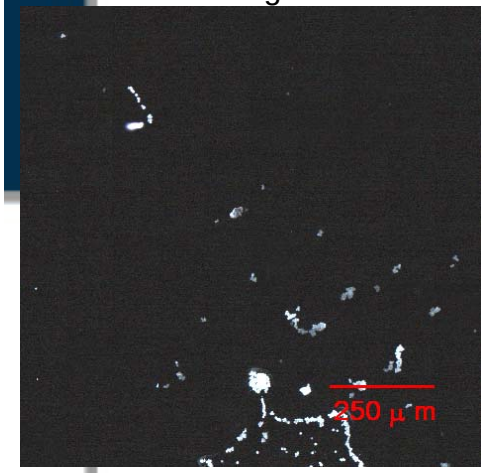

Binary Image

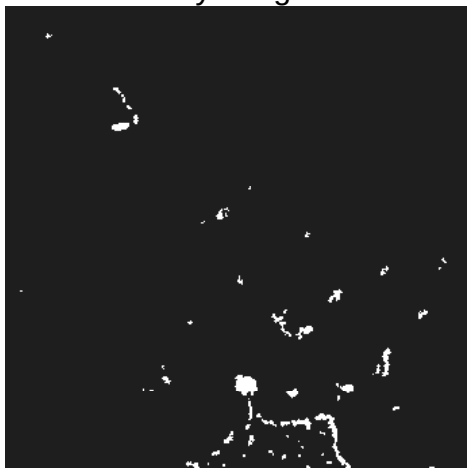

Detected Targets

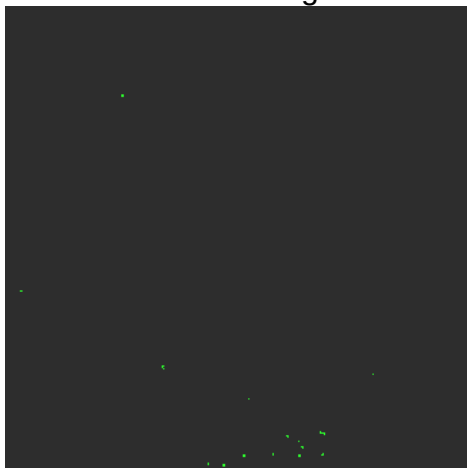

Overlay with ranked targets

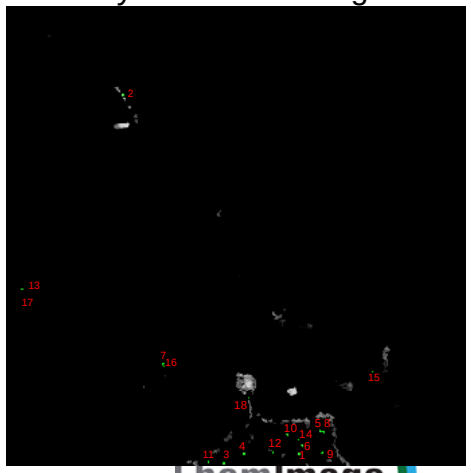

ChemImage

Task 5 Detection of 5 μm Polystyrene Sphere in Collected Indoor PM

BFR at 20x

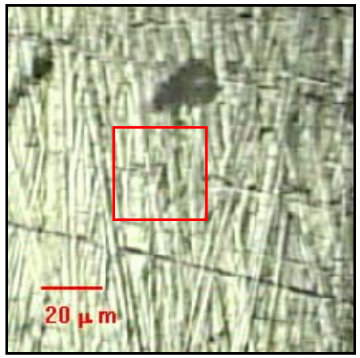

FLI at 20x

FAST Image @ 997 cm^{-1}

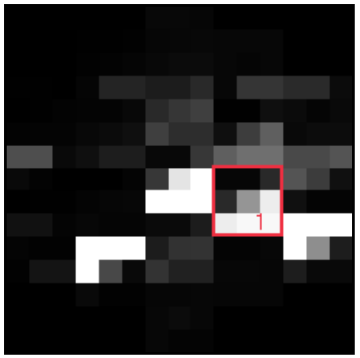

Blurred FAST Image @ 997 cm^{-1}

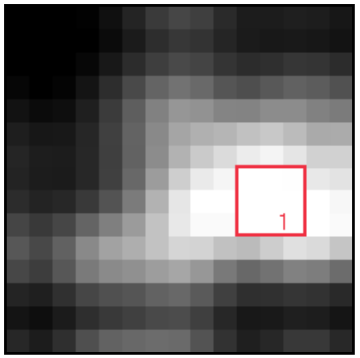

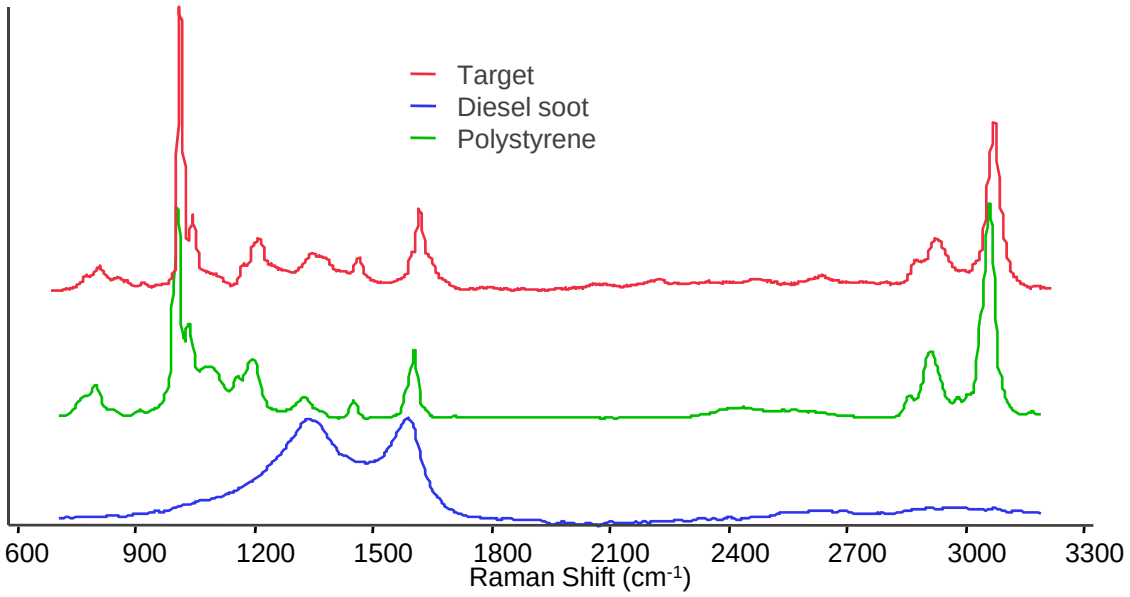

FAST Recon Steps: Cosmic, NIST, Truncate 300-3200cm^{-1}, Baseline, Normalize
Image Processing Steps: Gaussian Blur 3

ChemImage™

Task 5 Characterization of Collected Yellow Background at 100x

BFR at 100x

FLI at 100x

FAST Image @ 853 cm^{-1}

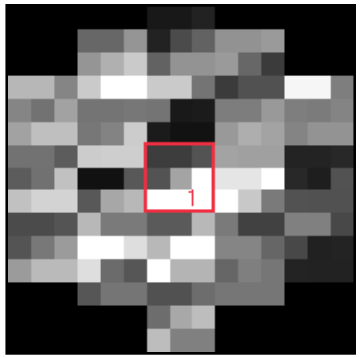

BFR at 100x after FAST

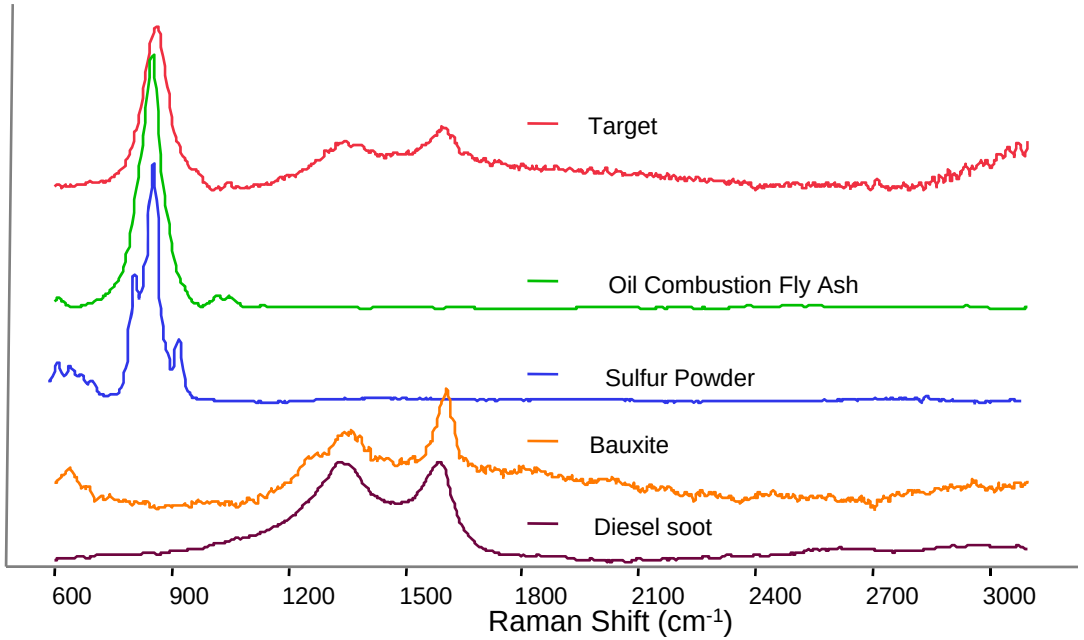

ChemImage™

Task 5 Targeting Performance of APICD Gen I

Date	1-Jun-07	13-Jun-07	13-Jun-07	**Summary**
Run #	**1**	**3**	**4**	
Analysis Time				
Time to Target (min)	3.31	2.7	3.6	**9.61**
Experiment Time (sec)	15.5	23.7	58.4	**97.6**
Photobleach Time (sec)	10	10	15	**35**
Exposure Time (sec)	10	10	10	**30**
Raman Expt Time (sec) /Particle	24.4	23.9	30	**26**
(Tfocus+Td) (sec) /Particle	70.2	78	78	**75**
Image Params				
Deposition Area (um2)				**1.94E+09**
Area Analyzed (um2)	1.04E+06	1.27E+06	8.86E+05	**3.19E+06**
% of Deposited Area Analyzed	254 FOVs			**0.17%**
Analyzed Particle Params				
# Particles	146	563	505	**1214**
# Respirable Particles	142	529	484	**1155**
# Fluorescent Particles	28	89	91	**208**
# Fluorescent Respirable Particles	15	60	59	**134**
% Respirable Fluorescent Fraction	10.56%	11.34%	12.19%	**11.6%**
Targeting Performance				
# Targets Classes				
# of PSMS Targets	11	20	44	**75**
Total Targeted Particles	13	18	46	**77**
# Correctly Targeted Threats	11	18	44	**73**
# Challenges (Fluo Particles)	28	89	91	**208**
True Positives	11	18	44	**73**
False Positives	2	0	2	**4**
False Negatives	0	2	0	**2**
True Negative	15	69	45	**129**
Sensitivity	100.0%	90.0%	100.0%	**97.3%**
Specificity	88.2%	100.0%	95.7%	**97.0%**
FN Rate	0.0%	10.0%	0.0%	**2.7%**

ChemImage™

Task 5 Raman Identification Performance of APICD Gen I

Date	1-Jun-07	13-Jun-07	13-Jun-07	**Summary**
Run #	**1**	**3**	**4**	
Raman Identification Performance				
Algorithm				MD
Spectral Range				800-1800; 2800-3200
#PCs				5
Library (Al; PSMS; Bg_Gmedia; Bt_Gmedia)				Library_070531
# Target Classes	4	4	4	**4**
# of TP Particles ID'd	5	3	11	**19**
# Challenges (# Targeted Particles)	13	18	46	**77**
Total # of ID Decisons	52	72	184	**308**
True Positives	5	3	11	**19**
False Positives	0	0	0	**0**
False Negatives	6	15	33	**54**
True Negative	41	54	140	**235**
Sensitivity	45.5%	16.7%	25.0%	**26.0%**
Specificity	100.0%	100.0%	100.0%	**100.0%**
FN Rate	54.5%	83.3%	75.0%	**74.0%**
FP Rate	0.0%	0.0%	0.0%	**0.0%**
Positive Predictive Value	100.0%	100.0%	100.0%	**100.0%**
Negative Predictive Value	87.2%	78.3%	80.9%	**81.3%**

ChemImage™

Task 5 Simulated APICD Gen II Data Logger Output

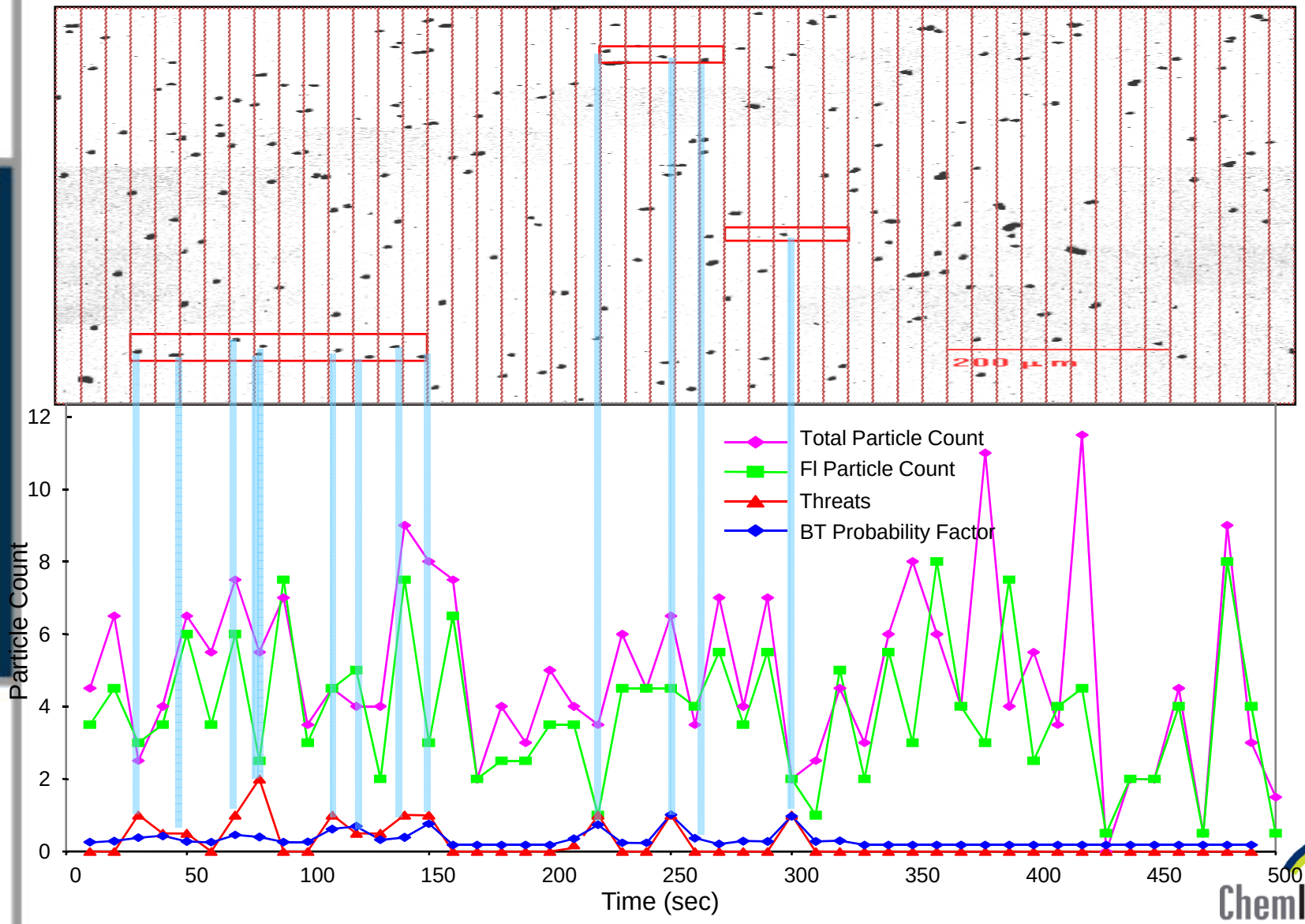

ChemImage™

Task 5 Modeling of APICD Gen II Device Based on Continuous Targeting and Detection

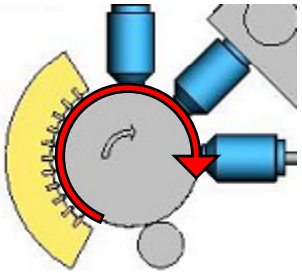

Aerosol Particulate Makeup Model

Component	Particles per liter
Non-Bio, Non-threat	900
Bio, Non-threat (targeted)	100
Bio, Threat (targeted)	25

Electrostatic Collector Model

Drum Diameter	3 inch
Collection Span	120 degree
Deposition Length	80 mm
Deposition Width	5 mm
Collection Rate	100 liters/min
Collection Efficiency	80%

Particulate Deposition Calculations

Component	Particles / mm^2 / sec
Non-Bio, Non-threat	3.0
Bio, Non-threat (*targeted*)	*0.3*
Bio, Threat (*targeted*)	*0.1*

Time for farthest particle to reach Raman Position

Collection Zone	1.48 min
Time to BF / TF	0.18
Spectral Imaging	0.55
Move to Raman	0.55
Total Time prior to Raman	2.76 min

ChemImage™

Task 5 Particle Accounting Model - 1

Process	Step #	Detection Sequence	ChemImage APICD Gen II Aerosol Sensor Particle Counting Model			Total Aerosols	Non-Bio Non-Threat Particles (NBNT)	Bio Non-Threat Particles (BNT)	Threat Agent Particles (BT)	Percent of Original Agent Particles
Assumptions	0		**Input Air Assumptions**							
			Biothreat Concentration (BT)	111	(#/liter)				111	9.99%
			NonBio Nonthreat Concentration (NBNT)	900	(#/liter)		900			81.01%
			Bio Nonthreat Concentration (BNT)	100	(#/liter)			100		9.00%
			Total Particle Loading:	**1,111**	(#/liter)	**1111**	900	100	111	100.00%
			Fluorescent Fraction Makeup							
			BT Fluorescent Fraction	**98%**	percent					
			BNT Fluorescent Fraction	**98%**	percent					
			NBNT Fluorescent Fraction	**2.5%**	percent					
			Total Fluorescent Particles	**229**	#/liter	**229.3**	22.5	98	109	20.6%
Electrostatic Collection		**Electrostatic Collection**	**Collect PM**							
			Collection Rate:	**50**	Liter/min					
			Particle Input Rate	926	particles / sec	**925.8**	750	83	93	
	1		CollectionTime	600	seconds					
			Air Volume Sampled During Collection	500	Liters					
			Particles Pulled In	555,500	particles	**555,500**	450,000	50,000	55,500	100.00%
			Total Collection Efficiency	**60%**	per Sceptor					
			Collection Segments	3	segments					
			Active Collection Segments	3	segment					
			Deposited Particles Makeup	333,300	particles	**333,300**	270,000	30,000	33,300	60.00%
			Deposition Area:							
			Deposition Width	10.0	mm					
			Drum Rotation Parameters:							
			Max Motor Rotation Rate	1.0	degree / sec					
Targeting		**Targeting**	**FLI Targeting**							
			Fluorescent Particles in FLI Targeting	5,012.9	particles	**5,012.9**	491.9	2,142.6	2,378.3	4.29%
	5	FLI Targeting	Apply FLI Targeting Algorithm to Generate List of Targets							
			FLI Targeting Sensitivity	**95%**						
			Fluorescent Particle Density in Active Deposition Area	76.8	particles / mm2					
			FCI Targeting							
	6	Sample Transfer	**Transfer Efficiency**	**99%**						
			Targeted Particles Transferred	3,115.2	particles	**3,115.2**	138.8	1,410.6	1,565.8	2.821%
			Distance Collection to FLI Objective	45	degree					
			Rotation Time to FCI from FLI							
	7	Focus at 20X	**FCI Focus Efficiency**	**90%**						
			FLI Targeted Particles Available for FCI Targeting	2,803.6		**2,803.6**	124.9	1,269.5	1,409.2	2.539%
			# of FCI FOVs	130						
			FCI Area Surveyed	65.3	mm^2					
			Fraction of the Depostion Segment Surveyed	8.18%	percent					
	8	Acquire FCI at 20x	**FCI Acquisition Efficiency**	**95%**						
			FLI Targeted Particles Available for FCI Targeting	2,663.5	particles	**2,663.5**	118.7	1,206.1	1,338.7	2.707%
			FCI Fields of View	1	FCI Fields of View					
			Fraction of the Targeting FOV Surveyed	**0.8%**	percent					
			Number of the Targeted Particles Surveyed	20.49	particles	**20.5**	0.9	9.3	10.3	

Task 5 Particle Accounting Model - 2

Process	Step #	Detection Sequence	ChemImage APICD Gen II Aerosol Sensor Particle Counting Model			Total Aerosols	Non-Bio Non-Threat Particles (NBNT)	Bio Non-Threat Particles (BNT)	Threat Agent Particles (BT)	Percent of Original Agent Particles
	9	FCI Targeting	Apply FCI Targeting Algorithm to Generate List of Targets							
			FCI Targeting Sensitivity	**95%**						
			FCI Targeting Specificity	**70%**						
			Targets Available for RCI Analysis	9.8	particles	**9.8**	0.3	2.6	6.8	0.012%
		Raman Detection	**Analysis**							
Raman Detection	10	Sample Transfer	**Transfer Efficiency**	**99%**						
			Targeted Particles Transferred	9.655	particles	**9.7**	0.3	2.6	6.8	0.012%
			Distance Collection to FLI Objective	45	degree					
			Rotation Time to Raman from FCI							
	11	Focus at 100X	Auto Find Targeted Particles							
			Find & Autofocus Efficiency	**90%**						
			Fraction of Particles to review	**100%**						
			Targeted Particles Available for Raman	8.8	particles	**8.8**	0.2	2.4	6.2	0.011%
			Targets in one FAST Sample Area	**1.0**	particles / FAST FOV					
	12	Acquire FAST RCI	Autoacquire RCI at 100x while maint focus between frames							
			RCI Acquisition Efficiency	**90%**						
			Particles Available for RCI Decision Making Algorithm	7.9	particles	**7.9**	0.2	2.1	5.5	0.010%
	13	Identification	Search against Mahalanobis Library							
			RCI BT Detection Sensitivity	**95%**						
			RCI Threat Specificity	**70%**						
			Particle Available for Combinatorial Decision-Making	4.4	particles	**4.4**	0.1	0.6	3.7	0.007%
			Decision							
Decision	14	System Report	Compare BT particles with set threshold							
			Misclassification	**95%**			Why?			
			Decide Air Safety Based On Particles' #	4.1	particles	**4.1**	0.1	0.6	3.5	0.006%
			The minimum Number of Threat Particles needed to Achieve Required FAR	**3**						
			Number of iterations to achieve Threat count	**1**	iterations					
		Regeneration	**Cleaning (Particles Added to the deposited ones)**							
			Cleaning is added here to allow particle accumulation to be accounted for in the overall particle counting							
Regeneration	15	Sample Transfer	Sample transfer to Regeneration Zone							
			Distance from RCI Zone to Collection Zone	107.5						
			Transfer Efficiency	**99%**						
	16	Surface Regeneration	Targeted Particles Transferred	4.1	particles	**4.1**	0.1	0.6	3.5	
			Cleaning Efficiency	**94.0%**						
			Residual Particles (Total)	0.246	particles	**0.00**	0			0.006%
			Residual BT, BNT, NBNT Particles (per FLI FOV)	11.211	particles / Targeting FOV					
			TOTAL Resudial Particles on the surface	19,998		**19,998.0**	16,200	1,800	1,998	

Task 5 APICD Gen II Performance Compared for 3 scenarios

Biothreat concentration = 9%, 50%, 91%

ChemImage APICD Gen II Aerosol Sensor Particle Counting Model			Total Aerosols	NBNT	BNT	BT
Bio Nonthreat Concentration (BNT)	100.0	(#/liter)			100.0	
NonBio Nonthreat Concentration (NBNT)	900.0	(#/liter)		900		
Biothreat Concentration (BT)	100.0	(#/liter)	9.0%			100
	1,000.0	(#/liter)	50.0%			1000
	10,000.0	(#/liter)	90.9%			10000
CollectionTime	300.0	seconds				
Particles in one FLI Targeting FOV	32.1	particles / Targeting FOV				
	131.0	particles / Targeting FOV				
	1,119.9	particles / Targeting FOV				
# of FLI FOVs	130.0	FOVs				
Fluorescent Particles in FLI Targeting	4,168.6	particles	4168.6	1311.8	1428.4	1428.4
	17,024.4	particles	17024.4	1311.8	1428.4	14284.1
	145,581.6	particles	145581.6	1311.8	1428.4	142841.4
FCI Analysis Time	300.0	seconds				
FCI Fields of View	1.0	FCI Fields of View				
Number of the Targeted Particles Surveyed	14.8	particles	14.8	2.4	6.2	6.2
	70.5	particles	70.47	2.43	6.18	61.85
	627.1	particles	627.1	2.4	6.2	618.5
Decide Air Safety Based On Particles' #	2.6	particles	2.6	0.2	0.4	2.1
	21.6	particles	21.6	0.2	0.4	21.0
	211.0	particles	211.0	0.2	0.4	210.5
Min # of Threat to achieve false Alarm Rate of 10^{-4}	10.0	RCI analysis time is restricted by the max of 10 threats				
Number of iterations to achieve Threat count	5.0	iterations				
	1	iterations				
	1	iterations				
Alarm raised	0.76	hrs	45.6	min		
	0.25	hrs	15.0	min		
	0.25	hrs	15.0	min		

Task 5 Time to Alarm Model for 50% Biothreat in PM

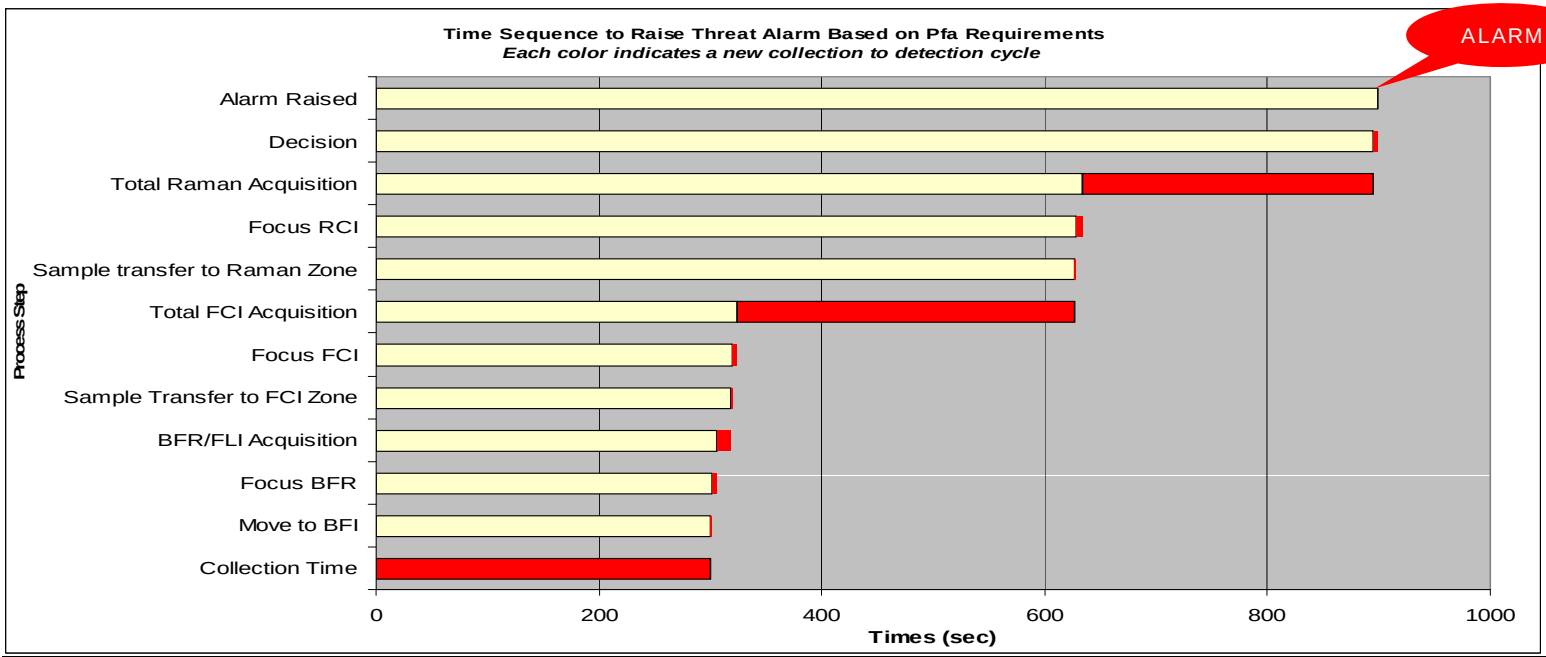

Steps	Time (sec) / Step	Base Time	Dead Time 1	Cycle 1	Dead Time 2	Cycle 2	Notes
1	**Collection Time**	300.0	0	300	0	0	Parallel to FCI
2	**Move to BFI**	2.1	300	2.0	0	0	Serial
3	**Focus BFI**	3.0	302	3.0	0	0	Serial
4-5	**FLI Acquisition**	13.0	305	13.0	0	0	Serial
6	**Transfer to FCI Zone**	2.3	318	2.3	0	0	Serial
7	**Focus FCI**	3.0	320	3.0	0	0	Serial
8-9	**Total FCI Acquisition**	303.0	323	303	0	0	Serial
10	**Transfer to Raman Zone**	2.3	626	2.3	0	0	Serial
11	**Focus RCI**	5.o	629	5.0	0	0	Serial
12-13	**Raman Acquisition**	154.3	634	154	0	0	Serial
14	**Decision**	5.0	788	5.0	0	0	Parallel
	Alarm Raised	1	**2745 sec (15 min)**				

Task 5 Time to Alarm Model for 9% Biothreat in PM

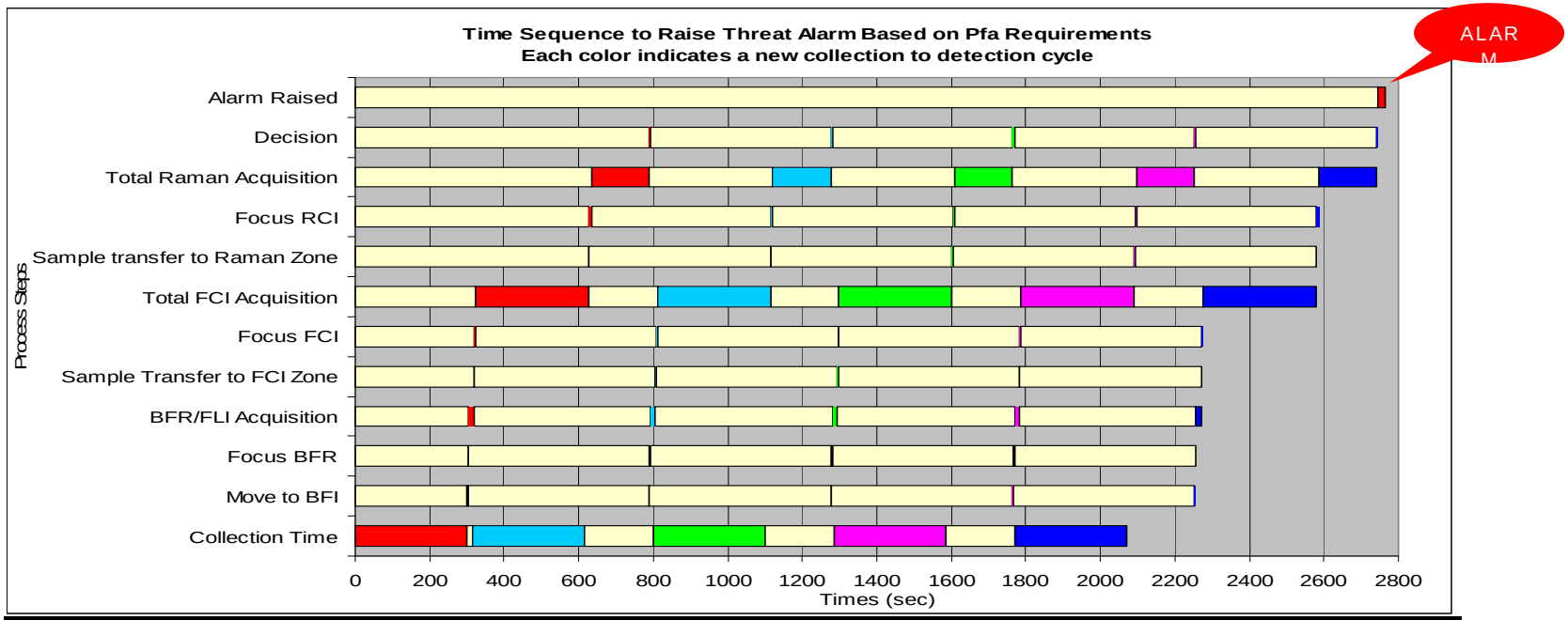

Steps	Time (sec) / Step	Base Time	Dead Time 1	Cycle 1	Dead Time 2	Cycle 2	Notes
1	**Collection Time**	300.0	0	300	15	300	Parallel to FCI
2	**Move to BFI**	2.1	300	2.0	300	2.0	Serial
3	**Focus BFI**	3.0	302	3.0	329	3.0	Serial
4-5	**FLI Acquisition**	13.0	305	13.0	2.0	13.0	Serial
6	**Transfer to FCI Zone**	2.3	318	2.3	486	2.3	Serial
7	**Focus FCI**	3.0	320	3.0	485	3.0	Serial
8-9	**Total FCI Acquisition**	303.0	323	303	185	303	Serial
10	**Transfer to Raman Zone**	2.3	626	2.3	486	2.3	Serial
11	**Focus RCI**	5.0	629	5.0	483	5.0	Serial
12-13	**Raman Acquisition**	154.3	634	154	334	154	Serial
14	**Decision**	5.0	788	5.0	483	5.0	Parallel
	Alarm Raised		**2745 sec (46 min)**				

Task 5 BT "Threat" Detection Simulation

Overlay of BFR and FLI images (Purple)

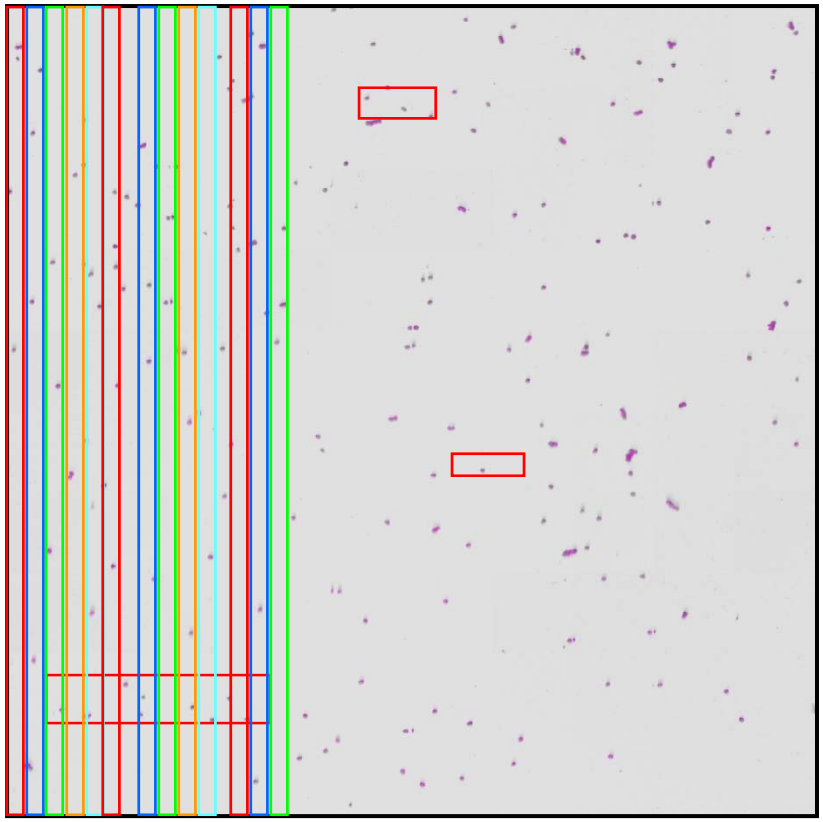

1 2 3 4 50

13 "threat" particles

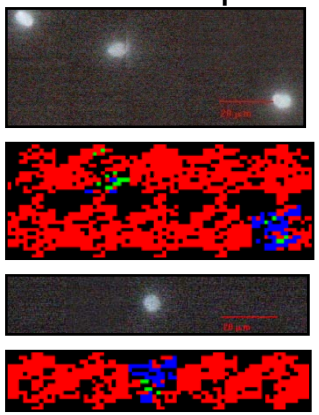

Total Particles:

BFR particles: 244 (224) Manual (CIX Count)

Max Chord 7.61±3.50 um

FLI particles: 192 (195) Manual (CIX Count)

Max Chord 7.08±3.13 um

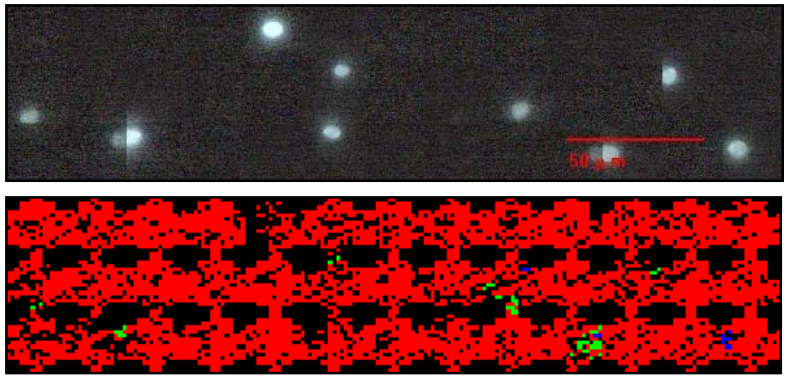

MD Classification, Probability 0.95, 800-1800 cm^{-1}

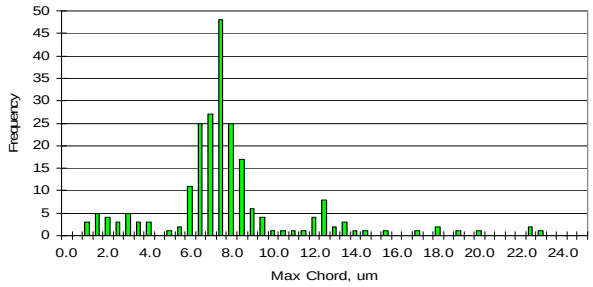

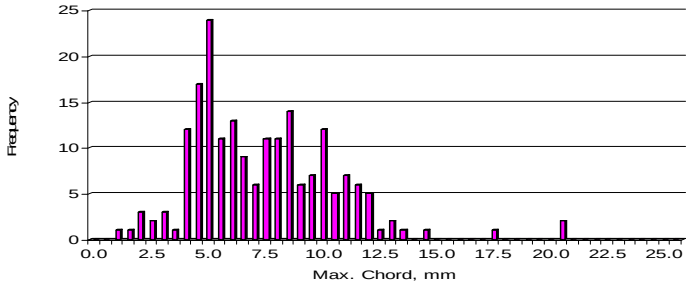

ChemImage™